From the *Walther Straub Institute for Pharmacology and Toxicology*

Dissertation

zum Erwerb des Doctor of Philosophy (Ph.D.) an
der

Medizinischen Fakultät der

Ludwig-Maximilians-Universität zu München

Characterization of a P2X7 BAC reporter mouse model and investigation of the P2X4/P2X7 interaction in mouse lung tissue

vorgelegt von

Antonio Ramírez Fernández

aus:

Málaga - Spanien

Jahr:

2023

Mit Genehmigung der Medizinischen Fakultät der

Ludwig-Maximilians-Universität zu München

First evaluator (1. TAC member): *Prof. Dr. nat. phil. Annette Nicke*

Second evaluator (2. TAC member): *Prof. Dr. Alexander Dietrich*

Third evaluator: *Prof. Dr. Arthur Liesz*

Fourth evaluator: *Prof. Dr. Markus Rehberg*

Dean: **Prof. Dr. med. Thomas Gudermann**

Datum der Verteidigung:

4 Oktober 2023

Table of contents

Abstract

P2X receptors (P2XR) comprise a family of ATP-gated, non-selective cation channels. Out of the seven members of the P2XR family (P2X1R-P2X7R), P2X7R presents important characteristics that make it unique. These are a) the low affinity for the ligand ATP, b) its long, intracellular C-terminus and c) the ability to induce the formation of a macropore under sustained stimulation that allows the passage of large molecules and that may eventually lead to cell death. The best characterized function of the P2X7R is the induction of NLRP3 inflammasome assembly for the activation of caspase-1 and release of pro-inflammatory cytokines IL-1β and IL-18.

The P2X7R is encoded by the *P2rx7* gene and is widely expressed in immune cells, where it has proved relevance as a drug target due to its role in inflammation and its demonstrated modulatory effects in various diseases. For example, P2X7R involvement has been found in infectious diseases, autoimmune disorders, and cancer. In the central nervous system, the P2X7R was shown to modulate neuroinflammation.

However, the cell type-specific localization and functions of the P2X7R in the central nervous system are incompletely understood. While its large intracellular C-terminus has been proposed to serve as a platform for the interaction with mediators of signaling pathways, details about the identity of these interaction partners, the signaling mechanisms and functional relevance of such interactions remain largely unknown. A physical interaction of P2X7R with the P2X4R subtype has been suggested, although proof of this interaction is mostly restricted to heterologous overexpression systems and evidence for this interaction *in vivo* is insufficient.

In an attempt to address these questions, two transgenic P2X7R reporter mouse models have been generated that express EGFP under the control of the endogenous *P2rx7* promoter. One of them expresses a soluble EGFP (sEGFP mouse) and the other one expresses a P2X7-EGFP fusion protein (P2X7-EGFP mouse). However, preliminary data revealed divergent distribution of the reporter proteins in the mouse brain.

In this project, a detailed characterization and comparison of both BAC transgenic mouse models was performed. Biochemical and histochemical approaches have been applied to compare the P2X4 and P2X7 expression levels in both mouse models and determine the cell-specific distribution of the EGFP reporter. In the P2X7-EGFP mouse model, this study confirmed that the endogenous P2X7 and P2X4 expression levels were unaffected and that the overexpressed fusion protein is found in microglia and oligodendrocytes. However, analysis of P2X4 and P2X7 levels in the sEGFP mouse model revealed an unexpected overexpression of both proteins, which is explained by the use of a different BAC clone and the respective recombination strategy. Immunohistochemistry experiments demonstrated divergent expression patterns of P2X7 and the sEGFP reporter and revealed its predominant localization in neurons. In conclusion, these results unveiled and explained inconsistencies in the reporter expression of the sEGFP mouse model.

In a second part of this thesis, I investigated the reported interaction between P2X7R and P2X4R using the transgenic P2X7-EGFP mouse model. In a biochemical approach the interaction of both receptors was evaluated by pull-down via EGFP-tag. Control experiments were performed upon expression of both subunits in *Xenopus laevis* oocytes and HEK293 cells. Our results confirmed a previously shown P2X4R-P2X7R interaction in *X. laevis* oocytes but revealed no proof of such an interaction in mouse lung and HEK293 cells. The possibility of a functional interrelation between P2X4R and P2X7R was further explored by comparison of the expression levels in both subunits in wildtype, P2X7-EGFP overexpressing mice and *P2rx4*$^{-/-}$ and *P2rx7*$^{-/-}$ knockout mouse models. Together, these data did not support an interaction or mutual interrelation of both receptors in the mouse lung.

Lastly, a preliminary comparative proteomic study was performed with wildtype, *P2rx7*$^{-/-}$ and P2X7-EGFP mice to study P2X7R signaling. To this aim, protocols for sample preparation were tested and samples from mouse hippocampus were submitted to liquid chromatography coupled to mass spectrometry (LC-MS) analysis. However, statistical analysis did not identify significantly enriched proteins. Therefore, a cell-specific approach was considered more promising and a protocol for microglia isolation from adult mouse brain was tested for future proteomic studies.

In summary, this study provided the first detailed characterization of the sEGFP P2X7 reporter mouse model and revealed important caveats for its use in basic research. It further showed evidence against the proposed interaction between P2X7R and P2X4R and finally describes a comparative proteomics approach to investigate P2X7R signaling cascades.

List of figures

Note: Figures 1, 2, 4, 5, 6 and 25 have been personally drawn using Adobe Illustrator.

List of tables

List of abbreviations

ABC Avidin-biotin complex

ADP Adenosine diphosphate

AIF-1 Allograft inflammatory factor 1

Akt Protein kinase B

AMP Adenosine monophosphate

APC(s) Antigen presenting cell(s)

ARTC2.1 Ecto-ADP-ribosyltransferase 2.1

ASC Apoptosis-associated speck-like protein containing a CARD

ATI Alveolar type 1 cell

ATP Adenosine triphosphate

BAC Bacterial artificial chromosome

BN-PAGE Blue native-polyacrylamide gel electrophoresis

BDNF Brain-derived neurotrophic factor

bp Base pair

BSA Bovine serum albumin

Bz-ATP 3'-O-(4-Benzoyl)benzoyladenosine 5'-triphosphate

CA Cornu ammonis

CARD Caspase activation and recruitment domain

CNS Central nervous system

CRF Corticotropin releasing factor

cRNA Complementary RNA

Cryo-EM Cryogenic electron microscopy

CXCR1 CXC motif chemokine receptor 1

CVD Cerebrovascular disease

DAB Diaminobenzidine

DAMP(s) Damage-Associated Molecular Pattern(s)

DAPI 4′,6-diamidino-2-phenylindole

DC(s) Dendritic cell(s)

DG	Dentate gyrus
dk	Donkey
DMEM	Dulbecco's modified eagle medium
DNA	Deoxyribonucleic acid
DPBS	Dulbecco's phosphate buffer saline
EC_{50}	Half maximal effective concentration
EDTA	Ethylenediaminetetraacetic acid
EGFP	Enhanced green fluorescent protein
FACS	Fluorescence-activated cell sorting
FASP	Filter-aided sample preparation
FRET	Förster resonance energy transfer
GENSAT	Gene expression nervous system atlas
GFAP	Glial fibrillary acidic protein
GFP	Green fluorescent protein
GL	Granular cell layer
GSDMD	Gasdermin D
gt	Goat
HEK	Human embryonic kidney
HEPES	4-(2-hydroxyethyl)-1-piperazineethanesulfonic acid
Hifα	Hypoxia inducible factor alpha
Iba1	Ionized calcium-binding adapter molecule 1
IF	Immunofluorescence
IFT81	Intraflagellar transport protein 81
IHC	Immunohistochemistry
IL-1β	Interleukin-1β
IP	Immunoprecipitation
JNK	Jun amino-terminal kinase
kb	Kilobases
kDa	Kilodalton

Lamp1 Lysosome-associated membrane glycoprotein 1

LC-MS Liquid chromatography coupled to mass spectrometry

LPS Lipopolysaccharide

MBP Myelin basic protein

MCAM Melanoma cell adhesion molecule

ML Molecular layer

mRNA Messenger RNA

ms Mouse

NeuN Neuronal nuclear protein

NG2 Neural/glial antigen 2

NGS Normal goat serum

NLRP3 NOD-like receptor family pyrin domain containing 3

NPC(s) Neural progenitor cell(s)

oATP Oxidized ATP

Olig2 Oligdendrocyte transcription factor 2

P2XR(s) P2X receptor(s)

P2YR(s) P2Y receptor(s)

pA Polyadenylation

pAb Polyclonal antibody

PAGE Polyacrylamide gel electrophoresis

PAMP(s) Pathogen-Associated Molecular Pattern(s)

PCR Polymerase chain reaction

PFA Paraformaldehyde

Pro-IL1β Pro-Interleukin-1β

PS Phosphatidylserine

PVDF Polyvinylidene fluoride

qPCR Quantitative PCR

rb Rabbit

RCSI Royal College of Surgeons in Ireland

RNA Ribonucleic acid

ROCK Rho-associated protein kinase

SAPK Stress-activated protein kinase

sEGFP Soluble EGFP

Slu Stratum lucidum

SOC Super optimal broth with catabolite repression

TAE Tris-acetate-EDTA

TALEN(s) Transcription activator-like effector nuclease(s)

TBS Tris buffered saline

TLR(s) Toll-like receptor(s)

VCAM1 Vascular cell adhesion molecule 1

WB Western blot

Wt Wildtype

ZFN(s) Zinc-finger nuclease(s)

ZnT3 Zinc transporter 3

1. Introduction

Adenosine triphosphate (ATP), first reported by Karl Lohmann (Langen & Hucho, 2008; Lohmann, 1929), is known by most as the cell principal energy reservoir. The high amount of energy that it takes to form the bond between the second and third phosphate group can be released by breaking it, which makes this molecule a good energy currency. Over the years, understanding of this molecule was expanded as new insights were discovered, in particular its suggested extracellular functions as a signaling molecule and a neurotransmitter (Burnstock, 1972; Burnstock et al., 1970; Drury & Szent-Györgyi, 1929; Emmelin & Feldberg, 1948; Holton, 1959).

This new role of ATP and the coinage of the term “Purinergic Signaling” by Geoffrey Burnstock was a matter of discussion and faced dissention from a certain part of the scientific community. Eventually, the first receptors for adenosine and its derivatives ATP, adenosine diphosphate (ADP) and adenosine monophosphate (AMP) were identified through study of dose-response effects caused by their application (*e.g.* changes of potential or accumulation of cyclic AMP), molecular cloning and discovery of antagonists (Blume et al., 1973; Cobbin et al., 1974; Kostopoulos et al., 1975; Kuroda et al., 1976; Valera et al., 1994; Webb et al., 1993). Soon, a classification was suggested for such receptors depending on their agonists: receptors activated by adenosine or AMP were termed P1 receptors (later named adenosine receptors), whereas those activated by ATP or ADP were classified as P2 receptors (Burnstock, 1978; Fredholm et al., 2001).

According to the initial proposed model (Burnstock, 1978), ATP released via exocytic vesicles would either activate P2 receptors from a neighboring cell or be rapidly cleaved into adenosine via nucleotidases, and the resulting adenosine molecules would then reach adenosine receptors at the prejunctional cell and modulate the release of ATP, creating a negative feedback loop (Figure 1). Current knowledge differs from this model, as ATP and its breakdown products are able to reach receptors both at the pre- and post-junctional cells. While adenosine is linked to anti-inflammatory processes, ATP is associated with inflammation. Furthermore, AMP and ADP are agonists for adenosine receptors and P2 receptors, respectively (Abbracchio & Burnstock, 1994; Rittiner et al., 2012; Silinsky et al., 1990; Silva-Ramos et al., 2020).

The release of ATP as a signaling molecule takes place in several types of cells across the organism *e.g.* in the nervous system, where ATP can be co-transmitted along with other neurotransmitters (Burnstock, 1976; Svensson et al., 2019). According to their mechanism of action, P2 receptors are classified in two families (Abbracchio & Burnstock, 1994; Burnstock & Kennedy, 1985). P2X receptors (P2XR) comprise a family of ionotropic receptors, and P2Y receptors (P2YR) are protein G-coupled receptors. Both families are widely distributed throughout the organism (Burnstock & Knight, 2004; Jacobson & Müller, 2016).

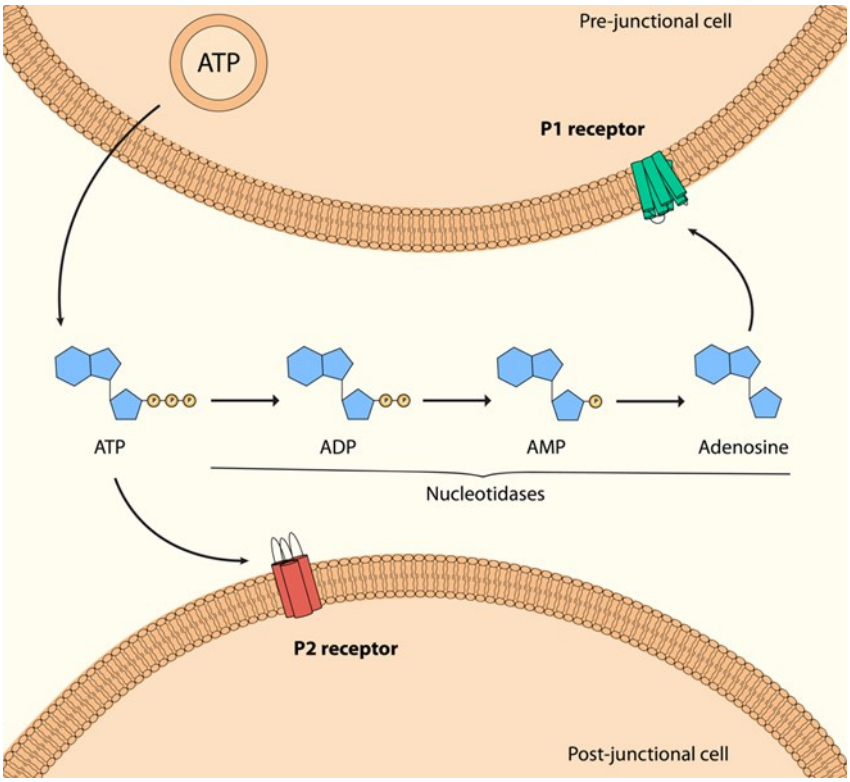

Figure 1: Negative feedback loop involving P1 (adenosine receptors) and P2 receptors *as suggested in their first proposed classification* (Burnstock, 1978).

1.1 P2X receptors

P2XRs, encoded by the *P2rx* genes, are a family of receptors that are non-selective cation channels and allow the passage of Na^+, K^+ and Ca^{2+} ions upon activation. Seven members of this family have been identified in and cloned from mammals (P2X1-P2X7), having their names assigned according to their chronological order of cloning (Kaczmarek-Hájek et al., 2012).

P2X receptors are encoded by 379 to 595 amino acids. The structure of P2X receptors consists of two transmembrane helical domains linked by a large extracellular loop that contains the biding site for the ligand, as well as for modulators and antagonists (Figure 2). Both N- and C-termini are located in the intracellular region in all the isoforms and are less conserved among the members of the family, whereas the extracellular region contains segments of amino acids that are more conserved. The different degrees of homology are responsible for the different ligand affinity and channel kinetics when comparing the different isoforms in different organisms (North, 2002).

The quaternary structure of P2X receptors consists of three subunits. Although channel activation was thought to require three molecules of the agonist, it was shown that only two molecules can activate a channel at times (Stelmashenko et al., 2012). Out of the seven isoforms, nearly all the members of the P2XR family are able to effectively show homotrimeric assembly, with the exception of P2X6R, which also has the shortest amino

acid sequence. In native tissues, P2X6R has been suggested to form heteromeric complexes with P2X2R (Resende et al., 2007; Schwindt et al., 2011) but also with P2X4R (Rubio & Soto, 2001). These combinations were also demonstrated via co-immunoprecipitation and functional studies in heterologous expression systems (King et al., 2000; Lê et al., 1998; Torres et al., 1999). The existence of heterotrimers expands the characteristics and dynamics of P2X receptors, although the specific subunit combinations in native tissues are incompletely understood. Aside of P2X6R, there are combinations for which good evidence has been reported over the years *e.g.* P2X2/3 or P2X1/5 (Saul et al., 2013; Torres et al., 1999), while others remain difficult to demonstrate in physiological conditions, such as P2X4/7. For further details about P2X4/7, refer to section 1.4.

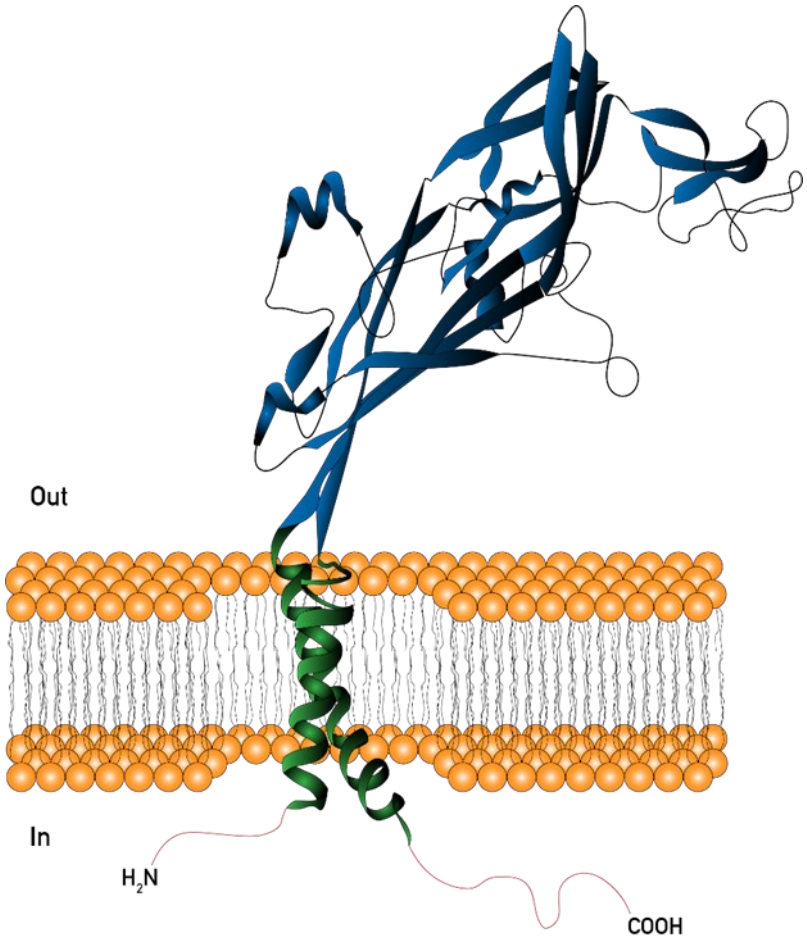

Figure 2: Schematic representation of a P2X monomer inserted in the plasma membrane. *Red: Intracellular N- and C-termini; green: transmembrane domains; blue: ectodomain.*

1.2 P2X7R

P2X7 receptor (P2X7R), the central core of this dissertation, represents the most dissimilar member within the P2XR family. The characteristics that make this channel unique among the P2X receptors are:

- It shows the lowest affinity for ATP (EC_{50}>1mM, up to 1000-fold over other isoforms). In fact, 3'-O-(4-Benzoyl)benzoyladenosine 5'-triphosphate (Bz-ATP), is a more potent agonist on this receptor (EC_{50}~100 µM) than ATP (Kaczmarek-Hájek et al., 2012).
- It has a long intracellular C-terminus, which has been reported to serve as a platform for the interaction with partners that might trigger signaling cascades not usually related to ion channels (Kopp et al., 2019).
- The P2X7 channel is the only member of the family that does not show desensitization upon sustained ligand application (Koshimizu et al., 1999; McCarthy et al., 2019). In fact, it has been demonstrated that, upon prolonged stimulation, the channel is able to induce membrane permeabilization by opening a macropore that allows the passage of large cations and fluorescent dyes such as YO-PRO1 or ethidium bromide. Although the molecular events that govern the opening of such macropore are not completely understood, it is known that it may lead to cell death (Kopp et al., 2019).

P2X7R activation enables the opening of a channel for the inward passage of Ca^{2+} and Na^{+} (Miller et al., 2011). In spite of studies arguing in favor of P2X7R being a channel for K^{+} efflux, it was shown that this is at least partially mediated by the two-pore domain K^{+} channel TWIK2 (Di et al., 2018) with functional relevance (refer to section 1.2.2.1). The presence of divalent cations (*e.g.* Cu^{2+}, Cd^{2+}, Ni^{2+}, Zn^{2+}, Ca^{2+}) lowers the ability of ATP to activate P2X7, possibly acting as allosteric inhibitors (Virginio et al., 1997).

1.2.1 Structure of P2X7R

With 595 amino acids, P2X7R is the largest protein in the P2XR family. When compared with other P2X isoforms, P2X7 shows the most variable sequence in the large extracellular loop (ectodomain) and the intracellular C-terminus (Chessell et al., 1998), which represents around 40% of the protein (Kopp et al., 2019). The structure of this domain was resolved recently for the rat P2X7R *in vitro* via single particle electron microscopy (Figure 3) and renamed as “ballast domain” (McCarthy et al., 2019). This study was a major breakthrough which revealed motifs and folds that opened new routes for P2X7R research (Figure 3). For example, residues of C- and N- termini form a “cap” in the cytoplasm that determines P2X7R desensitization rate. In relation with this, a cytoplasmic “anchor” C-cys domain undergoes palmitoylation that prevents desensitization. As for the ligand binding site, P2X7R ectodomain owns a binding pocket with a more narrow space that protects it from ligands and solvents in comparison with other P2XR isoforms, thus giving a reason for the low affinity that P2X7R has for ATP. The ballast domain was proved to be necessary for the opening of the so-called macropore *e.g.* through study of a naturally occurring truncated human P2X7R isoform called P2X7B that lacks from this domain and is unable to induce macropore formation (Adinolfi et al., 2010). Previously, it was suggested that the opening of this pore might require other interacting proteins such Pannexin-1 (Pelegrin & Surprenant, 2006).

Alternative splicing products apart from P2X7B have been characterized, studied, and compared to the canonical P2X7A (Andrejew et al., 2020; Jimenez-Mateos et al., 2019). Other isoforms lacking the carboxyterminal end are the human P2X7E or P2X7J. The latter, similarly to P2X7L, also lacks from part of the ectodomain (de Salis et al., 2022). Furthermore, P2X7J forms non-functional heterotrimers with other P2X7 subunits in a suggested protective role against ATP-related cell death, which is relevant in cancer cell survival (Y. H. Feng et al., 2006; Y.-H. Feng et al., 2006). Interestingly, P2X7k is a mouse isoform that expresses an alternative exon 1 (exon 1') and escapes deletion in a $P2X7^{-/-}$ mouse model (Nicke et al., 2009).

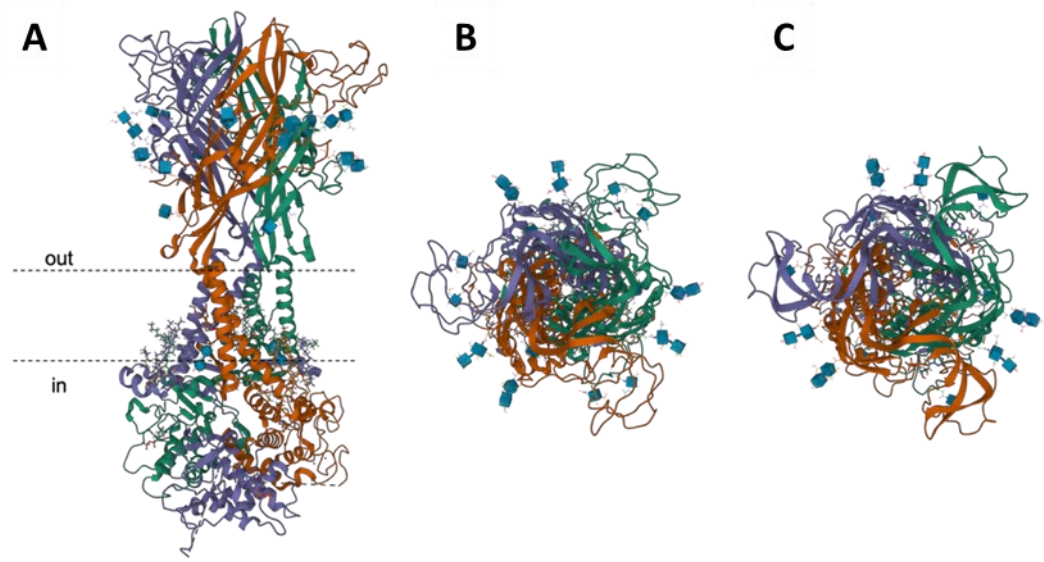

Figure 3: P2X7 trimer *as described by* McCarthy et al. (2019) *(A) Observation of the channel across the plasma membrane. (B, C) Observation of the channel from the outer side of the membrane in the (B) apo (PDB ID 6U9V) and (C) open (PDB 6U9W) states.*

1.2.2 Cellular and physiological functions of P2X7R

Some of the best described P2X7R functions include the synthesis and release of pro-inflammatory cytokines, activation of lipases, transcription factors, apoptosis, and induction of changes in the plasma membrane, among others (Kopp et al., 2019).

1.2.2.1 Role in inflammation

The most recognized function of P2X7R is its role in inflammatory processes and the synthesis and release of interleukin-1β (IL-1β). IL-1β is a pro-inflammatory cytokine that derives from the inactive form pro-interleukin-1β (pro-IL1β) that is cleaved by caspase-1 (Albalawi et al., 2017; Di Virgilio, 2007; Ferrari, Pizzirani, et al., 2006). Having a very low affinity for ATP means that P2X7R will be activated when the ATP concentration in the extracellular medium is high. In this situation, ATP acts as a Damage-Associated Molecular Pattern (DAMP) (Tanaka et al., 2014). DAMPs act upon tissue damage or recognition of Pathogen-Associated Molecular Patterns (PAMPS) such as bacterial lipopolysaccharide (LPS) (Di Virgilio et al., 2023). This is important for the recruitment of factors that play a role in immunity (Vénéreau et al., 2015).

Transcription of the NOD-like receptor family pyrin domain containing 3 (NLRP3) protein begins as a result of the signaling cascades triggered by toll-like receptors (TLRs) upon interaction with PAMP molecules such as LPS or biglycan (Babelova et al., 2009; De Nardo et al., 2014; Qu & Dubyak, 2009). As mentioned earlier, activation of P2X7R leads to Na^+ and Ca^{2+} influx and there is a compensatory K^+ efflux produced by P2X7R itself and the TWIK2 channel. Although the specific mechanisms of NLRP3 activation prior to NLRP3 inflammasome assembly are not clear, it has been suggested that NLRP3 inflammasome oligomerizes following K^+ depletion and/or Ca^{2+} increase in the cytoplasm (Figure 4). The complex is formed when NLRP3, that act as a sensor, recruits ASC (mediator), the apoptosis-associated speck-like protein containing a caspase activation and recruitment domain CARD. ASC oligomerizes creating the NLRP3 inflammasome complex (Lopez-Castejon & Brough, 2011). ASC recruits pro-caspase-1 forming the so-called ASC speck. This enables the self-catalytic activity of pro-caspase-1. Cleavage of pro-caspase-1 releases caspase-1 into the cytoplasm (Guo et al., 2015; Swanson et al., 2019). Caspase-1 cleaves both pro-IL1β into its active form IL-1β, and the auto-inhibited gasdermin D (GSDMD) into active GSDMD, which forms a membrane pore that allows secretion of mature IL-1β into the extracellular space. Once at the extracellular medium, IL-1β mediates inflammation by initializing the innate immunity (de Sá et al., 2023; Dubyak, 2012; Giuliani et al., 2017; Wang et al., 2021). GSDMD pores have been reported to trigger pyroptosis, a cellular process that involves death without affecting the surrounding cells (Liu et al., 2016). Additional aspects of P2X7R involvement in this process have been suggested, such as a possible direct interaction of P2X7R and NLRP3 prior to the NLRP3 inflammasome assembly (Franceschini et al., 2015; Silverman et al., 2009), which may allow an intrinsic ATPase activity of NLRP3 protein that it requires in order to oligomerize and begin the inflammasome assembly (Minkiewicz et al., 2013). The structure of the human NLRP3 inflammasome protein complex was resolved recently *in vitro* via cryogenic electron microscopy (cryo-EM) (Xiao et al., 2023).

The role of P2X7R in the synthesis and release of IL-1β was confirmed by the use of a knockout mouse model (*P2rx7*$^{-/-}$) whose macrophages showed impairment of IL-1β release after ATP stimulation (Solle et al., 2001b). As pro-IL1β levels remained stable, a conclusion of the study was that P2X7R activation by ATP plays a role in the cleavage of pro-IL1β into the active form IL-1β. However, that effect was compensated when applying LPS as a PAMP together with nigericine, a potassium ionophore that induces K^+ release from the cytoplasm to the extracellular environment. Therefore, both the Ca^{2+} uptake following P2X7R activation, and K^+ depletion seem to be mechanisms that can act independently to induce the assembly of NLRP3 inflammasome.

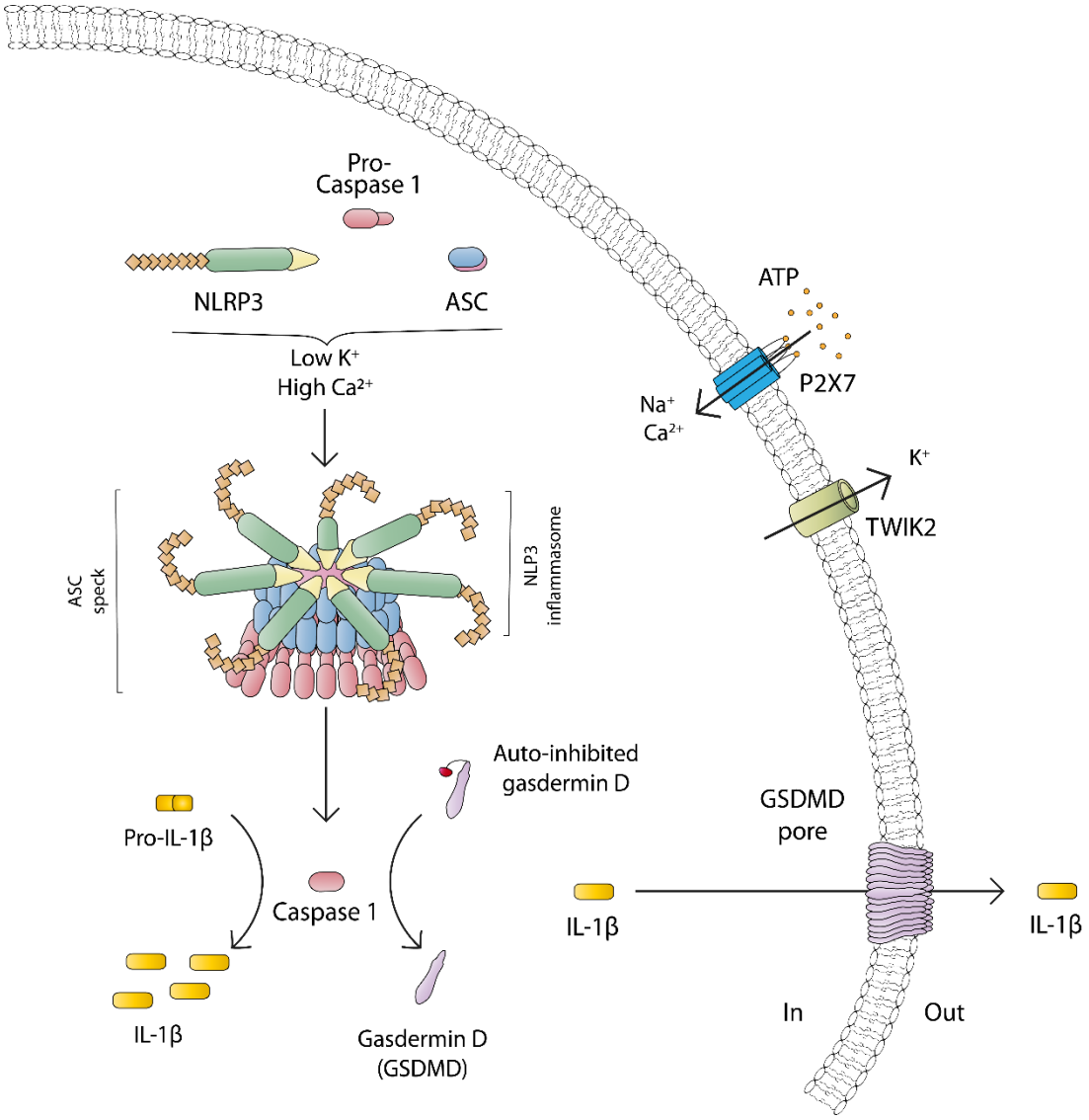

Figure 4: NLRP3 inflammasome assembly and release of IL-1β upon P2X7 activation by extracellular ATP *(Guo et al., 2015; Giuliani et al., 2017). K^+ depletion and Ca^{2+} increase resulting from ATP-mediated P2X7R activation induces recruitment and assembly of the NLRP3 inflammasome, leading to breakdown of pro-caspase 1 into its active form, which in turn generates IL-1β and GSMD. This allows the formation of the GSDMD pore and IL-1β release.*

1.2.2.2 Dual roles in cell death and growth

A dual role has been proposed for P2X7R in cell survival and death. Studies have suggested that the promotion of either one of these processes depends on the activation levels of this receptor (Adinolfi et al., 2005; Orioli et al., 2017). On the one hand, basal or low activation of P2X7 leads to changes in cell shape, growth and protective, trophic activity. On the other hand, high activation levels or prolonged stimulation of the receptor leads to cytotoxic activity that results in cell death.

P2X7R is involved in processes related to cell migration, survival and cell proliferation. Heterologous expression in P2X7R-lacking cells such as human embryonic kidney cells (HEK293) (Amoroso et al., 2012) and lymphoid cells that do not express this receptor (Baricordi et al., 1999) showed that, in absence of serum or low glucose conditions, P2X7

induces an increase of lactate production and activation of the Akt/HIFα axis in an autocrine/paracrine feedback loop that reprograms the cell metabolism as a way to meet the needs and allow cell survival. In human T lymphocytes, P2X7R shows mitogenic activity that can be reversed by the P2X7R antagonist oxidized ATP (oATP) (Baricordi et al., 1996). In microglia, P2X7R is involved in cell migration and proliferation (Bianco et al., 2006), an effect seen even when P2X7R is not activated, but only overexpressed (Monif et al., 2009). Also, P2X7R was shown to allow cell growth as reported in cancer cell lines CT26 (Adinolfi et al., 2012) and C6 (Wei et al., 2008). The induction of tumor growth was also reported for trimers of co-assembled P2X7B and P2X7A variants (Adinolfi et al., 2010). This effect was reversed by blockade of the receptor with antagonists that down-regulated the Akt/HIFα axis mentioned earlier (Amoroso et al., 2015).

However, P2X7R activation has been mainly linked to processes related to cell death, including pyroptosis, autophagy, necrosis, and apoptosis. As previously mentioned, prolonged stimulation of P2X7R induces pore formation that allows the passage of larger molecules. This may lead to depletion of intracellular ions and metabolites that are crucial for cell survival (Ferrari et al., 1997). In the dystrophic muscle, the opening of the macropore and cell death are linked to autophagy in myoblasts, but apoptosis in macrophages (Young et al., 2015). Phosphatidylserine (PS) flip, cytokine shedding and membrane blebbing are characteristic features of apoptotic processes mediated by P2X7R. It has been proposed that these and other processes induced by P2X7R activation such as Ca^{2+} increase in cytoplasm and mitochondria, cytoskeletal rearrangement and mitochondrial swelling are reversible processes that only lead to irreversible apoptosis once cytochrome-c is released from the mitochondria, which requires the Rho-associated protein kinase (ROCK) pathway to take place in parallel (Mackenzie et al., 2005). Upon priming with LPS, P2X7R cytotoxic effects are potentiated (Di Virgilio et al., 2023). Other studies on cell death induced by P2X7R activation showed certain pathways leading to cell death that are unrelated to IL-1β synthesis and release, in line with the reported cell death involving the SAPK/JNK pathway independently from caspase-1 (Humphreys, 2000; le Feuvre et al., 2002; Verhoef et al., 2003).

1.2.3 Localization of P2X7R

P2X7Rs are found widespread throughout vertebrate organisms. They are highly expressed in many immune cells, and also in cells of the nervous system. Controversy exists around this topic, as P2X7R expression in cell types such as neutrophils has been accepted although certain studies have shown the contrary (Karmakar et al., 2016; Martel-Gallegos et al., 2010; Suh et al., 2001). Existence of neuronal P2X7R is also widely accepted in the purinergic signaling field, although it has been challenging to demonstrate in biochemical or functional studies due to the lack of efficient antibodies and the low specificity of the available ligands (Kaczmarek-Hájek et al., 2018). Thus, the presence of P2X7 protein in neurons is still a subject of debate, with reports against and in favor of such localization (Illes et al., 2017; Teresa Miras-Portugal et al., 2017). Table 1 summarizes cell types in which P2X7 expression has been reported.

Cell type	References
Macrophages	(Bartlett et al., 2014; Jacob et al., 2013; Monif et al., 2009; Savio et al., 2018; Wewers & Sarkar, 2009)
Dendritic Cells (DCs)	(Bartlett et al., 2014; Mutini et al., 1999)
Lymphocytes T and B	(Adinolfi, Giuliani, de Marchi, et al., 2018; Yip et al., 2009)
Monocytes	(Bartlett et al., 2014; Lenertz et al., 2011; Savio et al., 2018)
Mast cells	(Idzko et al., 2014; Jiang et al., 2020; Monif et al., 2009; Savio et al., 2018)
Neutrophils	(Karmakar et al., 2016; Suh et al., 2001) (see Martel-Gallegos et al., 2010)
Eosinophils	(Ferrari, la Sala, et al., 2006; Mohanty et al., 2001; Müller et al., 2011)
Osteoblasts/Osteoclasts	(Bartlett et al., 2014; Lenertz et al., 2011)
Fibroblasts	(Bartlett et al., 2014; Morandini et al., 2014; Schilling et al., 1999)
Epithelial cells	(Bartlett et al., 2014; Morandini et al., 2014)
Endothelial cells	(Bartlett et al., 2014; Morandini et al., 2014; Wilson et al., 2007)
Salivary glands	(Morandini et al., 2014; Tenneti et al., 1998)
Pancreatic exocrine glands	(Morandini et al., 2014; Novak, 2008)
Neural Progenitor Cells (NPCs)	(Delarasse et al., 2009; Kanellopoulos & Delarasse, 2019; Messemer et al., 2013)
Microglia	(Bartlett et al., 2014; Cisneros-Mejorado et al., 2020; Idzko et al., 2014; Jacob et al., 2013; Jiang et al., 2021; Lenertz et al., 2011; Monif et al., 2009)
Oligodendrocytes	(Bartlett et al., 2014; Cisneros-Mejorado et al., 2020; Jiang et al., 2021)
Astrocytes	(Bartlett et al., 2014; Cisneros-Mejorado et al., 2020; Lenertz et al., 2011)
Neurons	(Teresa Miras-Portugal et al., 2017) (see Illes et al., 2017)

Table 1: Cell lines in which P2X7 localization has been reported

1.2.4 Pathophysiological roles of P2X7R

Taking into account the P2X7R functions and the cell types that show P2X7R expression, it has been taken as a potential drug target in several health conditions that range from infectious diseases to neurodegenerative disorders, cancer and cardiovascular or respiratory conditions, to name a few (Burnstock & Knight, 2018; Fuller et al., 2009; Sperlágh & Illes, 2014).

From the genetic perspective, *P2rx7* polymorphisms have been involved in mood disorders, as well as in the susceptibility and resistance to parasite invasion and infections provoked by intracellular pathogens (Fuller et al., 2009; Miller et al., 2011; Savio et al., 2018).

In immune cells, P2X7R is involved in pathological processes. ATP is released due to activation of antigen presenting cells (APCs) during processes of allograft rejection and subsequent graft versus host disease leading to systemic inflammation and life threat. In this regard, it has been suggested that P2X7R blockade might reduce the exacerbated immune response improving the patients' prognosis (Wilhelm et al., 2010). Similarly to its previously discussed role in cell death and survival, P2X7R is linked to either protection or susceptibility to infection depending on the severity of the pathogen's virulence. This dual involvement has been discussed in tuberculosis (Savio et al., 2018; Wirsching et al., 2020), while P2X7R has proved to be protective against other bacterial pathogens such as chlamydia and mycobacteria (Biswas et al., 2008; Darville et al., 2007; Morandini et al., 2014).

In the central nervous system, P2X7R activation and its role in neuroinflammation takes part in numerous pathologies. While its blockade has beneficial effects against glioblastoma progression (Delarasse et al., 2011; Drill et al., 2020), it showed again a dual neuroprotective and neurocytotoxic activity upon mild and severe cerebrovascular disease (CVD), respectively (Cisneros-Mejorado et al., 2020). Furthermore, P2X7R involvement in mood disorders (Deussing & Arzt, 2018; Ribeiro et al., 2019) and neurodegenerative diseases has been under extensive study during the recent years. The role of this receptor has been investigated in epilepsy (Conte et al., 2021; Doná et al., 2009; Engel et al., 2012), multiple and lateral amyotrophic scleroses (Bartlett et al., 2017; Ruiz-Ruiz, Calzaferri, et al., 2020; Ruiz-Ruiz, García-Magro, et al., 2020), Alzheimer's disease (Francistiová et al., 2020), schizophrenia (Calovi et al., 2020), and others (Calzaferri et al., 2020; Jimenez-Mateos et al., 2019). Therefore, it is considered as a potential therapeutic target (Calzaferri et al., 2021; Á. Sebastián-Serrano et al., 2019).

1.3 The BAC transgenic approach

Bacterial Artificial Chromosome (BAC) transgenic mice have been proved to represent powerful tools in basic and preclinical research since this technology was first developed (Yang et al., 1997) and applied to genetically modify laboratory mice. It has been widely

used because it allows the insertion of full genes along with their regulatory elements permanently into a mouse line. Taking advantage of this, the functions of an individual gene as well as the localization of a protein can be tested *in vivo*, *e.g.* by the use of appropriate reporter tags (Heintz, 2001; Kasatkina & Verkhusha, 2022; Roguev & Krogan, 2008).

This technology has been developed and used for multiple purposes and proved useful in the research on epithelial tissue (Kanayama et al., 2019; Birbach et al., 2009), and the immune system (Sparwasser & Eberl, 2007), among others. BAC transgenic mice expressing reporter genes are found in multiple studies *e.g.* AmCyan or GFP (Schmöle et al., 2015; Tsuda et al., 2017). In the CNS, this tool has allowed the visualization of protein targets in localization studies from specific cell types or regions of the brain, such as the spiny neurons or basal ganglia, as well as full expression patterns over the whole cerebrum (Shuen et al., 2008; Xu et al., 2016; Yang & Gong, 2005).

The proven utility of the BAC transgenic approach led to the creation of large scale projects such as the GENSAT project (http://www.gensat.org), which aimed to a) develop a database of BAC transgenic clones that include genes encoding EGFP-tagged versions of proteins that are expressed in the CNS; and b) to analyze the expression patterns of these proteins throughout the brain (Gong et al., 2010). The project was carried out in order to create a mouse brain atlas with images of region and cell specific expression for specific proteins, aiding in the research regarding their function in cell and tissue development (Gong et al., 2003; Zoghbi, 2003). The BAC transgenic mouse lines developed within this project have been used and reported in the literature using tissue-specific (Gerfen et al., 2013) as well as cell-specific (Srinivasan et al., 2016) approaches to analyze the distribution and functions of protein targets of study.

As part of the GENSAT project, a BAC transgenic mouse line (Tg(*P2rx7*-EGFP)FY174Gsat) is available and expresses a soluble EGFP protein under the control of the endogenous *P2rx7* promoter. The BAC clone was designed by insertion of the EGFP coding sequence inside exon 1 of the *P2rx7* gene with a stop codon and a polyadenylation site (pA) that was used to prevent additional overexpression of the P2X7 receptor (Figure 5A). Initial characterization of this model revealed EGFP localization in glia-like cells throughout the brain as well as neuronal expression. This mouse model has been described and used by several laboratories (Jimenez-Pacheco et al., 2013; Ortega et al., 2021).

In our laboratory, a BAC transgenic mouse model was created (Tg(RP24-114E20P2X7451P-StrepHis-EGFP)Ani) which expresses EGFP fused to P2X7 via a Strep-tag and a His-tag under the control of the endogenous *P2rx7* promoter (Figure 5B). Therefore, this mouse model shows an overexpression of P2X7 that overlaps with that of the wildtype mouse brain (Kaczmarek-Hájek et al., 2018). However, characterization of this model revealed no expression of P2X7-EGFP in neurons, but rather in microglia, oligodendrocytes and Bergmann glia, as well as a sparse distribution in astrocytes, unlike the GENSAT mouse model. Comparison of this model with the available

data from the GenSat mouse indicated differences in P2X7R localization in both models. However, a careful characterization of the GenSat mouse has not been performed.

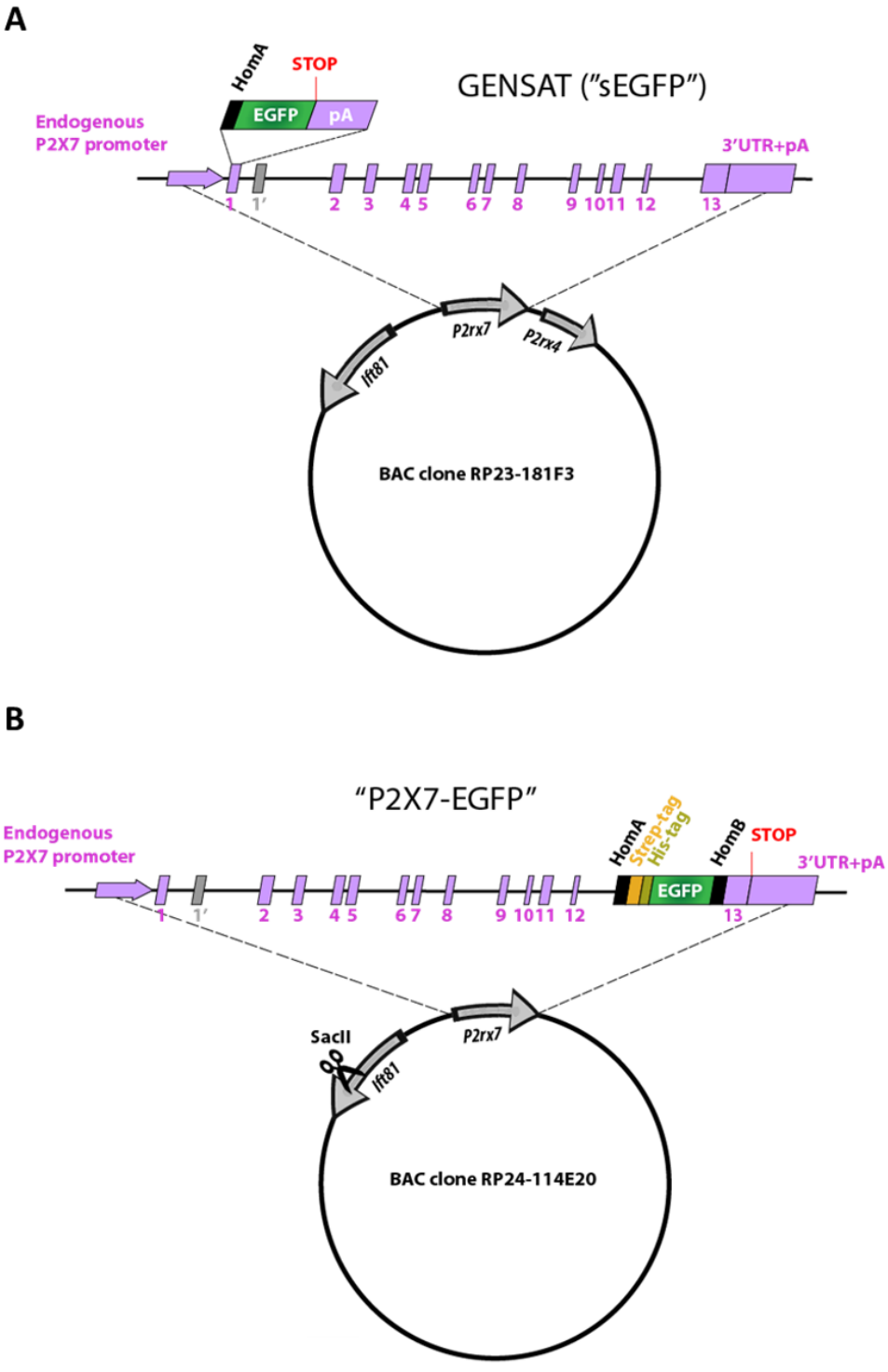

Figure 5: Schematic representation of the constructs used for the design of the reporter BAC transgenic mouse models used in this study. *In both cases, the gene Ift81 encoding for the intraflagellar transport protein 81 (IFT81) is inserted as a passenger gene. (A) The GENSAT P2X7 mouse line was designed by integration of the sEGFP squence (including the polyadenylation signal) at the start ATG codon of P2rx7 gene's exon 1. In this case, P2rx4 was also inserted as a passenger gene. (B) the P2X7-EGFP mouse model was designed by insertion of the Strep-His linker tags immediately upstream of the stop TGA codon of exon 13. Here, the Ift81 was erased by SacII linearization.*

1.4 P2X4R – interaction with P2X7R?

P2X4 is the member of the P2X family that shares the highest similarity with P2X7 (47% amino acid identity in humans). The *P2rx7* and *P2rx4* genes are located on the same chromosome in mice, rats and humans (Kopp et al., 2019; Saul et al., 2013). They also share a similar distribution, as P2X4R is present in immune cells, epithelial cells and cells from the nervous system such as microglia but also in neurons (Bowler et al., 2003; Illes et al., 2020; Ma et al., 2006; Xiang & Burnstock, 2005). However, P2X4R subcellular localization has been shown as predominantly lysosomal (Qureshi et al., 2007), where P2X4R might regulate lysosome Ca^{2+} trafficking and membrane events (Cao et al., 2015; Murrell-Lagnado, 2018). P2X4R is involved in processes related to release of pro-inflammatory cytokines, autophagy, and neurological disorders, like P2X7R. P2X4R is also involved in cardiac function and alcohol effects (Suurväli et al., 2017).

Heteromeric assembly of P2X4R with other P2XR isoforms has been reported *e.g.* with P2X6R (Lê et al., 1998). However, co-assembly with P2XR7 (Figure 6A) has been challenging to demonstrate *in vivo* and has been a subject of debate (Guo et al., 2007; Nicke, 2008). The question was raised first for P2XRs of airway ciliated cells, described as complexes that contain at least one P2X4 subunit, although characteristics of these resulted similar to those of P2X7R channels. Therefore, an interaction between P2X4 and P2X7 subunits, or a modulation of cilia P2X4R complexes by P2X7R, was suggested (Ma et al., 2006). This is in line with the findings of suggested heterotrimers in bone marrow-derived macrophages and HEK293 cells (Guo et al., 2007). Other studies point at a close interaction of P2X7R and P2X4R homotrimers (Figure 6B) rather than the heteromeric assembly (Antonio et al., 2011; Boumechache et al., 2009). These possibilities were also proposed after FRET analyses of heterologously expressed receptors in *Xenopus laevis* oocytes (Schneider et al., 2017) and HEK293 cells (Pérez-Flores et al., 2015).

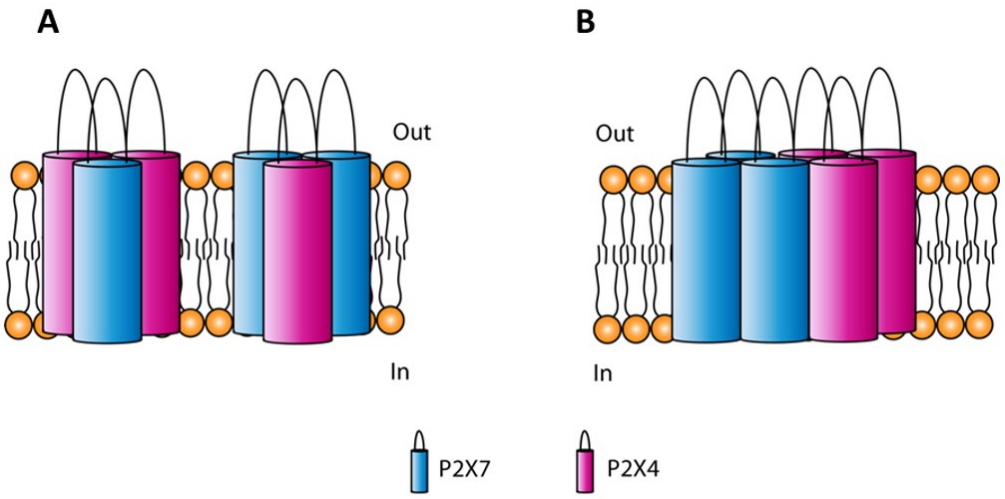

Figure 6: Representation of the models for P2X4/P2X7 interaction *as (A) heterotrimers and (B) interacting homotrimers. Note that the N and C-termini have been removed for simplification.*

Furthermore, a functional interrelation between P2X4R and P2X7R has been postulated. For example, P2X7R-induced macropore formation was reported to be negatively affected by P2X4R in HEK293 cells, but positively affected in murine macrophages (Casas-Pruneda et al., 2009; Kawano et al., 2012). It has also been discussed how silencing one of the *P2rx* genes induces an increase of the other as a compensatory effect (Weinhold et al., 2010).

1.5 Aim of the study

P2X7R localization and functions have been extensively studied through the last years. However, most of the available data that exists today are either inconclusive or only applicable *in vitro* or for heterologous expression systems due to the lack of reliable animal models and specific antibodies and ligands (Anderson & Nedergaard, 2006; Kopp et al., 2019). Therefore, involvement of P2X7R in health and disease remains under discussion because of the insufficient information about interactions and signaling pathways that are triggered or mediated by P2X7R. Through this project we focused on three aims:

- Comparison of the BAC transgenic mouse models that are available in our laboratory: As pointed out, previous reports mentioned region-specific and cell-specific distribution of the EGFP reporter that were divergent when comparing both models (Kaczmarek-Hájek et al., 2018). We aimed to provide a more detailed characterization and comparison of both mouse lines that will be useful for future research in the field.
- Investigation of the P2X4/P2X7 interaction: Heteromeric assembly of P2XRs has been shown for different isoforms, but evidence of functional interaction or interrelation between P2X4 and P2X7 receptors *in vivo* is lacking (Guo et al., 2007; Nicke, 2008). The recently generated P2X7-EGFP mouse model has been used in this project with the aim of studying the reported physical interaction or functional interrelation of P2X4 and P2X7 receptors, comparing it with heterologous expression systems that have been used in the past such as *X. laevis* oocytes and HEK293 cells (Pérez-flores et al., 2015; Schneider et al., 2017).
- Implementation of a proteomic approach to study P2X7R signaling pathways: As discussed, P2X7R involvement in health and disease has been studied, although the specific molecular mechanisms that govern P2X7R signaling pathways are not completely understood. Quantitative proteomics is a powerful tool in the investigation of cell signaling. It allows precise measurement of intermediaries from a signaling network under different genotypical backgrounds or under the environment of cells that respond to a certain stimulus (Woo et al., 2017). The last objective of this project was to develop a strategy to study general protein expression patterns in mice under different levels of P2X7 expression. We used our BAC transgenic P2X7-EGFP mouse model and compared it with the wildtype mouse and a *P2rx7*$^{-/-}$ mouse as a knockout model, in search for known or postulated P2X7R signaling intermediaries and aiming at the discovery of new ones. For this, we counted on the collaboration of Dr. Thomas

Fröhlich at the Gene Centre (Munich), who gave advice and performed the needed liquid chromatography coupled to mass spectrometry (LC-MS) experiments and statistical analysis.

2. Materials and Methods

2.1 Materials

2.1.1 Mouse models

Mouse line	Information	References
Tg(*P2rx7*-EGFP)FY174Gsat	sEGFP reporter, FVB/N background Males and females	(Gong et al., 2003; Jimenez-Pacheco et al., 2013; Ortega et al., 2021)
Tg(RP24-114E20P2X7451P-StrepHis-EGFP)17Ani	P2X7-EGFP reporter FVB/N and C57BL/6 backgrounds Males and females	(Kaczmarek-Hájek et al., 2018)
P2rx7$^{tmid(EUCOMM)Wtsi}$	*P2rx7*$^{-/-}$ C57BL/6 background Males and females	European Mutant Mouse Archive
P2rx4^{tm1Rass}	*P2rx4*$^{-/-}$	(Sim et al., 2006)

Table 2: Mouse lines used in this study.

2.1.2 Chemicals

Item	Manufacturer
Isoflurane (IsoFlo®)	Abbot
Precision Plus Protein™ All Blue Standards	Bio-Rad
n-dodecyl-β-D-maltoside	Calbiochem
4',6-diamidino-2-phenylindole (DAPI)	Carl Roth
Ampicilin	Carl Roth
Gentamicine	Carl Roth
Haematoxylin	Carl Roth
Kaiser's glycerol gelatine phenol-free	Carl Roth
Roti®-GelStain	Carl Roth
Tween® 20	Carl Roth
GFP-Trap®_A	Chromotek

Xylazine (Xylariem®)	Ecuphar N.V.
PefaBlock	Fluka
Ketamine	Medistar
Immobilon®-FL PVDF membrane	Merck
CD11b (Microglia) MicroBeads	Miltenyi Biotec
Gel Loading Dye Purple (6X)	New England Biolabs
Quick-Load® Purple 2-Log DNA Ladder	New England Biolabs
Dpn I enzyme	New England Biolabs
Bgl II enzyme	New England Biolabs
c0mplete™ EDTA-free Protease Inhibitor Cocktail	Roche
LightCycler® 480 multiwell plate 96	Roche
Tissue-Tek® O.C.T.™ compound	Sakura
Collagenase type IIa	Serva
Digitonin	Sigma-Aldrich
Low melting point agarose	Sigma-Aldrich
Nonidet™ P-40 (NP-40)	Sigma-Aldrich
Penicillin-Streptomycin (100x)	Sigma-Aldrich
SigmaFast™ DAB tablets	Sigma-Aldrich
Triton X-100	Sigma-Aldrich
Trypsin EDTA solution	Sigma-Aldrich
Fetal bovine serum	Thermo Fisher
Goat serum	Thermo Fisher
L-Glutamine	Thermo Fisher
Dulbecco's Modified Eagle's Medium (DMEM)	Thermo Fisher
DPBS	Thermo Fisher
PermaFluor™ mounting medium	Thermo Fisher

Table 3: Chemicals *used for the experiments described in the Methods section, including the manufacturer that provided them.*

2.1.3 Commercial kits

Item	Manufacturer
NucleoSpin® gel and PCR clean-up kit	Macherey-Nagel

Adult Brain Dissociation Kit, mouse and rat	Miltenyi Biotec
Gibson Assembly® master mix	New England Biolabs
iST-NHS kit	PreOmics
RNeasy plus mini kit	Qiagen
LightCycler 480 SYBR green I master	Roche
Random primed labeling kit	Roche
SapphireAmp® fast PCR master mix	Takara Clontech
mMESSAGE mMACHINE® T7/SP6 transcription kit	Thermo Fisher
ABC Vectastain® kit	Vectorlabs
Plasmid miniprep kit I peqGold	VWR Peqlab

Table 4: Commercial kits *used in this study and manufacturers that provided them. For further details, refer to the Methods section.*

2.1.4 Solutions and buffers

Solution	Composition
Homogenization buffer	0.1 M sodium phosphate buffer, pH 8.0 0.4 mM Pefablock® SC cOmplete™, EDTA-free (1 tablet/15 ml)
Extraction buffer	Homogenization buffer + 1% (v/v) NP40, 0.5 n-dodecyl-β-D-maltoside or 1% digitonin
Pull-down washing buffer	Extraction buffer + 500 mM NaCl
Pull-down elution buffer	0.2 M glycine pH 2.5
SDS sample buffer (5x)	0.3 M Tris/HCL; pH 6.8 5% (w/v) SDS 50% (v/v) glycerol 0.1% bromphenol blue
SDS-PAGE running buffer	25 mM Tris; 192 mM glycine 0.1% SDS
4x Stacking gel buffer	0.4% (w/v) SDS; 0.5M Tris-HCL, pH 6.8
4x Separation gel buffer	0.4% (w/v) SDS; 1.5M Tris-HCL, pH 8.8
Western blot transfer buffer (10x)	250 mM Tris; 1.92 M Glycin 7 mM SDS
Western blot transfer buffer (1x)	10% v/v Western blot transfer buffer (10x); 20% v/v Methanol
Odyssey® blocking buffer (TBS)	Supplied by LI-COR Biosciences

Western blot blocking buffer	50% (v/v) Odyssey® blocking buffer (TBS) 50% (v/v) TBS
TBS (10x)	1.4 M NaCl; 200 mM Tris/HCl, pH 7.4
TBS-T	TBS + 0.1% (v/v) Tween-20
SOC medium	2% (w/v) tryptone; 0.5% (w/v) yeast extract; 10 mM NaCl; 2.5 mM KCl; 10 mM $MgCl_2$; 10 mM $MgSO_4$; 20 mM glucose
TAE buffer	40 mM Tris; 20 mM Acetic acid; 1 mM EDTA
ND96 Ringer's solution	96 mM NaCl; 2 mM KCl; 1 mM $MgCl_2$; 1 mM $CaCl_2$; 5 mM HEPES, pH 7.4
PBS	137 mM NaCl; 27 mM KCl; 10 mM Na_2HPO_4; 1.8 mM KH_2PO_4, pH 7.4
PB Buffer	DPBS supplemented with 0.5% FBS
Immunostaining blocking solution	PBS supplemented with 0.2% Triton X-100 and 5% goat serum
Immunostaining blocking solution (adherent cells)	PBS supplemented with 4% bovine serum albumin and 4% goat serum

Table 5: Composition of solutions and buffers *used for the experiments described in the Methods section, as well as their detailed composition.*

2.1.5 Antibodies

Primary Antibody	Supplier	Identifier	Dilution
GFP rb pAb	Abcam	ab6556, AB_305564	IF 1:2000 DAB 1:5000
MBP rb pAb	Abcam	Ab40390, AB_1141521	IF 1:500
P2X4 rb pAb	Alomone	APR-002, AB_2040058	WB 1:1000 IF 1:200
GFP rat 3H9	Chromotek	3h9-100, AB_10773374	WB 1:1000
Olig2 ms 211F1.1	Millipore	MABN50, AB_10807410	IF 1:200
GFAP ms GA5	Millipore	MAB360, AB_11212597	IF 1:200
NeuN ms A60	Millipore	MAB377, AB_2298772	IF 1:500
NG2 rb pAb	Millipore	AB5320, AB_91789	IF 1:400
P2X7 ECD 7E2-rbIgG	Nolte lab (Kaczmarek-Hájek et al., 2018)	Nanobody rbIgG fusion construct	IF 0.1 µg/mL DAB 6.7 ng/mL
Lamp1 rat 1D4B	Santa Cruz Biotechnology	sc19992, AB_2134495	IF 1:200
Calbindin D28k (ms CB-955)	Sigma-Aldrich	C9848, AB_476894	IF 1:1000

Vinculin ms hVin-1	Sigma-Aldrich	V9131, AB_477629	WB 1:10000
P2X7 C-term (rb pAb)	Synaptic Systems	177003, AB_887755	WB 1:1500
Parvalbumin (ms 58E1)	Synaptic Systems	195011, AB_2619882	IF 1:500
Calretinin (ms 37C9)	Synaptic Systems	214111, AB_2619904	IF 1:200
ZnT3 (ms 180C1)	Synaptic Systems	197011, AB_2189665	IF 1:100
GFP (chk pAb)	Thermo Fisher	CA10262, AB_2534023	IF 1:400
Iba1 (rb pAb)	WAKO	019-19741, AB_839504	IF 1:100

Table 6: Primary antibodies *used in this study, including supplier, reference numbers and dilution.*

Secondary Antibody	Supplier	Identifier	Dilution
Cy5 gt anti-rb	Abcam	ab97077, AB_10679461	IF 1:400
800CW gt anti-ms	LI-COR	925-32210, AB_2687825	WB 1:15000
800CW gt anti-rb	LI-COR	926-32211, AB_621843	WB 1:15000
680RD dk anti-rb	LI-COR	925-68073, AB_2716687	WB 1:15000
680RD gt anti-rat	LI-COR	925-68076, AB_10956590	WB 1:15000
A488 gt anti-rb	Thermo Fisher	A11008, AB_143165	IF 1:400
A488 gt anti-chk	Thermo Fisher	A11039, AB_2534096	IF 1:400
A555 gt anti-rat	Thermo Fisher	A21434, AB_2535855	IF 1:400
A594 gt anti-ms	Thermo Fisher	A11032, AB_2534091	IF 1:400
A594 gt anti-rat	Thermo Fisher	A11007, AB_10561522	IF 1:400
A594 gt anti-rb	Thermo Fisher	A11037, AB_2534095	IF 1:400

Table 7: Secondary antibodies *used for this project, including the suppliers, reference numbers and dilutions.*

2.1.6 Equipment

Item	Manufacturer
Precellys® 24 homogenizer	Bertin Instruments
Mini Trans-Blot® cell	Bio-Rad
Nanoject II	Drummond Scientific
Typhoon™ Trio	GE Healthcare
CM1900 Cryostat	Leica
VT1200s	Leica
Odyssey® FC imaging system	LI-COR
GentleMACS™ Octo Dissociator with Heaters	Miltenyi Biotec
MACS® separator	Miltenyi Biotec
LightCycler® 480 system	Roche
NanoDrop™ 2000c	Thermo Fisher Scientific
Ultimate™ 3000 nano-LC	Thermo Fisher Scientific
Q-Exactive™ HF mass spectrometer	Thermo Fisher Scientific
Axio Imager M2	Zeiss

Table 8: Special Equipment *and manufacturers that provided them.*

2.2 Methods

2.2.1 Animal breeding

Mice were kept at the Walther Straub Institute of Pharmacology and Toxicology in Munich under standard conditions (water and food *ad libitum*, 12 h cycle light/dark, 22ºC). The mouse breeding conditions, handling and experimental procedures were carried out according to the German guidelines and approved by the government of Upper Bavaria (transcardial perfusion 55.2-1-54-2532-59-2016 and 55.2-2532.Vet_02-20-147). At weaning (3-4 weeks of age), ear punch biopsies were taken and used for genotyping.

2.2.2 Molecular biology

2.2.2.1 Nucleic acid preparation

2.2.2.1.1 Preparation of Plasmid DNA

Transformed *E. coli*, containing the desired DNA sequences subcloned in either the pNKS2 oocyte expression vector or the pcDNA 3.1 mammalian expression vector (for *X.*

laevis oocytes and HEK293 cells, respectively), were provided by my colleagues Anna Durner and Dr. Robin Kopp. *E. coli* cultures were grown overnight in SOC medium with 100 µg/mL ampicillin. *E. coli* cells were pelleted by centrifugation and the Plasmid mini-prep kit I peqGold was used to extract plasmid DNA according to the instructions of the manufacturer. The amount of DNA was quantified using a NanoDrop™ 2000c UV-Vis spectrophotometer.

2.2.2.1.2 cRNA synthesis

10 µg of plasmid DNA were linearized via digestion with 2 µL of the restriction enzyme for 2 hours at 37ºC. After verification of linearization via agarose electrophoresis, the DNA was purified with the Qiagen cleanup kit and cRNA was synthesized with the mMESSAGE mMACHINE® T7/SP6 transcription kit following the instructions of the manufacturer. Finally, the cRNA amount was quantified using the NanoDrop™ 2000c UV-Vis spectrophotometer and stored at -80ºC until usage.

2.2.2.2 Methods in Protein Biochemistry

2.2.2.2.1 Mouse euthanasia and tissue removal

Mice were euthanized by exposure to isoflurane followed by cervical dislocation. Organs of interest were removed quickly and snap-frozen in liquid nitrogen if not used immediately. Samples were kept at -80ºC for long-term storage until usage.

2.2.2.2.2 Protein extraction from mouse tissue

All the steps were carried out at 4ºC or on ice. Approximately 150 µg of mouse tissue were transferred to reinforced tubes containing 600 µL of homogenization buffer and homogenized using a Precellys® 24 homogenizer and 2.8 mm ceramic beads. Cell extracts were centrifuged at 1000 g for 10 minutes. The supernatants were collected, transferred to fresh tubes, and centrifuged at 21000 g for 45-60 minutes. The pellets were resuspended in 300 µL of extraction buffer in order to solubilize the membrane fraction. Lastly, a final centrifugation step of 15 minutes at 21000 g led to supernatants containing the crude membrane protein extracts.

2.2.2.2.3 Protein extraction from X. laevis oocytes

X. laevis females were kept at the Core Facility for Animal Models (CAM) at the Biomedical Center in Munich. Ovarian lobes were extracted and provided to our laboratory the day after the surgery. Lobes were torn in small pieces and incubated for approximately 100-180 minutes under gentle shaking at 16ºC in ND96 containing gentamicine and collagenase type IIA. Next, the single oocytes were incubated in Ca^{2+}-free Ringer's solution to remove follicular cells. These oocytes were transferred to ND96 solution supplemented with gentamicine (500 µL/mL) and selected for injection. Glass capillaries were transformed into needles by a micropipette puller and filled with RNAse free mineral oil

and the cRNA of interest. Using a Nanoject II injector, 25 ng of cRNA were injected at the interface between the animal and vegetal poles of each oocyte.

Two days post injection of cRNA and incubation of the oocytes at 16ºC in ND26 solution supplemented with gentamicine, 6-10 oocytes were homogenized by pippetting up and down with extraction buffer (~20 µL per oocyte). After 15 minutes of incubation on ice, crude membrane protein extracts were obtained by two subsequent centrifugation steps for 15 minutes at 4ºC and 15000 g, keeping the supernatant in both cases.

2.2.2.2.4 Protein extraction from HEK293 cells

All the steps were done either at 4ºC or on ice. Cells were detached from 6-well plates by repeated pipette flushing with 1 mL of sodium phosphate solution. After pelleting the cells by a five-minute centrifugation at 200 g, membranes were solubilized by mixing with an appropriate amount of extraction buffer (containing 0.5% n-dodecyl-β-D-maltoside). Samples were incubated for fifteen minutes and subsequently centrifuged at 21000 g for 10 minutes in order to get the crude membrane protein extracts in the supernatants.

2.2.2.2.5 Immunoprecipitation of GFP-tagged proteins

All the steps were performed on ice or in a refrigerated centrifuge (4ºC). 10-30 µL of GFP-trap slurry beads were washed per sample with 500 µL of pull-down washing buffer three times by 1 minute centrifugation at 1000 g, discarding the supernatant. Finally, 50 µL of pull-down washing buffer was added to the beads before the crude membrane protein extracts (~300 µL) were mixed with them and incubated for one hour at 4ºC on an end-over-end rotator. The mixture of proteins and beads was washed three times as described before. The pellets were finally suspended in 50 µL of pull-down elution buffer (pH 2.5) and incubated for 2 minutes with gentle shaking. The beads were spun down and the supernatants (containing EGFP-tagged protein complexes) were transferred to 5 µL of the pull-down Tris solution (pH 10.5).

2.2.2.2.6 SDS-Polyacrylamide Gel Electrophoresis (PAGE) and Western Blot analysis

A total of 30-50 µg of protein samples were incubated in 5x SDS sample buffer for 10 minutes at 40ºC prior to loading them onto the 8%-12% polyacrylamide gel. Proteins were separated according to their molecular weight applying 100 V through the stacking gel and increasing the voltage to 120-130 V for the separation gel. A fluorescence Typhoon™ Trio scanner was used to detect proteins containing EGFP. Proteins were transferred to methanol-activated polyvinylidene difluoride (PVDF) membranes in a tank blot system by applying a constant current of 20 mA at 4ºC overnight (16 hours). From this point, all the steps were carried out with gentle shaking. The membranes were blocked using the western blot blocking buffer for one hour at room temperature and subsequently incubated with the primary antibodies diluted in western blot blocking buffer overnight at 4ºC. After washing the membrane three times for 5 minutes with TBS-T, fluorescent-conjugated secondary antibodies were diluted in TBS-T and incubated on the membranes for one hour at room temperature. Finally, the membranes were washed three

times for 5 minutes with TBS-T and transferred to TBS before visualization on an Odyssey® Fc imaging system.

2.2.2.3 Immunohistochemistry

2.2.2.3.1 Mouse euthanasia and tissue removal

Mice were euthanized by injection of xylazine/ketamine/heparin and transcardially perfused with phosphate buffered saline (PBS, pH 7.4) followed by 4% paraformaldehyde (PFA) in PBS. Brains were removed and post-fixed using 4% PFA/PBS at 4ºC overnight. Brains were cryoprotected in 30 % sucrose/PBS solution for 72 hours at 4ºC.

2.2.2.3.2 Free-floating immunofluorescence staining

Brains were embedded in Tissue-Tek® OCT compound using plastic cryomolds and stored at -20ºC. Sections of 40 µm from the frozen brains were cut in sagittal projection using a CM1900 cryostat, placed in a solution containing 0.04% sodium azide/PBS and stored at 4ºC until usage. From this point, all the steps were performed while gently shaking the samples, unless specified. Slices were washed three times in PBS and blocked using the free-floating immunostaining blocking solution for two hours at room temperature. The blocked sections were incubated with primary antibodies overnight (12-24 hours) at 4ºC. The next day, slices were washed three times for five minutes with PBS and subsequently incubated with the secondary antibodies for two hours at room temperature and protected from the light. After additional washing with PBS three times for 5 minutes, 1 µg/mL DAPI solution was applied to the slices for 60-90 seconds at room temperature without shaking. After washing two times with PBS for 5 minutes, shaking was stopped, and the slices were placed onto glass slides and dried at room temperature for 20-60 minutes protected from the light. Samples were mounted using PermaFluor™ mounting medium and covered with cover slips. Samples were stored at 4ºC in the dark until visualization.

2.2.2.3.3 Diaminobenzidine (DAB) immunostaining

Brains were embedded in 5% low melting temperature agarose/PBS compound using 6 well plates as molds. The brains were protected with parafilm and aluminum foil and incubated for one hour at room temperature. Once the low melting temperature agarose solution was solid, blocks containing the brains were extracted from the wells and sections of 30 µm were cut in sagittal projection using a VT1200s vibrating microtome using 0.40 mm aplitude and 0.18 mm/s speed. The slices were placed in a solution containing 0.04% sodium azide/PBS and stored at 4ºC until usage. From this point, all the steps were performed while gently shaking the samples and at room temperature, unless specified. Slices were peroxidase blocked with 1% H_2O_2/PBS for 30 minutes. Samples were washed with 0.1% Triton X-100/PBS three times for five minutes. The slices were then blocked with 10% Normal Goat Serum (NGS)/0.1% Triton X-100/PBS for one hour and subsequently incubated with primary antibodies in 5% NGS/PBS overnight (12-24 hours) at 4ºC. Samples were washed three times for ten minutes with 0.1% Triton X-100/PBS.

Then, biotinylated secondary antibodies were incubated on the samples in 10% NGS/PBS. Additional washing with PBS was applied three times for ten minutes and the brain slices were incubated with the ABC Vectastain® kit for 90 minutes. After washing three times with PBS for ten minutes each, DAB substrate was added to the samples for four minutes and finally washed three times again for ten minutes with PBS before mounting and drying on glass slides at room temperature. Counterstaining was carried out by rinsing with PBS for ten minutes and applying hematoxylin for 40 seconds. The brain slices were rinsed with running distilled water for five minutes, dehydrated with ethanol at increasing concentrations (70%, 80%, 100% for 150 seconds each) and xylene (ten minutes) before embedding with Phenol free Kaiser's glycerol gelatine and covering using coverslips. Samples were stored at room temperature until visualization.

2.2.2.3.4 Immunofluorescence staining of cells

All the steps were carried out at room temperature, unless specified. Two days after transfection, cells grown on poly-L-lysine coated coverslips were fixed by 3.7% PFA/PBS for ten minutes. Excess of PFA was removed by exchange with PBS. Samples were stored at 4ºC until usage. The cells were permeabilized by 0.5% Triton X-100/PBS (10 minutes) and blocked using 4% Bovine Serum Albumin (BSA)/4% NGS/PBS for one hour. The primary antibodies were diluted in 2% BSA/PBS and incubated overnight (12/24 hours) at 4ºC in a humidity chamber. The coverslips were washed six times in washing buffer (0.1% BSA/PBS) and the secondary antibodies were applied for 1 hour. After rinsing the coverslips with washing buffer six times, DAPI solution was applied for 1-3 minutes before 6 further washing steps followed by 2 washes with distilled water. Finally, the cells coverslips were mounted on glass slides using PermaFluor mounting medium. Samples were stored at 4ºC until visualization.

2.2.2.4 Cell culture

2.2.2.4.1 Transfection of adherent HEK293 cells

Cells were seeded on 6-well plates in serum-free medium. The next day, cells at 70-80% confluency were transfected using the Turbofect™ transfection reagent. Per each well, 1 µg of DNA was added to 100 µL of serum-free medium and subsequently mixed with 2 µL of vortexed transfection reagent. After incubating the mixture for 15-20 minutes at room temperature, 100 µL were added drop by drop to each well and the plates were gently tilted to ensure even distribution of the mixture over the seeded cells.

2.2.2.4.2 Isolation of microglia from adult mouse brain

The brains were quickly removed, washed with cold D-PBS, and cut into small pieces discarding the cerebellum and brainstem. From this point on, all the steps were carried out on ice or at 4°C. The brain pieces were placed in a gentleMACS™ C-tube containing 1950 µL of enzyme mix 1 before adding 30 µL of the enzyme mix 2 and running the 37C_ABDK_01 program on a gentleMACS™ Octo Dissociator with Heaters. From this point on, all the steps that involved handling of the samples were carried out inside the

cell culture hood using sterile materials. The tubes were spun for a short time, samples were collected and run through a MACS® SmartStrainer (70 µm) on top of a 50 mL falcon tube. 10 mL of D-PBS were added to the remaining brain pieces of the C-tube and run through the strainer in order to ensure maximum sample amount. The suspension was centrifuged at 300 g for 10 minutes and the supernatant was discarded. The samples were resuspended in 3100 µL D-PBS before mixing with 450 µL of Debris Removal Solution and a 2 mL overlay of D-PBS applied gently to avoid mixing. After centrifugation (4ºC, 3000 g, 10 minutes) the top two phases were discarded and the bottom phase was mixed with fresh D-PBS up to a total volume of 15 mL. The samples were gently inverted three times and centrifuged (1000 g, 10 minutes), and the supernatants were discarded. Each sample was resuspended in 1 mL of Red Blood Cell Removal Solution and stored at 4ºC for ten minutes before adding 10 mL of fresh D-PBS. The cell suspension was pelleted by centrifugation (300 g, 10 minutes) and resuspended in 90 µL of PB buffer. Then, 10 µL of the CD11b MicroBeads were added and the samples were kept at 4ºC for 15 minutes. The cell suspensions were centrifuged (300 g, 10 minutes) and the pellets were mixed with 500 µL of PB buffer. For the magnetic separation, LS columns were attached to a MACS® separator placed in a magnetic field. Each column was rinsed with 3 mL of PB buffer before applying the cell suspension. The columns were rinsed three times with 3 mL of PB buffer. Finally, each column was retrieved from the magnetic field and placed on top of a 15 mL falcon tube which collected the microglia suspension after running 5 mL of PB buffer by pushing the solution using a plunger. Each sample was centrifuged (300 g, 10 minutes), the pellets of cells were resuspended in microglia cell culture medium and subsequently seeded on poly-L-lysine coated coverslips. The microglia cell cultures were maintained by replacement of 50% of the medium on alternate days until fixation.

2.2.2.5 Proteomics

2.2.2.5.1 Preparation of samples for proteomic analysis

Protein samples from mouse tissue were prepared using the PreOmics iST-NHS kit, a modification of the Filter-Aided Sample Preparation (FASP) protocol for sample preparation (Wiśniewski et al., 2009), according to the instructions of the manufacturer. In short, 100 mg of mouse tissue were disrupted in reinforced tubes containing 50 µL of Lyse-NHS buffer using a Precellys® 24 homogenizer and 1.4 mm ceramic beads. Samples were transferred to fresh tubes and lysis was allowed in a heating block (95 ºC, 1000 rpm, 10 minutes). Digestion of the samples was carried out by incubation with 50 µL of complemented Digest buffer for 3 hours on a heating block at 37 ºC and 500 rpm. The samples were transferred to cartridges and washed through several centrifugation steps (2250 g, 3 minutes) using 200 µL of the Wash buffers 1 and 2. In the last step, the Elute buffer was added and the flow-through protein samples were collected in fresh tubes. The samples were air-dried at 45 ºC and resuspended in 100 µL of the LC-Load buffer.

2.2.2.5.2 Proteomic analysis via liquid chromatography coupled to mass spectrometry

LC-MS analysis was carried out by Dr. Thomas Fröhlich (Gene Center, Munich). Purified samples were injected in an Ultimate™ 3000 nano-LC system coupled online to a Q-Exactive™ HF mass spectrometer. Initially, proteins were run through a PepMap™ 100 column (100 µm x 2 cm, 5 µm particles) and subsequently separated on an PepMap™ RSLC C18 column (75 µm x 50 cm, 2 µm particles). Solvent A consisted of 0.1% formic acid/water, whereas solvent B consisted in 0.1% formic acid/acetonitrile. The flow was set to 250 nL/min, with a gradient duration of 160 minutes of 5-25% solvent B followed by a 10-minute raise to 40%. Mass spectrometry spectra were acquired using a top 15 data-dependent acquisition method. Processing of raw data was carried out using MaxQuant (v.1.6.7.0) (Tyanova et al., 2016) with the built-in search engine Andromeda (Cox et al., 2011) and the mouse subset of the Uniprot database. Intensities were normalized via MaxLFQ approach (Cox et al., 2014), and volcano plots were generated using two-tailed Student's t-test and a permutation-based FDR cut-off of 0.05, setting an s0-parameter of 0.01 to consider fold changes (Tusher et al., 2001).

3. Results

3.1 Comparison of P2X7 reporter mouse models and investigation of P2X7 localization

3.1.1 Biochemical analysis of P2X7 and P2X4 protein levels

The first step in the study and comparison of both BAC transgenic mouse models was the investigation of the P2X7 levels in tissue from both mouse lines via western blot experiments. As previously mentioned, *P2rx7* and *P2rx4* are neighboring genes in the mouse genome. Therefore, P2X4 levels were also tested to check for passenger gene transgenesis of *P2rx4* in the BAC clones.

Taking crude membrane extracts from mouse lung of the P2X7-EGFP and the sEGFP models, western blot was carried out running samples from both mouse lines and the wildtype mouse as a reference. The membranes were stained with antibodies targeting P2X4 and P2X7 as well as vinculin for standardization (Figure 7).

In the P2X7-EGFP mouse (Figure 7B), P2X4 levels did not show significant differences in comparison with the wildtype mouse. As for P2X7, apart from the bands corresponding to the endogenous protein, there is a second band around the 100 kDa mark corresponding with the fusion protein P2X7-EGFP, in line with previous results (Kaczmarek-Hájek et al., 2018). Overall, combination of both bands brings the total relative amount of P2X7 to an approximate three-fold overexpression in comparison with the wildtype mouse.

Western blot results from the sEGFP lung samples (Figure 7A) showed an overexpression of P2X4 of approximately eight-fold in comparison with the wildtype mouse, thereby revealing the presence of *P2rx4* in the BAC clone as a passenger gene. Surprisingly, the sEGFP mouse also showed a three-fold overexpression of P2X7 protein in comparison to the wildtype mouse. This result was unexpected, as the insertion of a STOP codon after the EGFP coding sequence should prevent P2X7 receptor overexpression. These results were confirmed by collaborators from the group of Tobias Engel at the Royal College of Surgeons in Ireland (RCSI) via qPCR on brain tissue (Ramírez-Fernández et al., 2020).

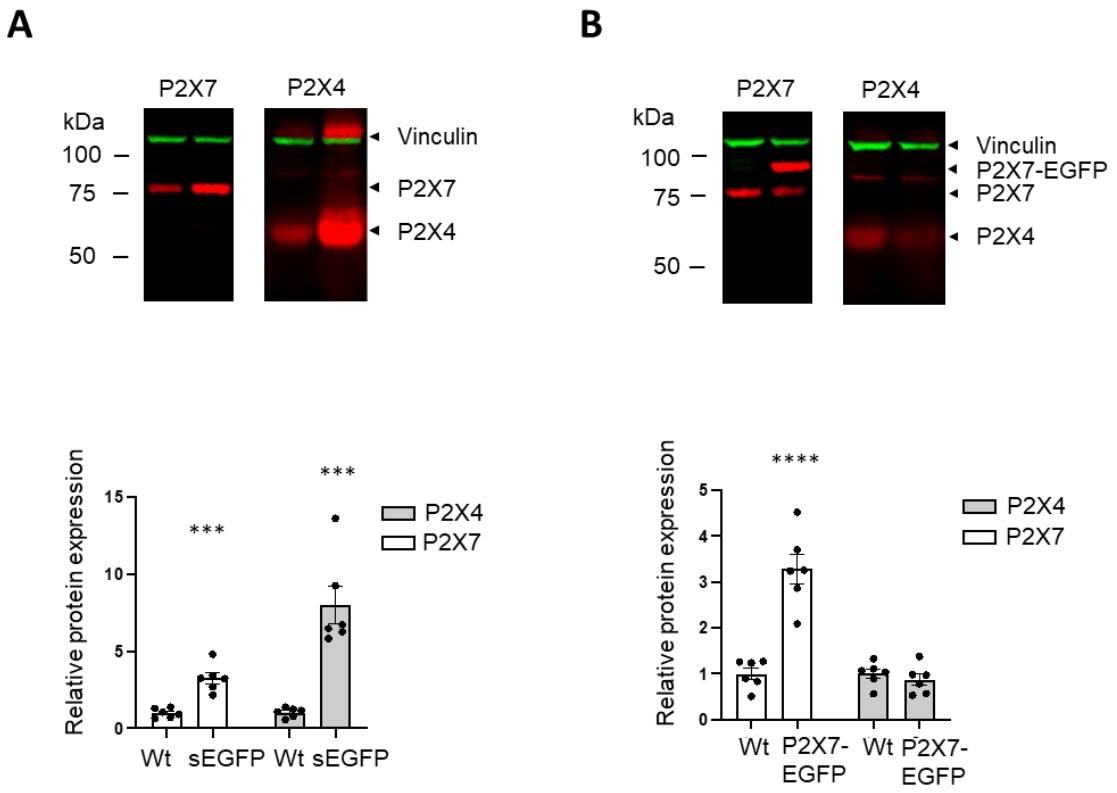

Figure 7: Comparison of P2X7 and P2X4 protein levels in (A) P2X7-EGFP and (B) sEGFP BAC transgenic mice. *A representative western blot experiment using anti-P2X4 antibodies, anti-P2X7 antibodies (both in red) and anti-vinculin antibodies (green) as a loading control is shown. Crude membrane extracts were obtained from mouse lung using 0.1% NP40 detergent and 50 µg of total protein were loaded in each well. Two independent experiments were performed with a total number of six mice of both sexes (10-35 weeks of age). Mann-Whitney test was carried out in order to assess significance (**p<0.01). A version of this figure has been published* (Ramírez-Fernández et al., 2020) *under the Creative Commons Attribution 4.0 International License.*

3.1.2 Study of P2X4, EGFP and P2X7 localization in sagittal mouse brain sections

Following these observations, a question was raised regarding the *P2rx4* insertion in the BAC clone of the sEGFP mouse and whether the distribution of the overexpressed P2X4 protein would replicate that of the wildtype mouse brain. Immunofluorescence staining was used to compare the distribution of the overexpressed P2X4 in the sEGFP model with the wildtype mouse in sagittal brain slices (Figure 8). The observed distribution patterns were overlapping in the brain, with higher density in regions from the hippocampus and the cerebellum, where the staining was particularly intense in the Purkinje cell layer. These results are also in line with other transgenic mouse models that include the *P2rx4* gene in their BAC clone and were generated via knock-in (Bertin et al., 2020) and BAC transgenesis (Xu et al., 2016) using mCherry and TdTomato as reporter proteins, respectively. The authors of these studies highlight the sparse expression in soma from neurons of the cortex, the granular and pyramidal cell layers of the hippocampus, as well as the Purkinje cell layer of the cerebellum.

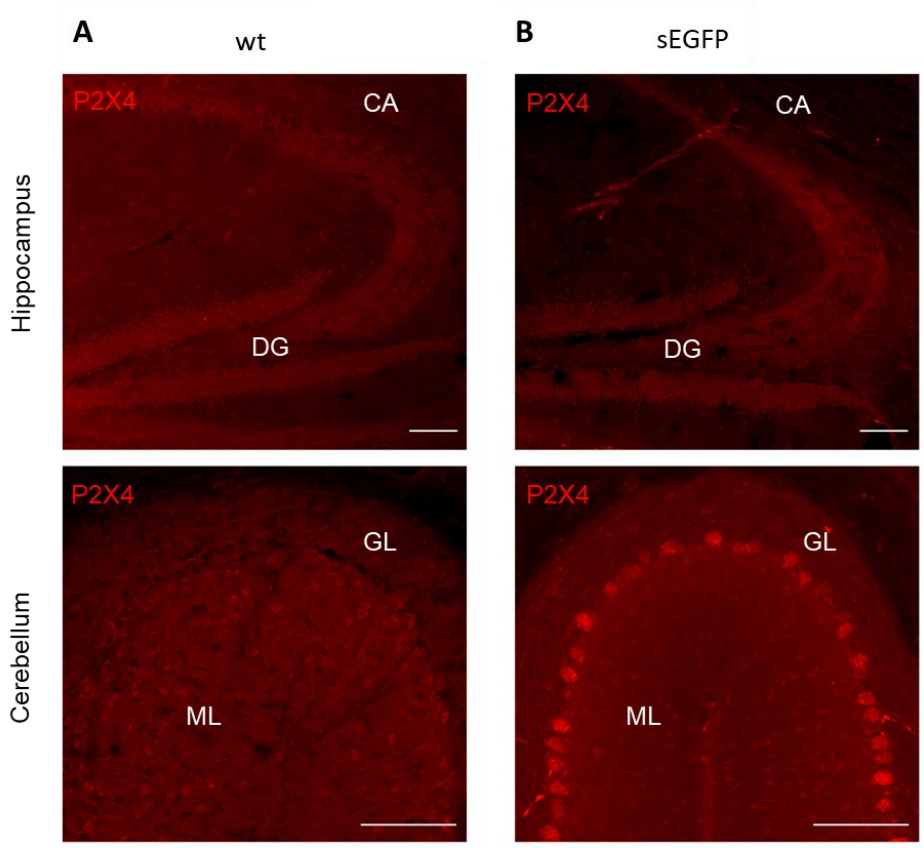

Figure 8: P2X4 immunofluorescence showing the increased level of expression in the wildtype mouse (A) in comparison with the sEGFP mouse (B). *Sagittal sections from dentate gyrus of the hippocampus (upper) and cerebellum (lower) are shown. Representative images from three independent experiments with three different animals are shown. CA, cornu ammonis; DG, dentate gyrus; ML, molecular layer; GL, granular layer. Scale bars 100 µm. A version of this figure has been published* (Ramírez-Fernández et al., 2020) *under the Creative Commons Attribution 4.0 International License.*

As found in a preliminary comparison (Kaczmarek-Hájek et al., 2018), expression of the reporter EGFP differed in the soluble EGFP mouse model (www.gensat.org) in comparison to the P2X7-EGFP mouse throughout the brain. In particular, this comparison emphasized the neuronal expression of the sEGFP reporter, whilst the P2X7-EGFP mouse model showed predominant distribution of the reporter in microglia.

Immunofluorescence staining with an anti-GFP antibody (Figure 9) also revealed clear differences between the two models in brain slices. Most remarkably, sEGFP showed a very localized distribution in the hippocampus, the cerebellum, and the caudate putamen, whereas P2X7-EGFP was more evenly distributed throughout the mouse brain with higher density in the cortex, *substantia nigra*, cerebellum and medial habenula. Interestingly, it even appeared to have a lower fluorescence signal in the caudate putamen and hippocampus.

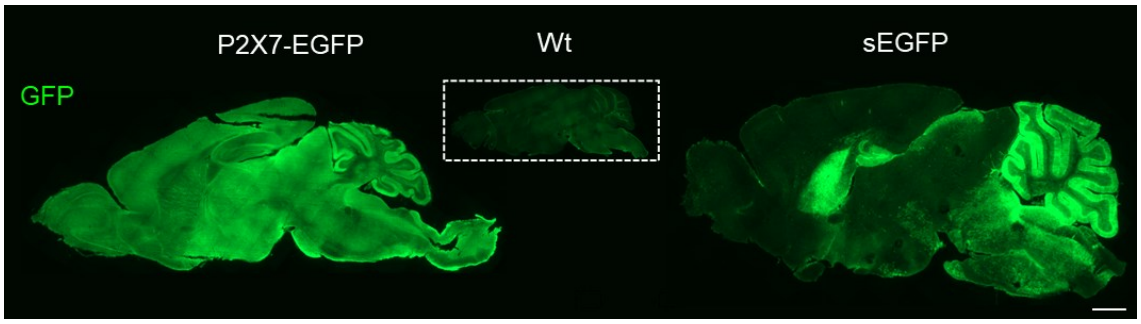

Figure 9: Comparison of general expression patterns of EGFP in both mouse models and the wildtype mouse*. Immunostainings were performed using an anti-GFP antibody on sagittal brain slices. The intensities were adjusted individually to prevent saturation, and representative images from three independent experiments with different animals are shown. Scale bar 1mm. A version of this figure has been published* (Ramírez-Fernández et al., 2020) *under the Creative Commons Attribution 4.0 International License.*

Although immunofluorescence staining was useful for the comparison of EGFP distribution over the brain, direct comparison of the two mouse lines applying the same acquisition parameters was not possible because the signal intensities needed individual adjustment in order to avoid saturation of the resulting images. Another inconvenient is that immunofluorescence staining using low-specificity antibodies has limitations because acquisition adjustments may lead to low signal-to-noise ratio and poor imaging quality. A similar problem emerged when this approach was applied for the study of P2X7 expression patterns, given the poor specificity of the available antibodies.

Diaminobenzidine (DAB) staining was proposed as an alternative experiment for the evaluation of P2X7 and EGFP distribution over the mouse brain. The brown precipitate generated by oxidation of DAB leads to stable staining that can be visualized directly or by light microscopy, making this technique a convenient option for general analysis of protein distribution patterns at the tissue level. Furthermore, this technique allows the generation of reliable results because the staining intensity can be controlled by increasing the incubation time of the DAB substrate at the oxidation step when the antibodies lack from sensitivity.

The DAB assay protocol was developed and optimized first using the anti-GFP antibody, taking that the results had been visualized previously via immunofluorescence staining. This experiment confirmed the predominance of EGFP expression throughout the molecular layer of the cerebellum in both models (Figure 10) which also showed a striped pattern that might correspond to Bergmann glia. As for the hippocampus, the P2X7-EGFP showed a limited localization in the shape of a rim surrounding the molecular layer of the dentate gyrus, and it was absent in the granular layer. In contrast, we found a predominance of sEGFP in the granular layer of the dentate gyrus, as well as the entire molecular layer. Of note, the EGFP signal was intense in single, neuron-like cells of the pyramidal cell layer of the CA region as well as in the region where mossy fibers corresponding with the Stratum lucidum of the CA3 region are localized.

Over the entire brain, the P2X7-EGFP showed again a more homogeneous distribution of the reporter, although regions such as the cortex, olfactory bulb, hypothalamus and

substantia nigra showed stronger staining. The sEGFP mouse brain shows a more intense and localized signal of the reporter, clearly highlighted in the caudate putamen and superior colliculus.

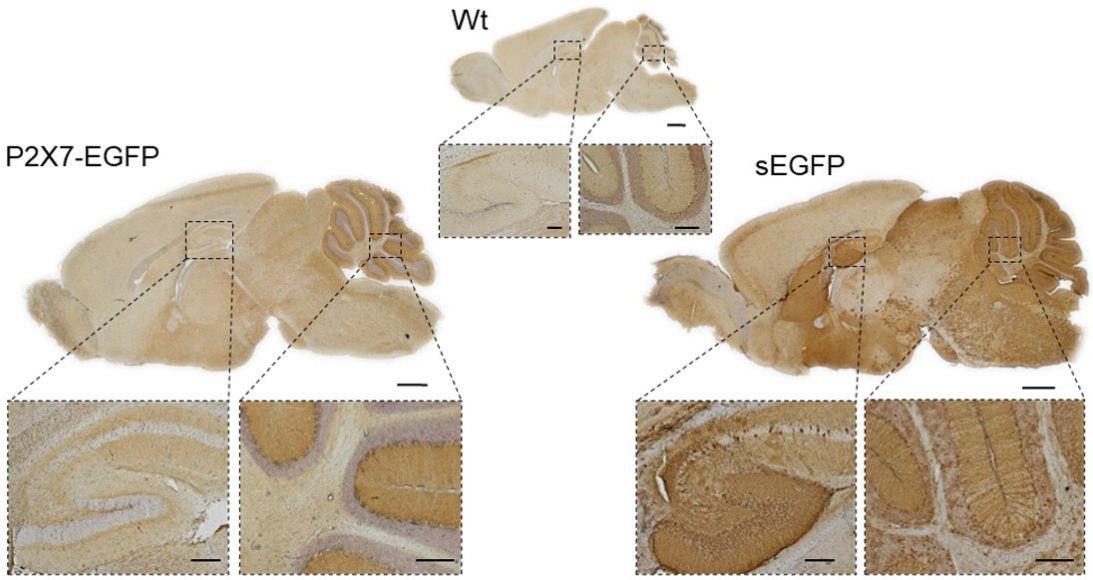

Figure 10: Comparison of EGFP distribution in the brain of both BAC transgenic mouse models and the wildtype mouse (negative control) by DAB staining*, using haematoxylin for counterstaining. Representative images of sagittal brain slices from three independent experiments with 3 different animals are shown. Scale bars 1 mm (200 µm in insets). A version of this figure has been published* (Ramírez-Fernández et al., 2020) *under the Creative Commons Attribution 4.0 International License.*

As pointed out previously, taking the advantages of DAB staining and the limitations of the available anti-P2X7 antibodies, this experiment was carried out using an anti-P2X7 nanobody on both BAC transgenic mouse models and allowed comparison of their P2X7 expression patterns with that of the wildtype mouse, using a $P2X7^{-/-}$ model as a negative control (Figure 11).

Surprisingly, the sEGFP model showed a P2X7 distribution that did not correspond with the one seen for the EGFP reporter, even though the expression of both proteins should be controlled by the P2X7 endogenous promoter. The P2X7 expression patterns seen in both models were similar when compared to the wildtype mouse, as P2X7 distribution matched the one seen for the EGFP in the P2X7-EGFP mouse, with a higher intensity in the molecular layer of the cerebellum, as well as a fine rim around the molecular layer of the dentate gyrus.

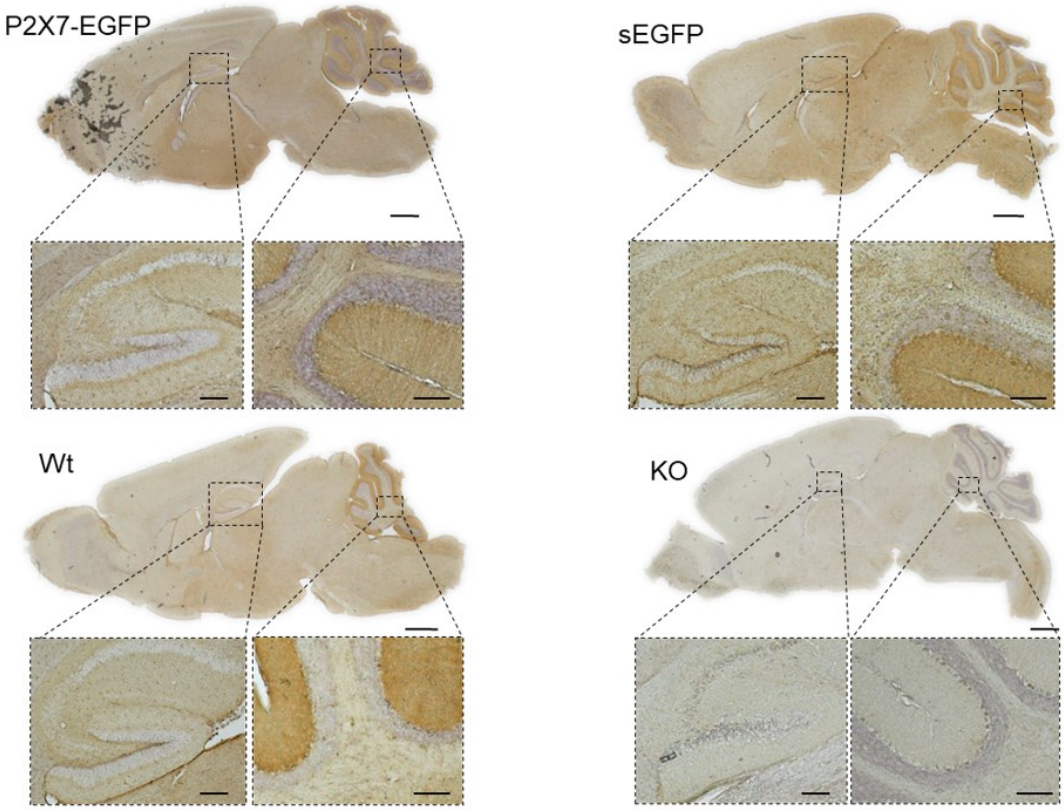

Figure 11: Comparison of P2X7 receptor distribution in both transgenic mouse models and wt mice by DAB staining *using an anti-P2X7 nanobody on brain slices. P2X7 knockout mouse were used as a negative control. Haematoxylin was added for counterstaining. Representative images of sagittal brain slices from three independent experiments with 3 different animals are shown. Scale bars 1 mm (200 µm in insets). A version of this figure has been published* (Ramírez-Fernández et al., 2020) *under the Creative Commons Attribution 4.0 International License.*

3.1.3 Comparison of cell type-specific EGFP localization in the mouse hippocampus

Given the unexpected differences seen between the expression patterns of EGFP and P2X7 in the sEGFP mouse model, we proceeded to perform immunostainings on sagittal brain slices of both BAC transgenic mouse models using antibodies against EGFP and specific marker proteins in order to study the cell type-specific distribution of the reporter.

3.1.3.1 Microglia

Microglia cells are the resident macrophages of the CNS, where they play a dual role in immunity and remodeling upon tissue damage (Ginhoux et al., 2013). P2X7 expression and function has been extensively characterized in microglia due to its involvement in proliferation and neuroinflammation (Bhattacharya & Biber, 2016; Ren et al., 2022; Territo & Zarrinmayeh, 2021). Thus, this cell type was chosen in the first place for a detailed

comparison between the expression of the EGFP reporter in the BAC transgenic mouse models.

Brain sections were stained with anti-GFP and anti-Iba1 antibodies (Figure 12). Iba1 (Ionized calcium binding adaptor molecule 1), also known as Allograft inflammatory factor 1 (AIF-1) is a cytoskeletal protein expressed by microglia and macrophages. We observed no co-localization of Iba1 and GFP in the sEGFP mouse model, where the EGFP staining confirmed the distribution in aforementioned regions such as the granular layer of the dentate gyrus and the Stratum lucidum of the hippocampus, and it also revealed a high signal in the Purkinje cell layer of the cerebellum. In contrast, co-localization was clear in the observed regions of the P2X7-EGFP mouse model, revealing expression of the P2X7-EGFP fusion protein in microglia.

However, the different expression patterns of the reporter and P2X7 receptor in the sEGFP mouse led to the question of whether the endogenous receptor is expressed by microglia of this model, even though the reporter is absent. FACS analysis carried out by our collaborators from the University Medical Center Hamburg-Eppendorf (Hamburg) confirmed the expression of P2X7 in microglia (Ramírez-Fernández et al., 2020) and gave further proof of inconsistencies in the sEGFP mouse model.

3.1.3.2 Oligodendrocytes

Oligodendrocytes are the cells that constitute the myelin sheaths in the CNS. Therefore, their function is crucial since they collaborate in maintaining the efficiency and speed of axonal action potential transmission (Collins & Bowser, 2017). P2X7 has been related to oligodendrocyte development and function, being involved in oligodendrocyte-mediated axonal damage, which has a relevance in neurodegenerative diseases such as amyotrophic lateral sclerosis or multiple sclerosis (Matute, 2008; Y. F. Zhao et al., 2021). The oligodendrocyte transcription factor 2 (Olig2) is a cytoplasmic marker for oligodendrocytes in the brain (Figure 13). The co-immunostaining using anti-GFP and anti-Olig2 antibodies gave similar results as those for microglia, given that the presence in the same cells was found for EGFP and Olig2 in the samples from the P2X7-EGFP mouse (see insets for a detailed view of Olig2 expressed over the cytoplasm, surrounded by the EGFP that is expressed over the cell membrane). However, different results were seen in the sEGFP mouse model, where Olig2 and EGFP were detected separately in different cells.

Although Olig2 is used as a general oligodendrocyte marker, it has been suggested that this protein is predominantly expressed by neural progenitor cells (NPCs) and oligodendrocytes at intermediate stages of development, but not in mature oligodendrocytes (Bradl & Lassmann, 2010). In order provide further confirmation of P2X7-EGFP localization in mature oligodendrocytes that form the myelin sheaths, P2X7-EGFP mouse brain slices were stained for EGFP in combination with an anti-MBP antibody, which is specific for the Myelin Basic Protein (MBP), a marker for mature oligodendrocytes in the brain. Signs of co-localization detected in the cortex and the fiber tracts of the cerebellum, being

particularly higher in the fibers from the striatum pallidum and the hilus of the hippocampus (Figure 14).

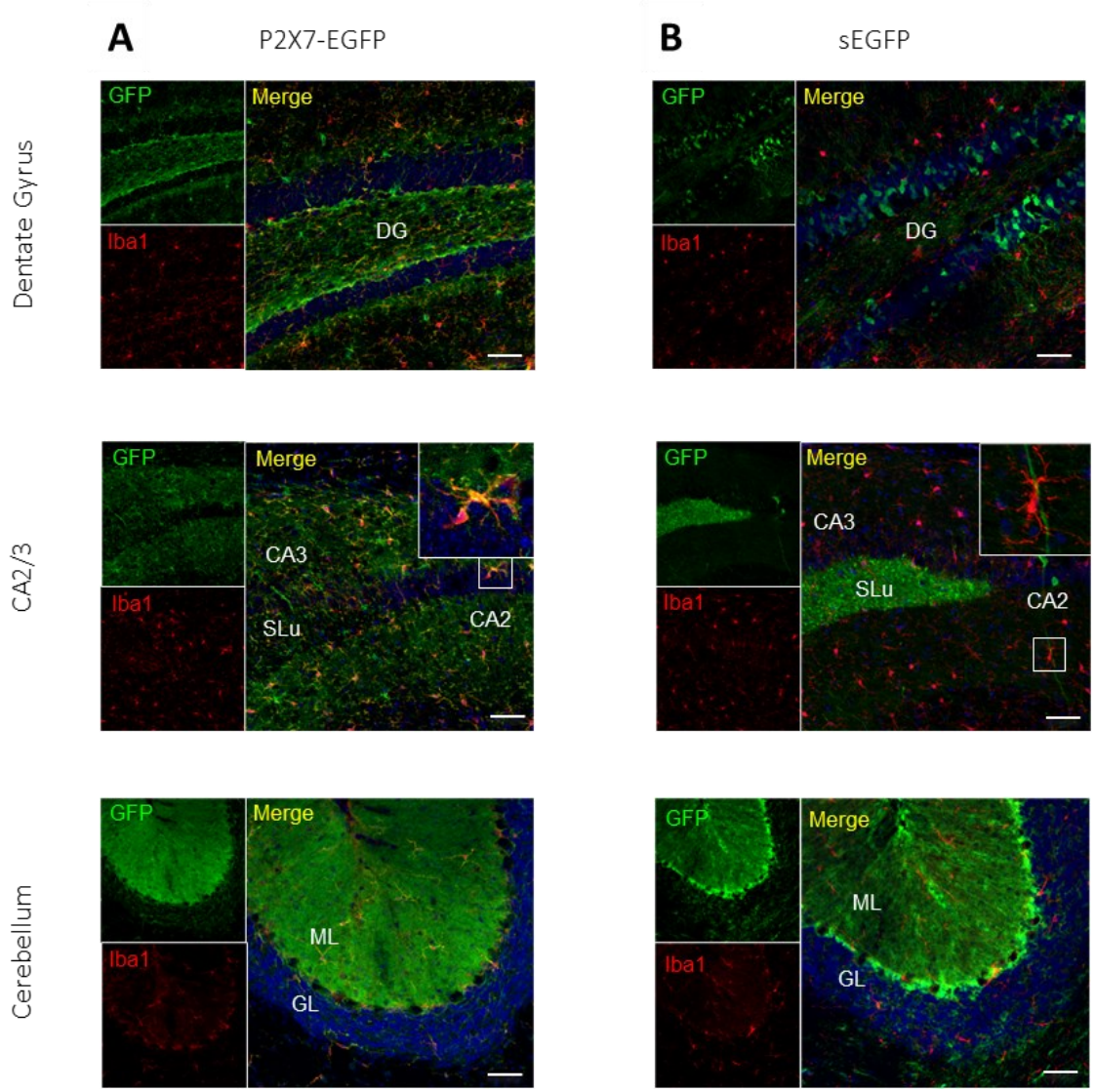

Figure 12: Cell type-specific EGFP localization in both reporter mouse models with a focus in microglia. *Samples were stained with anti-GFP and anti-Iba1 antibodies, and DAPI for nuclear counterstaining. Representative images from three independent experiments are shown for the dentate gyrus and the CA2/3 region of the hippocampus as well as the cerebellum. SLu, stratum lucidum; CA, cornu ammonis; DG, dentate gyrus; ML, molecular layer; GL, granular layer. Scale bars 50 µm. A version of this figure has been published* (Ramírez-Fernández et al., 2020) *under the Creative Commons Attribution 4.0 International License.*

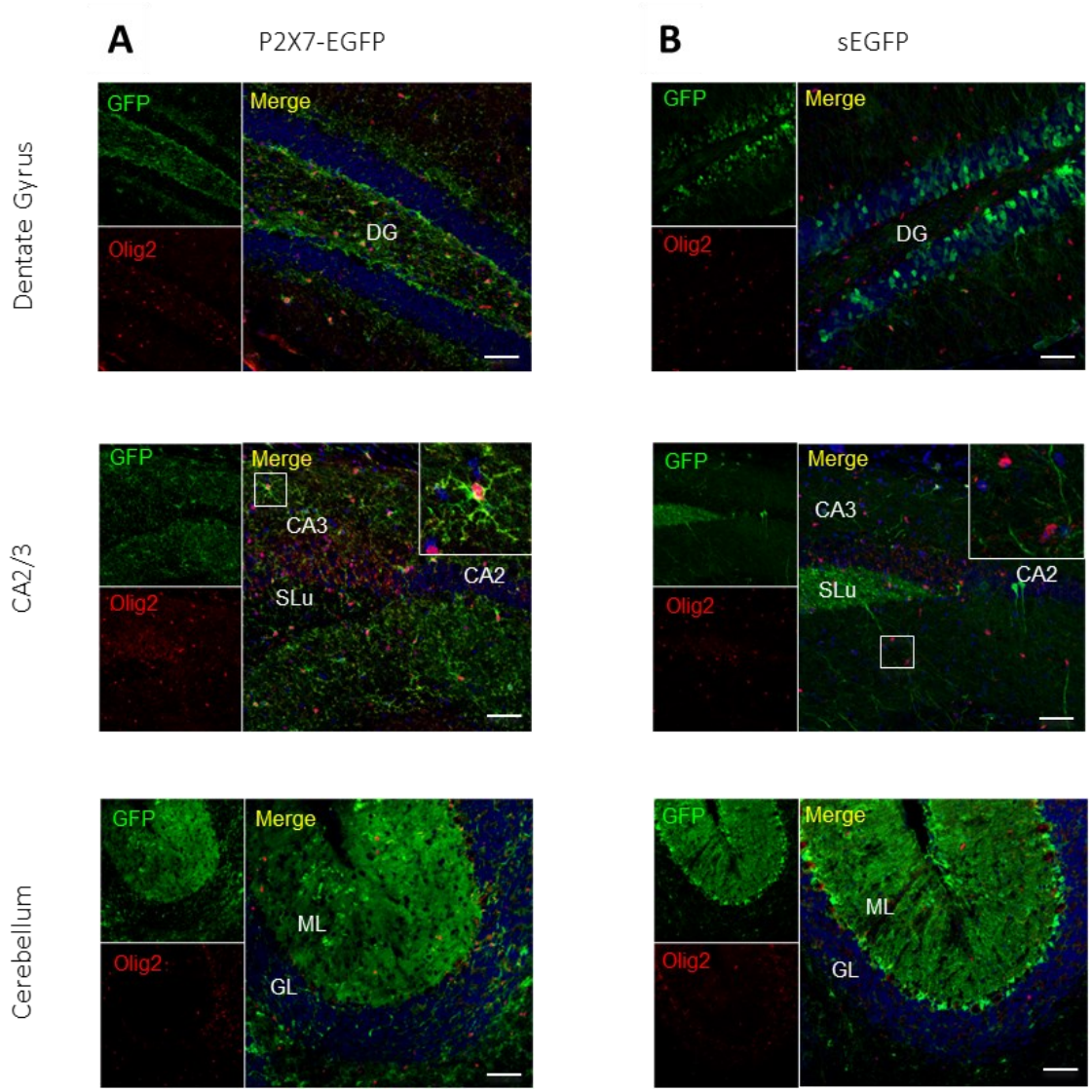

Figure 13: Cell type-specific EGFP expression in both reporter mouse models with a focus in oligodendrocytes. *Sagittal brain sections were treated using anti-GFP and anti-Olig2 antibodies, as well as DAPI for nuclear counterstaining. Representative images of sagittal brain slices from three independent experiments using three different animals from each line are shown for the dentate gyrus and CA2/3 region of the hippocampus as well as the cerebellum. SLu, stratum lucidum; CA, cornu ammonis; DG, dentate gyrus; ML, molecular layer; GL, granular layer. Scale bars 50 µm. A version of this figure has been published* (Ramírez-Fernández et al., 2020) *under the Creative Commons Attribution 4.0 International License.*

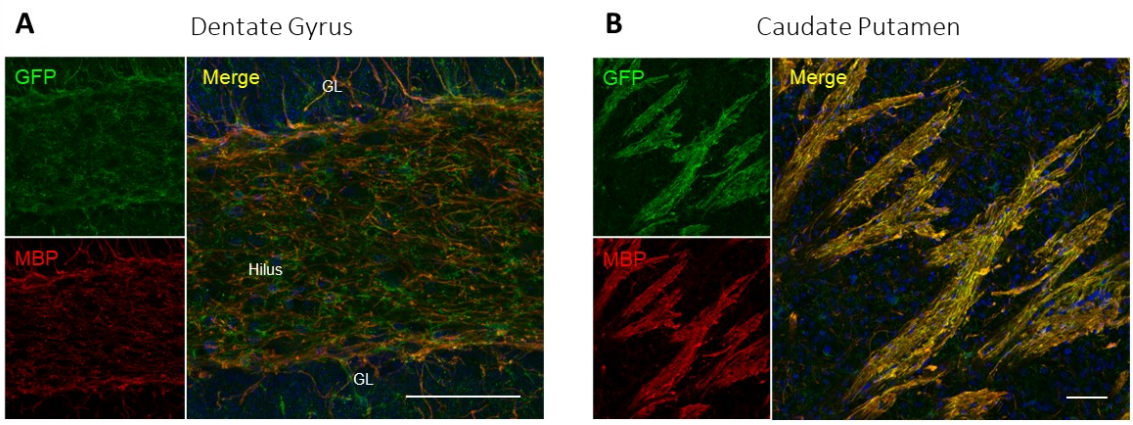

Figure 14: Cell-specific EGFP expression in P2X7-EGFP mouse oligodendrocytes using an antibody against the oligodendrocyte marker MBP*. Sagittal brain sections were treated using an anti-GFP and anti-MBP antibodies and DAPI for nuclear counterstaining. Representative images from 3 independent experiments are shown for the hilus of the (A) dentate gyrus of the hippocampus, as well as the (B) striatum pallidum of the caudate putamen. GL, granular layer. Scale bars 50 µm.*

3.1.3.3 Neurons

As already discussed, the existence of neuronal P2X7Rs has been a subject of debate, and there have been studies supporting and opposing it. While part of the scientific community argues that P2X7R-mediated effects on neurons are in fact produced by P2X7Rs from microglia, astrocytes and oligodendrocytes, pharmacological approaches *in vitro* provide arguments in favor of neuronal P2X7Rs given the effects of P2X7 antagonists on neuronal cultures (Teresa Miras-Portugal et al., 2017). However, evidence has been subject to doubt. For example, the purity of these cultures relies on previously known markers such as synaptophysin, which has been recently proved to be expressed by astrocytes as well. Others point at the existence of P2X7Rs in NPCs arguing that the expression of this receptor decreases over the development and differentiation process (for references, see Illes et al., 2017).

As mentioned in section 1.3, localization of EGFP in neurons has been reported in the sEGFP mouse, while it appeared absent in this cell type in the P2X7-EGFP model. To clarify this question, we tested a combination of anti-GFP and anti-NeuN antibodies to check for the neuronal expression of the reporter in sagittal brain slices from both models (Figure 15). The neuronal nuclear protein (NeuN) is generally used as a marker for neuronal development and differentiation.

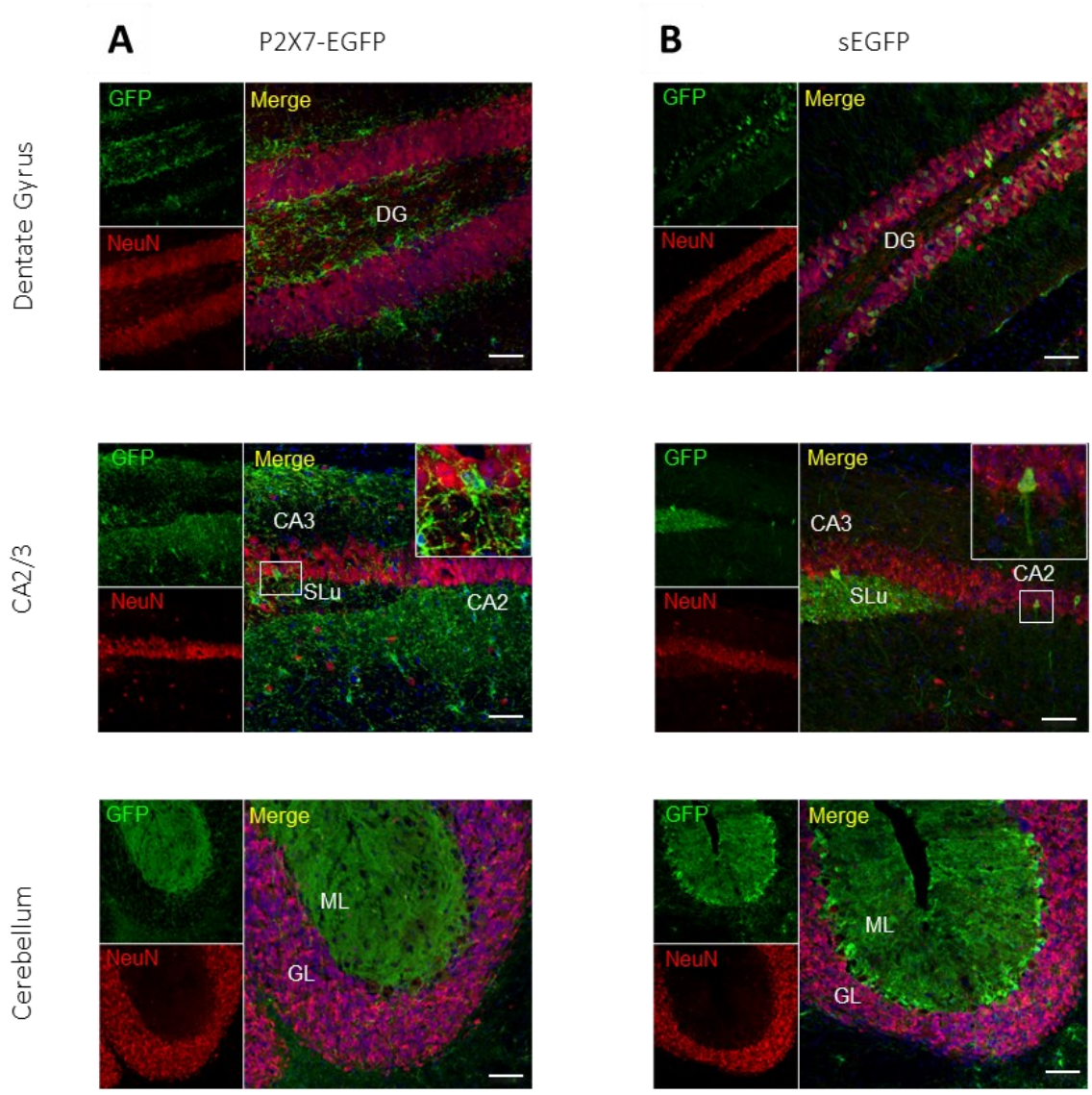

Figure 15: Comparison of cell type-specific EGFP expression in both reporter mouse models by co-staining with the neuronal marker NeuN. *Samples were stained using anti-GFP and anti-NeuN antibodies, and DAPI for nuclear counterstaining. Representative images of sagittal brain slices from three independent experiments using three different animals are shown for the dentate gyrus and CA2/3 region of the hippocampus as well as the cerebellum. SLu, stratum lucidum; CA, cornu ammonis; DG, dentate gyrus; ML, molecular layer; GL, granular layer.Scale bars 50 µm.*

Taking the positive EGFP signal of the sEGFP mouse model in neuron-like cells from the granular layer of the dentate gyrus, the pyramidal layer and the mossy fiber tract from the Stratum lucidum of the CA3 region and the Purkinje cell layer, as well as other cells that are sporadically EGFP-positive in the molecular layer of the cerebellum, we next aimed to identify the specific neuronal or other cell types that express EGFP at high levels in these regions of the brain.

Cerebellar calbindin-1 (calbindin-D28k) in Purkinje cells is known for its role in the regulation of motor coordination, with relevance in pathologies such as ataxia and dementia (Barski et al., 2003; Schmidt et al., 2003). In this regard, an antibody was tested targeting calbindin-1 (calbindin-D_{28k}), and its partial co-localization with EGFP suggests the expression of this reporter in Purkinje cells of the cerebellum (Figure 16A). Apart from Bergmann glia-like cells, the molecular layer showed EGFP staining in cells that were identified as either stellate or basket cells, given the sporadic co-localization of EGFP with parvalbumin (Figure 16B), a protein involved in Ca^{2+} regulation in interneurons from the molecular layer (Braun, 1990). Furthermore, other cells from this region showed EGFP-positive signal that co-localized with NG2 (Figure 16C). In spite of its common use as a marker for oligodendrocytes, the neural/glial antigen 2 (NG2) is expressed from early stages of development in neural progenitor cells (NPCs), which later differentiate into neurons, oligodendrocytes or astrocytes (Tsoa et al., 2014).

Following these observations, we aimed to test antibodies against further neuronal markers in the search for information about the EGFP staining seen in the mossy fibers from the stratum lucidum at the hippocampal CA3 region in the sEGFP mouse model. The markers chosen for co-immunostainings were calbindin-1, calretinin and the zinc transporter ZnT3. In the mossy fibers, calbindin-1 regulates sprouting with functional relevance in memory processes (Martinian et al., 2012). Calretinin is another protein involved in Ca^{2+} regulation and is related to Calbindin-1, although its expression in this region of the hippocampus has been reported for non-pyramidal neurons (Gulyls et al., 1992; Rogers, 1989). Lastly, ZnT3 expression in the mossy fiber region has been reported to modulate synaptic transmission through transport of zinc into synaptic vesicles. Even though antibodies targeting calbindin-1 and ZnT3 showed a positive signal in this region, we found no co-localization with EGFP. Neither was the case for calretinin, which was not even expressed in this region (Figure 17). Taken together, these results indicate that the EGFP-positive signal in this region might correspond with projections from the EGFP-positive neurons of the pyramidal cell layer of the hippocampus.

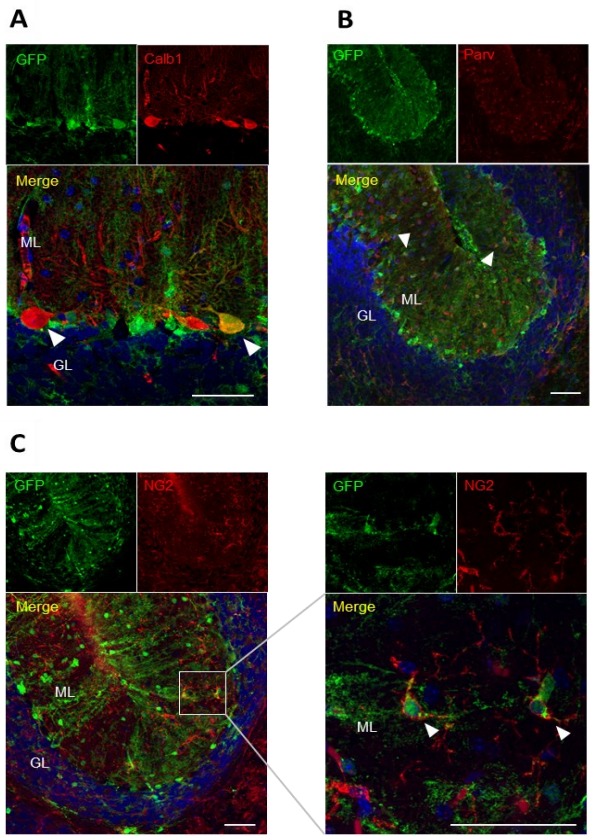

Figure 16: Images from the cerebellum of the sEGFP mouse model stained with anti-GFP and antibodies against Calbindin1 (A, Purkinje cells), parvalbumin (B, basket and stellate cells) and NG2 (C, NPCs). *Arrows point at specific cells that show co-localization of EGFP with the specific marker, except for calbindin1, in which a cell that does not show EGFP expression is also highlighted. Representative images from 3 independent experiments using three different mice are shown for the dentate gyrus and CA2/3 region of the hippocampus as well as the cerebellum. ML, molecular layer; GL, granular layer. Scale bars 50 µm. A version of this figure has been published* (Ramírez-Fernández et al., 2020) *under the Creative Commons Attribution 4.0 International License.*

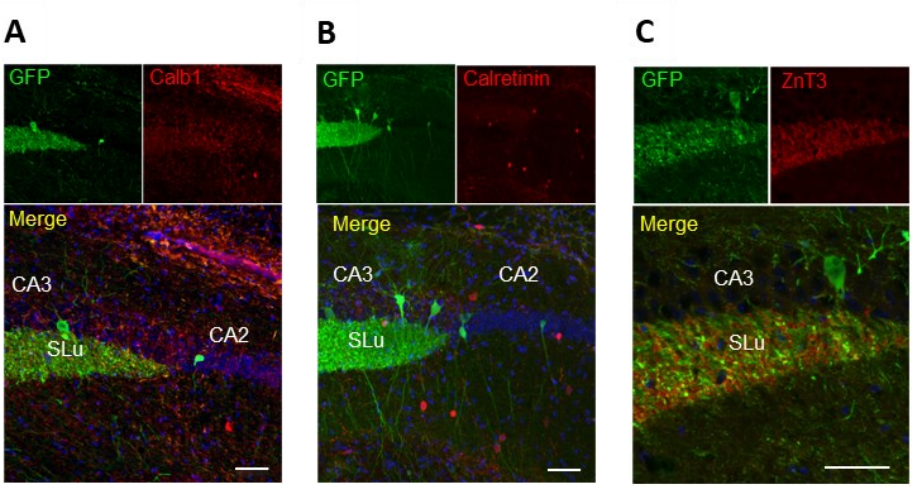

Figure 17: Images from the CA2/3 region of the hippocampus of the sEGFP mouse model stained with anti-GFP and antibodies against Calbindin1, calretinin and ZnT3 targeting neurons from the mossy fiber region of the stratum lucidum. *Representative images from sagittal brain sections of three independent experiments with three different animals are shown for the dentate gyrus and CA2/3 region of*

the hippocampus as well as the cerebellum. SLu, stratum lucidum; ML, molecular layer; GL, granular layer.Scale bars 50 µm. A version of this figure has been published (Ramírez-Fernández et al., 2020) *under the Creative Commons Attribution 4.0 International License.*

Finally, we had a more detailed look at the expression of P2X4 in the neurons of the Purkinje cell layer of the cerebellum from the sEGFP mouse (Figure 18). In this regard, the high level of expression of P2X4 allowed the visualization of patterns that conciliate with the reported intracellular localization of this receptor (Figure 18A). Therefore, additional experiments were carried out using an antibody against the Lysosome-associated membrane glycoprotein 1 (LAMP1) in order to study the P2X4 localization in lysosomes. However, we could not see co-localization of P2X4 and LAMP1 in our samples (Figure 18B).

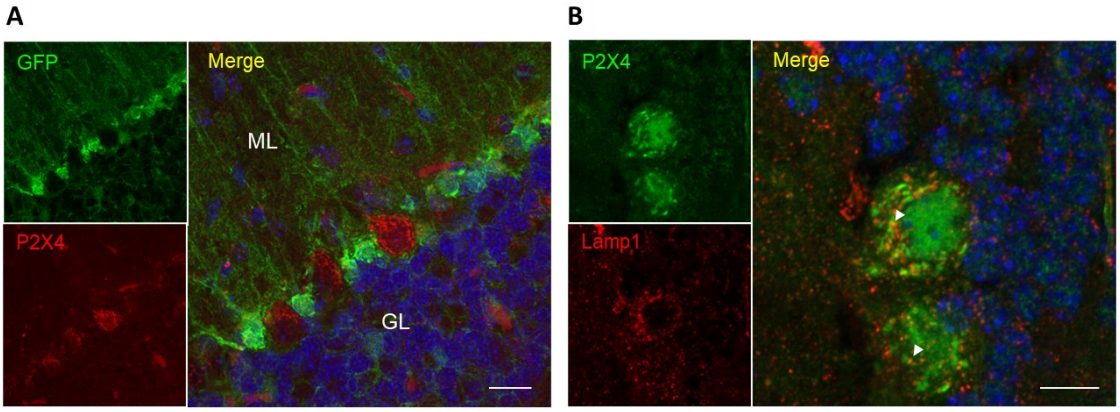

Figure 18: Images from the cerebellum of the sEGFP mouse model stained with anti-GFP, anti-P2X4, and anti-LAMP1 antibodies targeting neurons from the Purkinje cell layer. *Representative images from 3 independent experiments are shown from sagittal brain slices. ML, molecular layer; GL, granular layer. Scale bars 50 µm (A), 10 µm (B). A version of this figure has been published* (Ramírez-Fernández et al., 2020) *under the Creative Commons Attribution 4.0 International License.*

From these experiments, we learned that the sEGFP mouse model shows high reporter expression in the granular layer of the hippocampus and the Purkinje cell layer of the cerebellum. However, a question that remains unanswered is why there is an only sporadic expression of EGFP in the pyramidal cell layer. As mentioned above, EGFP-expressing cells from this layer might be responsible for the staining detected in the mossy fibers from the stratum lucidum at the CA3 region of the hippocampus. However, this needs to be confirmed given the negative co-localization of EGFP with the markers calbindin-1 and ZnT3.

Additional steps were proposed that included the implementation of a protocol to isolate embryonic neurons, which might be tested in immunostainings and morphology studies with the aim of investigating the expression of the reporter and the P2X7 receptor in neurons of the available mouse models, as well as the consequences of P2X7 ablation for neurons of the *P2rx7*$^{-/-}$ mouse. These experiments were planned to be done in the course of a laboratory rotation in the research group of Prof. Beáta Sperlágh at the Institute of Experimental Medicine (MTA-KOKI) in Budapest, Hungary. However, because of

the advance of the Covid-19 pandemic across Europe in March 2020, this laboratory visit was interrupted before significant progress could be made.

3.1.3.4 Astrocytes

Astrocytes are crucial for the regulation of homeostasis in the interstitial medium and the correct function of the neural network. The presence and function of P2X7 in astrocytes has also been under discussion, although its expression and involvement in NLRP3 inflammasome assembly, cytokine release and inflammatory responses has become more accepted in the recent years (Albalawi et al., 2017; Lu et al., 2017; Y. F. Zhao et al., 2021). Co-immunostainings of sagittal brain tissue slices were carried out for EGFP and the glial fibrillary acidic protein (GFAP), a marker for astrocytes (Figure 19). However, none of the samples tested with either of the reporter mouse models showed co-localization of EGFP with GFAP.

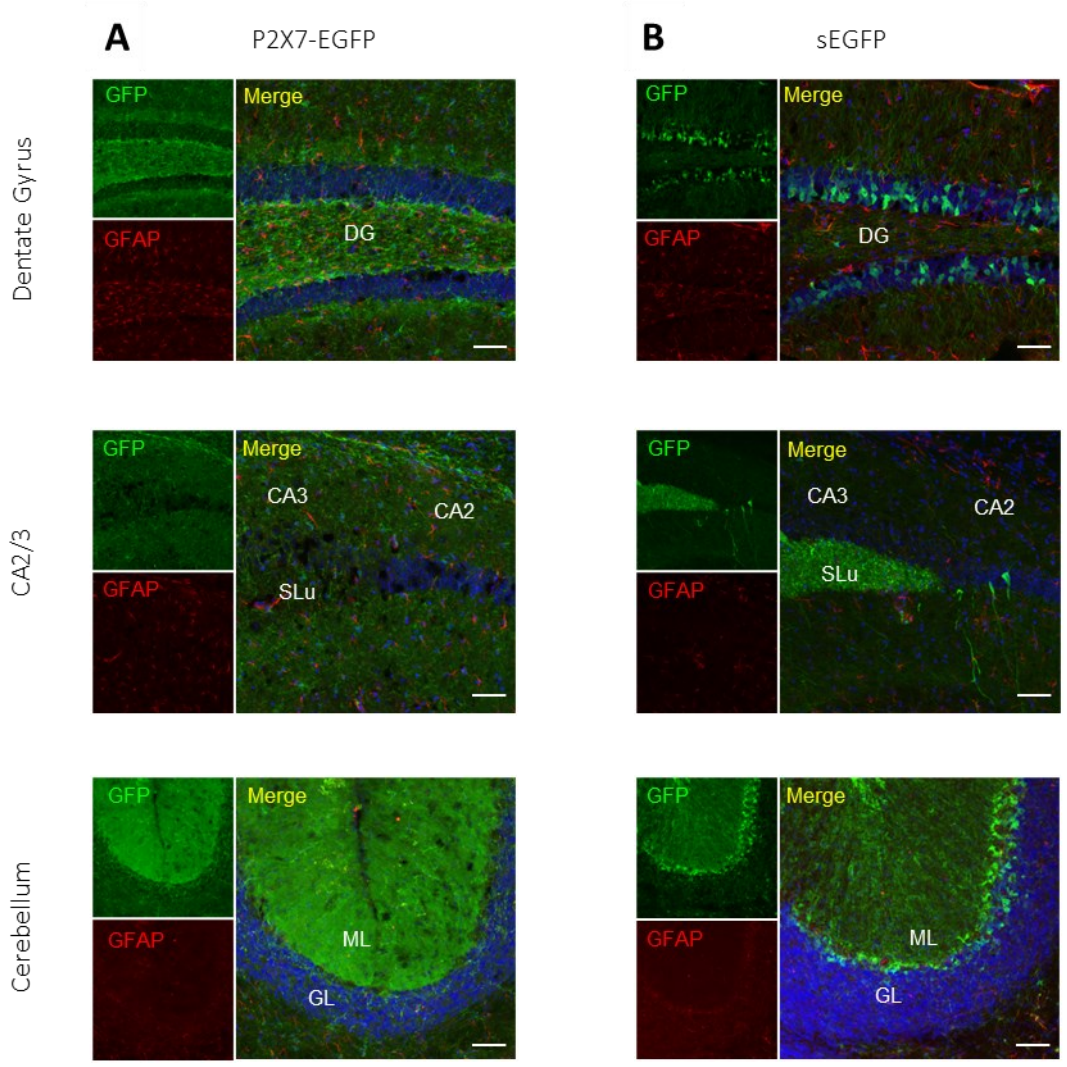

Figure 19: Cell-specific EGFP expression in both mouse models with a focus in astrocytes. *Samples were treated using anti-GFP and anti-GFAP antibodies, using DAPI for nuclear counterstaining. Representative images of sagittal brain slices from 3 independent experiments are shown for the dentate gyrus and CA2/3 region of the hippocampus as well as the cerebellum. SLu, stratum lucidum; CA, cornu ammonis; DG, dentate gyrus; ML, molecular layer; GL, granular layer.Scale bars 50 µm.*

3.2 Re-investigation of a P2X4-P2X7 interaction or functional interrelation using the BAC-transgenic P2X7 reporter mouse model

3.2.1 Pull-down assays on *X. laevis* oocytes expressing P2X7+P2X4 and P2X7-EGFP+P2X4

As mentioned above (section 1.4), studies providing evidence for and against a physical interaction between the closely related homomeric P2X4 and P2X7 receptors have been published in the literature (Antonio et al., 2011; Boumechache et al., 2009; Nicke, 2008). However, a large proportion of the studies that supported this hypothesis relied on the overexpression of the receptors in heterologous expression systems.

Once the validity of the BAC-transgenic P2X7-EGFP mouse model was confirmed, we next used this model to re-investigate the discussed P2X4R-P2X7R interaction, aiming for a higher degree of proximity to the physiolgical conditions. This assumption is based on the advantages that the BAC transgenic mouse brings, as it shows only moderate overexpression of P2X7 and it allows working with native tissue. Furthermore, the EGFP-tag enables visualization of both P2X4 and EGFP-tagged P2X7 receptors via fluorescence microscopy by co-staining with antibodies targeting P2X4 and EGFP. This is not feasible in the wildtype mouse since antibodies against P2X4 and P2X7 are both raised in rabbit. Lastly, the EGFP-tag gives the possibility to pull down EGFP and interacting proteins from complex samples.

As a positive control, we first performed co-immunoprecipitation experiments in *Xenopus laevis* oocytes, where a P2X4-P2X7 interaction was previously demonstrated via FRET experiments (Schneider et al., 2017). The injection of cRNA encoding for each of the receptors into *X. laevis* oocytes represents a valuable tool because it allows for the generation of protein that is quantifiable in short times. Furthermore, the ratio of expression from each receptor can be controlled by adjusting the proportion of cRNA that is injected into the oocytes, which provides an additional advantage.

RNA encoding for P2X4 and P2X7, as well as P2X4 and P2X7-EGFP, was injected into *X. laevis* oocytes. After the homogenization of the oocytes and protein extraction, co-purification experiments were carried out with anti-GFP nanobodies, followed by western blot using anti-GFP in combination with anti-P2X7 or anti-P2X4 antibodies to study the physical interaction of the receptors (Figure 20).

In agreement with the aforementioned study (Schneider et al., 2017), the Western blot revealed an interaction of P2X7-EGFP and P2X4 in *X. laevis* oocytes, given that the anti-P2X4 antibody showed a positive signal after the immunoprecipitation. Of note, a size shift takes place in the bands corresponding with the anti-GFP antibodies in the eluates. This is due to the low-pH glycine buffer used to detach the immunoprecipitated complexes from the GFP-Trap beads. In the negative control, in which non-tagged P2X7 and P2X4 were co-expressed, neither EGFP nor P2X4 and P2X7 were detected in eluates.

However, in the mouse lung samples, the pull-down extracts were negative for the anti-P2X4 antibody in all the wildtype and P2X7-EGFP samples. To exclude a dissociation of the complexes exerted by the detergent chosen for the membrane solubilization (NP40), the experiment was repeated using two other non-denaturing detergents, n-dodecyl-β-D-maltoside and digitonin, which is considered as a mild detergent. The results showed different degrees of efficiency during the protein extraction and pull-down processes. However, all of them gave a negative result for this interaction in the mouse tissue.

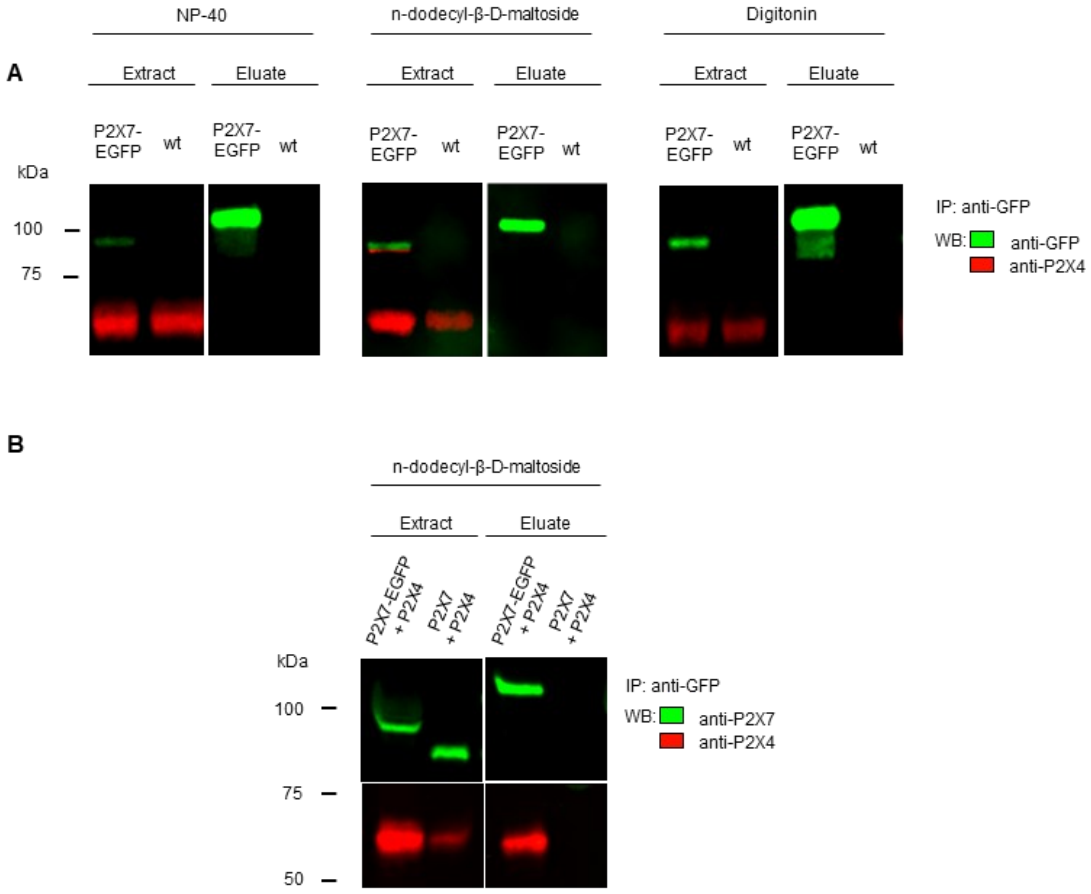

Figure 20: Western blot experiments following immunoprecipitation of P2X7 via the EGFP-tag from protein extracts of mouse lung and Xenopus laevis oocytes*. (A) Solubilization with three different detergents (1% NP-40, 0.5% n-dodecyl β-D-maltosyde and 1% digitonin) from wt and P2X7-EGFP mouse lung. (B) Co-purification of P2X4 with P2X7 upon expression in X. laevis oocytes and extraction with 0.5% n-dodecyl β-D-maltoside. Protein bands were stained with antibodies against P2X7, EGFP and P2X4 as indicated. Note that there is a size shift in the GFP bands from the eluates due to the low-pH glycine buffer used during the pull-down experiment. Representative results from at least three experiments are shown.*

From these data, we conclude that there is an interaction between P2X4 and P2X7-EGFP in *X. laevis* oocytes, in accordance with the previous report (Schneider et al., 2017). However, this interaction could not be detected applying the same pull-down approach in lung tissue from the BAC transgenic P2X7-EGFP mouse line. Thus, it is possible that expression of both receptors in oocytes might lead to artefactual interaction of P2X4 and P2X7-EGFP upon exacerbated expression under non-physiological conditions. We next focused on reproducing the conditions of this experiment in HEK293 cells,

aiming for an *in vitro* assay that might reproduce the conditions of the native mammal tissue with higher fidelity, as different regulatory events might take place that do not occur in oocytes.

3.2.2 Pull-down experiments with HEK293 cells

To test this hypothesis, we chose HEK293 cells as a heterologous expression system to study the interaction of both receptors as this system reproduces better the physiological conditions of the mammalian tissue. We transfected DNA encoding for P2X4 in both wt HEK293 cells as a negative control and a HEK293 cell line that was stably transfected with P2X7-EGFP (Figure 21).

After the preparation of protein extracts and pull-down with GFP-trap beads, the eluates did not show P2X4 positive bands, as the P2X4 signal corresponding to the stably transfected P2X7-EGFP HEK293 cells was not distinguishable from the background signal. This is in contrast with previous studies, where P2X4 was successfully co-purified with P2X7 from transfected mammalian cells and also from primary cells (Guo et al., 2007). However, as seen in figure 21, the P2X4 bands in the extract were more intense than those of the stably transfected P2X7-EGFP receptor, indicating that the stably transfected cells express rather low amounts of P2X7. A double transfection of DNA encoding for P2X7-EGFP and P2X4 might lead to higher amounts of protein and show artefactual positive results, due to aggregation of the unphysiologically overexpressed protein.

In summary, based on these data, we conclude that the high overexpression of these proteins in *X. laevis* oocytes leads to an aggregation of receptors during synthesis that result in the positive results of the co-purification assay. However, in lung tissue from the P2X7-EGFP BAC transgenic mouse model and in transfected HEK293, which more realistically reproduce the physiological conditions, a moderate overexpression is not able to induce an interaction of P2X7 and P2X4 that can be detected using these methods.

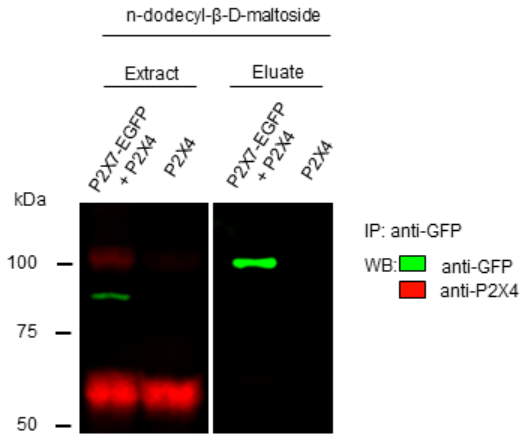

Figure 21: Western blot experiments following GFP-tag immunoprecipitation from protein extracts of HEK293 cells *under the treatment with 0.5% n-dodecyl β-D-maltosyde during the protein extraction and immunoprecipitation. Protein bands were stained with antibodies targeting P2X4 and EGFP. Representative results from at least 3 independent experiments are shown.*

3.2.3 Mutual interrelation of P2X4 and P2X7 receptors

Previous studies have shown that changes in expression levels of one of these receptors is able to influence the expression of the other, giving proof of a functional interrelation between both P2XR subtypes. This has been proposed for the mouse kidney and in dendritic and epithelial cells, to name a few (Craigie et al., 2013; Weinhold et al., 2010; Zech et al., 2016). Conversely, other studies were not able to find a functional interrelation in immune cells and microglia (Kawano et al., 2012; Trang et al., 2020).

Therefore, our next step was to analyze such an interrelation of both receptors comparing the effect of different levels of expression in the mouse lung. For this, western blot experiments were performed with lung samples from the wildtype and our P2X7-EGFP mice, as well as the P2X7$^{-/-}$ and P2X4$^{-/-}$ models (Figure 22).

Results from these experiments were pooled with the ones previously obtained by my colleague Dr. Robin Kopp and, in spite of showing certain degrees of variability, no significant differences were found between the expression of each receptor in either knockout model in comparison with the wildtype mouse. Furthermore, overexpression of the P2X7 receptor in the P2X7-EGFP mouse lung did not lead to a significant alteration of P2X4 levels. Therefore, we found no proof of an interrelation between P2X4 and P2X7 in these mouse models.

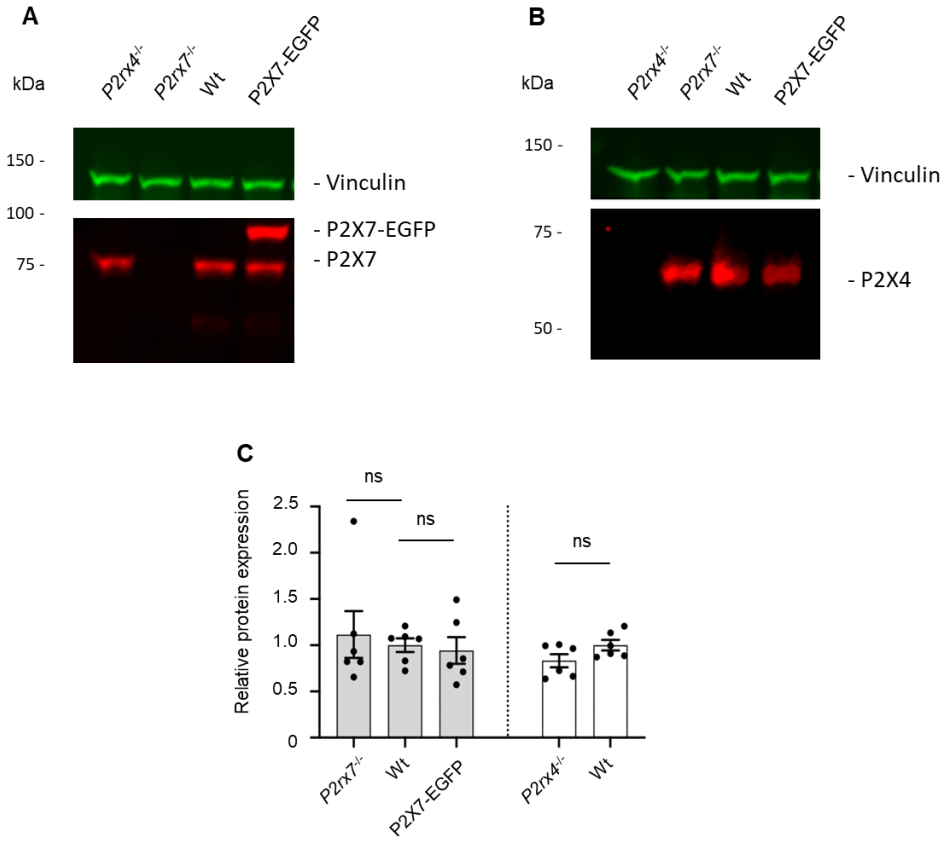

Figure 22: Western blot experiments to explore interrelation of P2X4R and P2X7R. *Deletion or overexpression of P2X7 does not affect the P2X4 protein level and vice versa. Comparison of P2X7 and P2X4 protein levels in the P2rx4-/-, P2rx7-/-, wildtype and the P2X7-EGFP mouse model (tg). A representative*

*western blot experiment using anti-P2X4, anti-P2X7 (red) and anti-vinculin (green) as a loading control is shown. 50 µg of total protein from mouse lung were loaded in each well, and the two independent experiments were performed with at least five mice of both sexes in total (10-35 weeks of age). Mann-Whitney test was carried out to determine significance. Grey bars: P2X4; white bars: P2X7 (**p<0.01).*

3.3 Comparative proteomic analysis of tissue/cells from wt and *P2rx7*$^{-/-}$ and P2X7-EGFP mice

3.3.1 Comparing of protocols for mass spectrometry experiments from mouse hippocampus samples

Although the role of P2X7R in cytokine release and inflammation has been extensively studied, other functions of this receptor and the exact signaling mechanisms that are triggered by P2X7R activation are not completely understood (Bartlett et al., 2014; De Marchi et al., 2016; Kopp et al., 2019). Discovery and investigation of the intermediaries that are involved in P2X7R signaling will lead to further insights about its role in health and disease. Therefore, a proteomic approach was proposed for this project which aimed to quantitatively compare general protein expression patterns in the mouse tissue under P2X7 ablation (knockout, P2X7$^{-/-}$ mouse), P2X7 physiological levels (wildtype mouse), and P2X7 overexpression (P2X7-EGFP BAC transgenic mouse).

Several protocols were compared for the preparation of samples from mouse tissue prior to liquid chromatography coupled to mass spectrometry. These included the tissue dissociation and generation of membrane extracts that would be subject to precipitation (using acetone or trichloroacetate), based on a previous protocol (Bruderer et al., 2017), and finally delivered to the mass spectrometry facility for the later digestion, alkylation, and fractionation of the samples prior to LC-MS. However, another method was tested later which proved more effectiveness and reliability. This was a modified protocol from a commercial kit provided by PreOmics GmbH based on the FASP protocol for sample preparation (Wiśniewski, 2018). This protocol included key steps such as the tissue dissociation, digestion and alkylation of the samples, and purification of the proteins before the delivery of the samples for LC-MS analysis.

Hippocampal samples were taken from P2X7$^{-/-}$, wildtype and P2X7-EGFP mice in order to assess possible differences in protein expression patterns in the absence of P2X7 or upon its overexpression. After processing the lung tissue following the PreOmics protocol, samples were analyzed in the laboratory of Dr. Thomas Fröhlich (Gene Zentrum, Munich).

Analysis of the samples revealed differences in several proteins when comparing the mouse genotype backgrounds in pairs (Figure 23). However, no robust candidates were found that showed statistically significant differences in their expression levels after running a false-positive test, given the high Q-value calculated in the preliminary analysis.

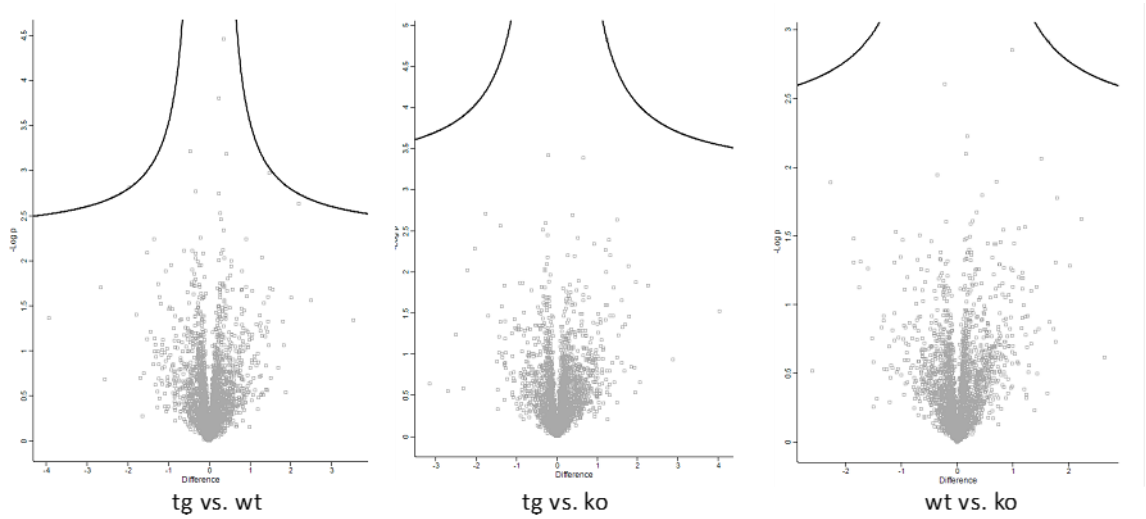

Figure 23: Volcano plot comparing hits obtained by mass spectrometry on mouse hippocampus from our three genetic backgrounds (N=5). *The X axis represents fold difference, while the Y-axis shows -Log p-value.*

3.3.2 Development of a protocol to isolate microglia from adult mice as an alternative to mouse tissue experiments

P2X7 protein is highly expressed in the brain and it has been identified in several cell types of different regions (refer to section 1.2.3). In the hippocampus, P2X7-EGFP is highly expressed in microglia and oligodendrocytes but distribution in astrocytes and neurons could not be proved in this study. Therefore, the previous proteomic analysis might have failed to identify major changes in protein expression since it included many different cell types that can be expected to produce a high background. Thus, we decided to investigate possible effects of P2X7 deletion or overexpression using a cell-specific approach in a cell type that is known to have a high level of P2X7 expression. We opted for microglia since it is a cell type that has been widely studied for its P2X7 expression, and it is of great relevance in P2X7R-induced neuroinflammation. Therefore, investigation of P2X7R signaling in this cell type might provide insights for P2X7R function in the CNS, which is a matter of discussion, as already mentioned.

With this objective, I adapted and optimized a protocol provided by Miltenyi Biotec B.V. & Co. for the isolation of microglia from adult mouse brain. The development of this protocol resulted in effective isolation of microglia cells which was verified by immunofluorescence staining using antibodies targeting Iba1 and EGFP on the obtained primary cultures from the *P2rx7*$^{-/-}$, wildtype and P2X7-EGFP mice at 3, 7 and 14 days *in vitro* (Figure 24).

In the future, the protocol will need to be upscaled in order to prepare samples of the needed amount of protein for mass spectrometry. This procedure will be useful in the preparation of samples for mass spectrometry and the analysis of general protein expression patterns under the three genotype backgrounds.

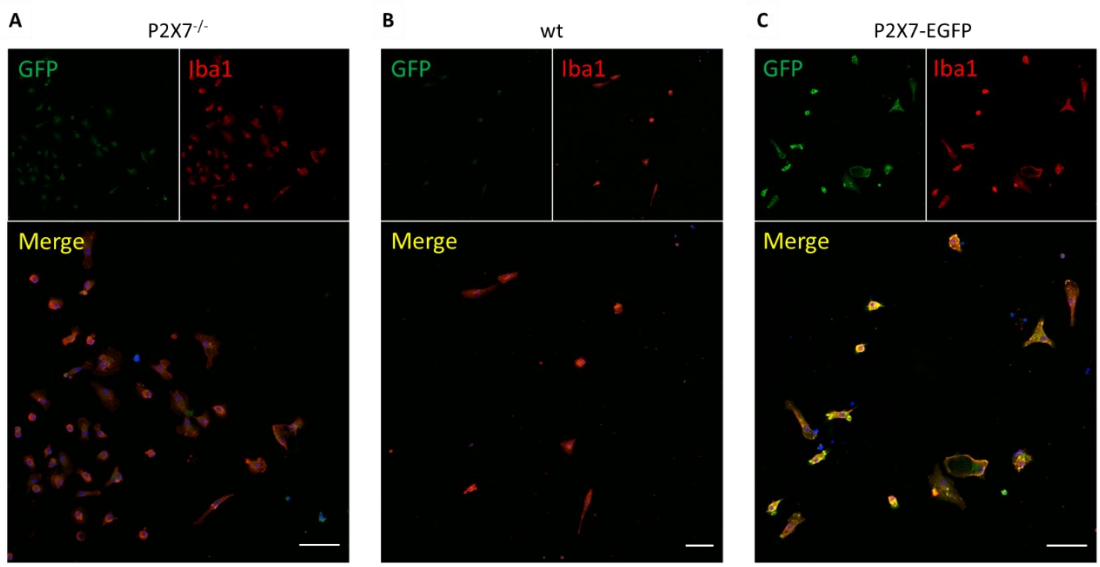

Figure 24: Immunofluorescence images of microglia cells isolated from adult mouse brain stained with antibodies targeting Iba1 (red) and GFP (green) of P2rx7$^{-/-}$, wildtype and the P2X7-EGFP mice *at 7 days in vitro, showing DAPI as a nuclear staining. Representative images from 3 independent experiments are shown. Scale bars 50 µm.*

4. Discussion

4.1 Comparison of P2X7 reporter mouse models and investigation of P2X7 localization

The ionotropic P2X receptors have arisen as potential therapeutic targets due to their reported involvement in health and disease (Burnstock & Kennedy, 2011; Khakh & North, 2006; North & Jarvis, 2013). From the seven members of this family, P2X7R has attracted special interest because of characteristics that make it unique, namely its low affinity for the agonist ATP, its large intracellular C-terminus and its ability to induce the formation of a macropore under sustained stimulation (Kopp et al., 2019). However, questions remain unanswered regarding the tissue and cell type distribution of this receptor, as well as the interaction partners and the signaling events triggered by P2X7R activation. Strategies have been developed with the aim of studying P2X7 distribution and function in the organism, among which mice represent a good option due to advantages such as the genetic proximity to humans, the short generation time, and simplicity to handle.

A number of mouse models have been designed to study P2X7R (Sluyter et al., 2023; Urbina-Treviño et al., 2022). A *P2rx7*$^{-/-}$ mouse from the European Mouse Mutant Archive (*P2rx7*$^{tm1d(EUCOMM)Wtsi}$) was generated by using the Cre/LoxP system and has been used for this dissertation (Kaczmarek-Hájek et al., 2018). Humanized mouse models have also been generated, one of them (*P2rx7*$^{tm1.1(P2RX7)Jde}$) by substitution of the murine *P2rx7* exon 2 via knock-in (human *P2rx7* exons 2 to 13), which results in humanized P2X7R whose expression is controlled by the murine *P2rx7* promoter (Metzger et al., 2017).

However, a careful characterization of the available mouse models is needed in order to obtain results that are consistent and reliable. In P2X7 research, some of these models have failed to meet the expectations. For example, this is the case of commercially available *P2rx7* knockout mouse models generated by Pfizer (Solle et al., 2001) and GlaxoSmithKline (Sikora et al., 1999). The first of these was generated by deletion of exon 13 and showed partial expression of truncated variants of the receptor. The latter exhibits expression of the P2X7k receptor as a result of the expression of the alternative 1' exon in the *P2rx7* gene (Masin et al., 2012).

The lack of reliability of some of the available mouse models and the absence of selective agonists, as well as the poor specificity of antibodies (Anderson & Nedergaard, 2006) has led to a constant debate over the last years in terms of the tissue distribution and cell-specific localization of P2X7R. Taking this into account, the development of reporter mouse models is a promising alternative because it allows the direct detection of the protein and/or its site of expresssion *in situ* in cases where it is not possible to label the target specifically and effectively with antibodies or other tools. In comparison with other reporter proteins, the use of EGFP has been well established in animal models, and the

possibility of designing fusion proteins by addition of an EGFP tag allows subcellular visualization of protein targets, which is another great advantage (Serganova & Blasberg, 2019).

In this project, we used and compared two different BAC transgenic mouse models that were generated using different approaches. In one of them (Kaczmarek-Hájek et al., 2018), the reporter protein EGFP is fused to the receptor (P2X7-EGFP). In the other one (Gong et al., 2003), EGFP is expressed as a soluble protein (sEGFP from GenSat). In both cases, the protein expression is controlled by the *P2rx7* endogenous promoter which is present in the BAC. Thus, both models were designed to induce a reporter distribution that mimics the expression patterns of the endogenous P2X7 receptor in the wildtype mouse. However, a preliminary comparison of the mouse models, based on the limited information available for the sEGFP mouse, indicated divergent cell-specific distribution of the reporters (Kaczmarek-Hájek et al., 2018). Therefore, a more detailed characterization and comparison of cell type- and region-specific expression was needed.

4.1.1 P2X7 and P2X4 expression levels

In the western blot experiments described above, P2X7-EGFP protein levels were around three times higher in comparison to the endogenous P2X7 protein in the transgene and wildtype mouse. This is in line with a previous report and is explained by the integration of several copies of the modified BAC clone (Kaczmarek-Hájek et al., 2018). The transgenic P2X7 can easily be differentiated from the endogenous receptor by its higher molecular weight. As the *P2rx4* gene is not present in this BAC clone, we did not observe any significant differences in the level of expression of P2X4 when compared to the wildtype mouse. This is also a supporting argument against a functional relationship between both receptors, as levels of P2X4 are not altered upon P2X7 overexpression, something that will be discussed later on.

In contrast, the sEGFP mouse model shows a P2X4 overexpression that is explained by the presence of the *P2rx4* gene in the BAC clone. However, P2X7 was unexpectedly overexpressed in this model as well. A possible assumption based on the overexpression of P2X7 and P2X4 is that this mouse model might show phenotypical differences, given the role of both receptors in cytokine release and inflammation (Adinolfi, Giuliani, De Marchi, et al., 2018; Kanellopoulos et al., 2021; North, 2002). It has been reported that both P2X7R and P2X4R have a role in lung disease, retinal dystrophy or protection against bacterial infection, to name a few (Csóka et al., 2018; Martínez-Gil et al., 2022; Wiley & Gu, 2012; Winkelmann et al., 2019), Moreover, both receptors have attracted an increasing interest due to their involvement in pathophysiology of the CNS, having a suggested role in spinal cord injury, neuropathic pain, or multiple sclerosis (Andrejew et al., 2020; North & Jarvis, 2013; Tozaki-Saitoh et al., 2022). For example, our collaborators from the Tobias Engel's laboratory at the RCSI (Dublin, Ireland) confirmed that the sEGFP mice experience a decreased neurodegeneration following *status epilepticus* (Ramírez-Fernández et al., 2020).

4.1.2 General expression patterns of P2X4, EGFP and P2X7

Ectopic gene expression may occur as a consequence of the BAC transgenesis. Taking the overexpression of *P2rx4* in the sEGFP mouse model, I focused on P2X4 expression over the brain of this mouse and compared it to the wildtype mouse in order to check for possible aberrant patterns in the distribution of this receptor. However, we have not detected abnormal patterns in the immunofluorescence stainings making use of the anti-P2X4 antibody and comparing this model with the wildtype mouse. However, striking results were found in the study of the reporter EGFP distribution on the brain slices, given that the expression pattern of the sEGFP model was remarkedly different to the P2X7-EGFP mouse.

While the P2X7-EGFP mouse showed a widespread reporter distribution throughout the brain, the sEGFP mouse showed a much more localized expression of EGFP. In the cerebellum, EGFP signal was increased in the molecular layer, as well as the area of the Bergmann glia and the Purkinje cell layer. A high signal was also evident in the superior colliculus and pons as well as the caudate putamen region which, similarly to the cerebellum, is also related to motor function.

These differences brought up further incongruencies when I compared the endogenous and overexpressed P2X7 distribution in both mouse models using the *P2rx7*$^{-/-}$ model as negative control. The distribution patterns observed by the use of an anti-P2X7 nanobody did not show the differences that were found in the GFP reporter between the two BAC transgenic mouse models. Surprisingly, the receptor showed identical distribution in both mouse lines. This distribution pattern was indeed overlapping with the anti-GFP staining pattern of the P2X7-EGFP mouse. Therefore, there is a mismatch between the distribution of the soluble EGFP and P2X7 protein in the sEGFP mouse model, even though the genes responsible for P2X7 and EGFP are controlled by the same promoter. This is an important limitation of P2X7R localization studies that have based their conclusions on the expression patterns of the soluble EGFP reporter in this mouse model (Jimenez-Pacheco et al., 2016; Ortega et al., 2021; A. Sebastián-Serrano et al., 2016).

4.1.3 Differences in cell type-specific EGFP localization in the mouse brain

After comparing the general distribution of EGFP in the mouse brain and revealing differences between the two mouse models, I proceeded to perform co-immunostainings using antibodies targeting GFP and different cell-specific markers in order to evaluate de cell-specific distribution of the reporter.

The divergent cell-specific distribution of EGFP in the BAC transgenic mouse models is a new point of discussion regarding the ectopic reporter expression in the sEGFP. As demonstrated, the sEGFP mouse model showed co-localization of EGFP and the marker NeuN, corresponding with neurons, in contrast to the P2X7-EGFP model in which EGFP

co-localized with Iba1 (microglia) as well as Olig2 and MBP (oligodendrocytes), as reported before (Kaczmarek-Hájek et al., 2018).

In the hippocampus, the sEGFP model showed high signal from the anti-GFP antibody in single cells from the granular layer of the dentate gyrus and the pyramidal cell layer of the CA region. Most likely, projections of these cells are the ones that show high GFP signal in the mossy fiber region from the stratum lucidum in CA3 (Figure 17 in results). However, the exact neuronal cell type corresponding with these GFP-positive fibers could not be identified. The marker calretinin was not found in this region, in agreement with the assumption that the mossy fibers derive from pyramidal neurons. However, we also found absence of co-localization between GFP and ZnT3, or calbindin-1, although these markers were indeed expressed in this area.

This region might be of interest, as it shows an increase of the brain-derived neurotrophic factor (BDNF) following seizures (Danzer & McNamara, 2004). BDNF has been linked to P2X7R, and specially to P2X4R. For example, activation of P2X7R and P2X4R has been proposed to mediate in the physical exercise-induced increase of BDNF levels that results in the modulation of synaptic plasticity and amelioration of neuronal damage during stroke (Sun et al., 2023). Moreover, P2X4 activation upon nerve injury promotes BDNF release in Schwann cells and microglia, which leads to remyelination (Domercq & Matute, 2019). Therefore, overexpression of both receptors and the increase of BDNF could be a reason for the decreased neuronal damage that has been found in the sEGFP mice following status epilepticus (Ramírez-Fernández et al., 2020). However, it must be reminded that, while EGFP signal is present in this region, this has not been the case for the P2X7 receptor as shown via immunofluorescence and DAB staining (Figures 10 and 11). With the data that is available in our laboratory, such a relationship between BDNF and P2X receptors in the stratum lucidum of the sEGFP mouse can only be suggested for P2X4, which is highly expressed in the pyramidal cell layer and stratum lucidum of the CA3 region (Figure 8).

In the cerebellum, the EGFP pattern was more similar between the two BAC transgenic mouse models, with a higher intensity of the staining in the molecular layer (Figures 9 and 10). However, single, neuron-like cells attracted our attention in the case of the sEGFP mouse (Figure 16). In the Purkinje cell layer, occasional EGFP staining might represent Purkinje cells, given the co-localization with the marker Calbindin-1. In the molecular layer, immunostaining revealed intermittent co-localization of EGFP with parvalbumin and NG2. Parvalbumin-positive cells might be basket or stellate cells, cell types that receive excitatory inputs from axons of the granular cell layer (also known as parallel fibers) and communicate with each other and with Purkinje cells through inhibitory signals (Brown et al., 2019).

Taken together, in the P2X7-EGFP mouse model, EGFP is present in microglia and oligodendrocytes. However, the soluble EGFP from the sEGFP mouse shows predominant expression in neurons from the Purkinje cell layer and the basket and stellate cells from the molecular layer of the cerebellum as well as sparse distribution in single neurons

from the granule cell layer of the dentate gyrus and the pyramidal cell layer from the CA region of the hippocampus, whose axons are projected within the mossy fiber region of the stratum lucidum. Lastly, NG2-positive cells that might correspond to NPCs show EGFP expression. Therefore, a possibility might be proposed that EGFP is expressed in early stages of cell development in the NPCs but only remains to be expressed when cells differentiate into neurons and not into oligodendrocytes nor astrocytes, or at least not at levels above the detection limit.

4.1.4 The sEGFP BAC transgenic mouse model construct

In this project, we have uncovered inconsistencies in the sEGFP mouse model reporter expression, which does not correlate with that of the P2X7-EGFP nor with the endogenous P2X7 distribution in the sEGFP mouse itself. There are several factors that may account for the aberrant distribution of the reporter protein.

To understand these discrepancies, we need to take the BAC construct designs into consideration. The P2X7-EGFP construct was generated by addition of the reporter cDNA through a linking sequence to the very C-terminus of the receptor. This means that the *P2rx7* gene was nearly unchanged. In contrast, the sEGFP mouse construct was generated by insertion of the sequence encoding EGFP into the exon 1 of the *P2rx7* gene. For simplicity, only one homology arm was used, and the BAC plasmid was not resolved in this cloning strategy. The sequence of the P2rx7 gene was interrupted by a STOP codon and polyadenylation signal (Gong et al., 2010). Therefore, a modification of the gene structure must be considered. The interruption of the *P2rx7* gene in the BAC construct might lead to silencing of key regulatory elements that govern the expression of the gene. Moreover, absence of distal regulatory elements that modulate gene expression of either *P2rx7* or the genes surrounding the insertion site of the BAC might be considered. For example, there is a possibility that regulation of the P2X7k variant through expression of the alternative exon 1' could be altered as a consequence.

The recombination strategy also explains the overexpression of the P2X7 receptor in the sEGFP mouse model. This was unexpected because the insertion of a stop codon and a polyadenylation signal after the sequence that encodes for EGFP should have prevented the expression of the *P2rx7* gene. However, an amplification and sequencing strategy (designed and performed by my colleague Anna Durner) confirmed the duplication of the homology domain A used for the recombination (from 332 bp upstream of the transcription start to 163 bp downstream of the transcription start). This was duplicated because only one homology arm was used, and the BAC was not resolved (Gong 2010). This strategy, known as the one-step RecA method (Yang, 2009), simplified the generation of the transgenic mouse lines developed within the GenSat project. A consequence of this is the presence of a second transcription start codon ATG due to the duplication of the homology domain, thus allowing *P2rx7* transcription in the BAC clone. However, it should be borne in mind that the P2X7 protein levels measured in the sEGFP mouse were much lower than P2X4, and this is likely due to the alteration of regulatory elements

of the *P2rx7* gene. However, an interrelation effect of both receptors cannot be excluded (Casas-Pruneda et al., 2009; Weinhold et al., 2010).

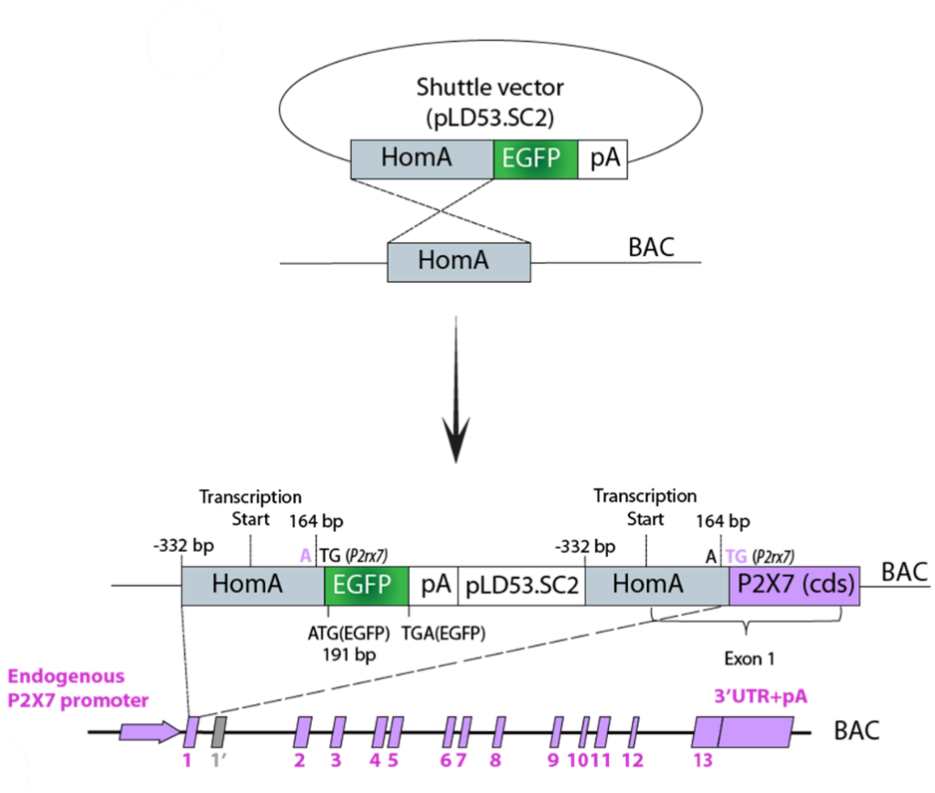

Figure 25: BAC design in the sEGFP mouse model. *The one-step RecA method resulted in the duplication of the homology domain (HomA) and led to a second transcription start codon ATG that enables P2rx7 gene expression. Below, a representation of the P2rx7 gene inserted in the BAC clone is shown, and the boxes represent the exons and the 3'UTR+polyA tail. 1' is the alternative exon 1 whose expression leads to the P2X7k variant.*

4.1.5 The BAC transgenic approach

The use of BAC transgenic mouse models in biomedical research has greatly advanced the investigation of protein expression and function *in vivo*. Major advantages that this technology brings are the possibility of reproducing the distribution of an endogenous protein thanks to the possibility of including a complete gene along with regulatory sequences in the BAC construct, its transmission to the progeny and the possibility of including reporter genes that allow for the localization or even direct visualization of a protein. In addition, they provide only moderate overexpression of target genes, which is of interest because it leads to gene expression levels that are close to the physiological conditions.

BAC transgenic mouse lines have also been used to develop Cre driver lines. This system uses a Cre recombinase that is activated under specific conditions (*e.g.* expression under the control of the promoter of a gene that is specific for a particular cell type) and exerts recombination on a target gene that is flanked by the LoxP sequences, the target sites of the Cre recombinase. These systems are used for the generation of conditional

reporter and knockout mouse lines (Kaczmarek-Hájek et al., 2018; Kim et al., 2018; Requardt et al., 2009; X. F. Zhao et al., 2019).

However, the BAC transgenic approach has important disadvantages that might account for inconsistencies in some of the models that have been developed (Beil et al., 2012). Firstly, the untargeted insertion of large amounts of DNA from the BAC chromosome might alter the gene structure at the insertion site. Thus, a certain degree of genome instability might be considered responsible for possible deletion or mutation in the DNA. Secondly, the BAC chromosome might lack distal regulatory elements involved in the cell type-specific expression and this could lead to incorrect localization (ectopic expression) and function of the protein of interest. Thirdly, there are features that escape control in the design of the BAC strategy, such as the number of copies and the lack of specificity of the integration site. Insertion into a region where it is under the control of another promoter, or changes in the gene structure of the inserted gene, might also lead to aberrant distribution of the BAC encoded protein, as well as variability in the expression levels of the affected gene, meaning overexpression or underexpression. Therefore, thorough studies are needed in order to validate a BAC transgenic mouse model.

Other BAC transgenic mouse models showing ectopic expression of the reporter gene have been described in the literature. For example, following the crossing of reporter mouse models with cre-driver lines and generation of three cre-dependent microglia-specific Cx3cr1 mouse lines, a careful analysis revealed that one of them, expressing GFP, showed “leakiness” in different cell types while the two others were showing specific GFP signal in microglia (X. F. Zhao et al., 2019). Here, it was suggested that one of the original reporter mice was responsible for the ectopic GFP distribution. However, there is controversy regarding the possible transient expression of Cx3cr1 in neurons and astrocytes that might be responsible for the ectopic distribution. In a different example, studies point out differential expression patterns of the target protein corticotropin-releasing factor (CRF) from reporter mouse models not only depending on the reporter of choice *e.g.* tdTomato or GFP (Hooper & Maguire, 2016), but also on the strategy chosen for the transgenesis *e.g.* BAC or Cre-loxP system (Chen et al., 2015).

It has even been suggested that BAC transgenesis should be replaced by other technologies in order to overcome the drawbacks mentioned above (Beil et al., 2012). These are mainly focused on the “designer nucleases”, namely the Zinc Finger Nucleases (ZFNs) and Transcription Activator-Like Effector Nucleases (TALENs). Here, direct injection of DNA or mRNA encoding for these nucleases into the cytoplasm of zygotes leads to synthesis of such enzymes, which generate targeted double strand breaks in the host DNA. Simultaneous microinjection of the gene sequence of interest into the pronucleus results in the knock-in of such sequence at the nuclease-generated insertion site.

In summary, it is necessary to carefully plan the generation strategy and carry out a careful study and characterization of the resulting transgenic mouse models before applying them in biomedical research and drawing conclusions that might be misleading.

The sEGFP mouse model has been used in the study of the central nervous system, for example regarding P2X7 localization in neurons (Jimenez-Pacheco et al., 2016; Martínez-Frailes et al., 2019). However, the results shown in this dissertation suggest that the reliability of this mouse model is compromised given the leaky expression patterns of the reporter EGFP over the brain and the overexpression of P2X7. Therefore, findings obtained using this mouse model in previous studies should be taken cautiously and re-evaluated.

4.2 Re-investigation of the physical interaction or functional interrelation between P2X4 and P2X7 receptors

4.2.1 Evidence for and against a physical P2X4/P2X7 interaction

The interaction of P2X4 and P2X7 has been discussed in chapter 1.4, stating that P2X4 is the most similar subunit to P2X7 within the P2X family, and that they are co-expressed in different cell types in mammals (Guo et al., 2007; Ma et al., 2006; Novak, 2011; Xiang & Burnstock, 2005). Furthermore, similar cellular functions have been attributed to P2X7 and P2X4, and roles have been proposed for both receptors in several diseases, especially in the lung and the central nervous system (Domercq & Matute, 2019; Martínez-Gil et al., 2022; Savio et al., 2018; Zech et al., 2016).

In our studies, we used HEK293 cells and mouse tissue as model systems to evaluate the physical interaction of P2X4R and P2X7R, making use of the P2X7-EGFP fusion construct in order to pull down protein complexes of interest from our samples, as described previously. *X. laevis* oocytes were used as a positive control, since an interaction between both receptors had already been reported based on FRET analysis in this system (Schneider et al., 2017).

After performing protein extraction, pull-down and western blot from mouse lung tissue, the signal from the antibody targeting P2X4 was missing from the blot, meaning that P2X4 protein was not contained in the EGFP-bound complexes. A first assumption might be that, in the mouse tissue, the interaction of both receptors is either missing or only transient. The experiment was done using three different non-denaturing detergents NP-40, n-dodecyl-β-D-maltoside and digitonin to exclude a breakdown of complexes during the purification. In particular, digitonin is known as a mild detergent that depends on cholesterol in order to induce an increase in membrane permeability without causing major membrane disruption (Sudji et al., 2015). However, in none of the samples a signal corresponding with P2X4 was found after the pull-down step. In contrast, P2X4 was present in the eluates of the *X. laevis* oocytes' samples, confirming an interaction in this system.

Following the experiments in mouse lung tissue, a similar approach was applied to HEK293 cells (used as a negative control) and HEK293 cells that were stably transfected

with DNA encoding for the fusion protein P2X7-EGFP. Both were transfected with DNA encoding for P2X4, assuming that this would be a model that might reproduce better the physiological conditions of a mammalian tissue. However, the results were similar to those obtained with the mouse lung, as P2X4 was present in the extracts but appeared absent in the pull-down eluates of both the HEK293 cells (negative control) and the HEK293 expressing P2X7-EGFP.

In conclusion, an interaction between P2X4 and P2X7 could not be found in the mouse tissue, nor in transfected HEK293 cells. This interaction was only confirmed using *X. laevis* oocytes as a heterologous system that expresses both receptors at levels that are high enough to provoke an interaction that can be detected with the tools that are available in our laboratory.

4.2.2 Methodological aspects and limitations

Xenopus laevis oocytes represent a valuable option as a heterologous expression system (Bröer, 2003; Tammaro et al., 2008) because they allow for a fast protocol and the protein amount can be adjusted depending on the cRNA amount that is injected in the oocyte. This is an advantage of this model in comparison to HEK293 cells because, even though the procedure with HEK293 cells is faster, *X. laevis* oocytes offer a wider range to work with in terms of controlling the protein expression levels of the target. In this case, the receptors were expressed by the oocytes at levels that were higher than in mouse tissue or HEK293 cells. This made possible that an interaction was detected after pull-down, but it might be argued that such interaction could be an artifact, product of an exacerbated synthesis of both receptors at levels that are not found in physiological conditions.

The lack of evidence of an interaction shown in mouse tissue and HEK293 cells conflicts with previous reports where the interaction was found in primary epithelial cells and macrophages as well as alveolar epithelial cells (Guo et al., 2007; Hung et al., 2013; Pérez-Flores et al., 2015; Weinhold et al., 2010). Even though the P2X7-EGFP mouse model shows an overexpression of the P2X7 receptor, this is only mild and might not be sufficient in order to prove an interaction with P2X4R that is stable and above the detection limit. Moreover, it should be noted that P2X7R is mostly expressed in the cell membrane, whereas P2X4 shows predominance in lysosomes (Kanellopoulos et al., 2021; Murrell-Lagnado, 2018). Thus, even if they are co-expressed in several cell types, they do not share full subcellular distribution, and this is something to take into account when evaluating the possibility of a long-term interaction between both receptors.

Lastly, our experiments in HEK293 cells show higher expression of P2X4 than P2X7-EGFP, meaning that transient transfection might lead to higher protein amounts in comparison with the stable transfection. Indeed, a recent comparison of HEK293 cells that were transiently and stably transfected with P2X7 revealed large amounts of intracellular protein in case of the former and small amounts of membrane-localized P2X7 in case of

the latter (unpublished data from the laboratory). This might be a reason why the interaction between both receptors could not be demonstrated, in contrast with a previous report (Guo et al., 2007).

Although the described experiments and results obtained in the study of the discussed interrelation between P2X4 and P2X7 gave no evidence of such an event, there are limitations of this approach, and the following aspects should be taken into consideration.

1) These studies have been applied to whole mouse lung tissue, although other tissues or specific cell populations might be more suitable due to a higher expression of P2X4 and P2X7. For example, in the salivary gland, an interaction has already been suggested in the form of heterotrimers (Casas-Pruneda et al., 2009) based on functional experiments where P2X4R and P2X7R were co-expressed, exhibiting ATP-induced currents that would not be explained by the activation of either receptor alone. However, blue native-polyacrylamide gel electrophoresis (BN-PAGE) experiments failed to detect any association of the receptors after purification from salivary gland (Nicke, 2008). Furthermore, the tissue-specific approach might be not sufficient in order to get valid conclusions on this aspect based on the heterogeneity of cell types involved. Thus, a cell-specific approach might lead to more precise findings if applied to cell types that express both isoforms.
2) Limitations of the pull-down experiments should be taken into consideration. Although the co-immunoprecipitation of P2X4 and P2X7-EGFP in *X. laevis* oocytes might be a result from an actual interaction, it may be assumed that such event might be a result from the tendency of P2X4 to aggregate when expressed at high levels. Examples are found in this dissertation (figures 7, 20 and 21), where P2X4 aggregated even in the presence of the SDS buffer. Whether this aggregation events occur at the plasma membrane or at subcellular compartments is a remaining question from our study. As already mentioned, an argument against the interaction of P2X4 and P2X7 subunits is that P2X4 shows predominant distribution in lysosomes (Kanellopoulos et al., 2021). However, both receptors have roles in vesicle trafficking, and it is possible that the interaction only takes place at specific subcellular levels (Murrell-Lagnado & Frick, 2019; Qu & Dubyak, 2009). The possibilities might range from the trans-Golgi network to the very endoplasmic reticulum during protein synthesis. It has been shown that exacerbated gene expression might lead to stress at the endoplasmic reticulum, ineffective protein folding and aggregation (Hamdan et al., 2017; Li & Sun, 2021).

4.2.3 Future perspectives

Given the limitations of these studies, there are further experiments that can be suggested for future investigations. As discussed, the HEK293 cells that are stably transfected with P2X7-EGFP show lower protein amount of P2X7-EGFP than P2X4 when transiently transfected with DNA encoding for P2X4. Thus, an additional experiment could be to use double-transfected HEK293 cells that show transient expression of both

P2X4 and P2X7-EGFP. This might lead to higher amount of both proteins, possibly allowing for a detectable interacting complex. However, a positive result in this case might also account for artefactual interaction. Repetition of the oocyte experiments with lower expression levels and use of a proper positive control, such as the P2X2R/P2X3R heteromer (Saul et al., 2013), would also be an alternative experiment.

As for the mouse tissue, we have previously shown that the BAC transgenic P2X7-EGFP mouse model exhibits only mild overexpression of P2X7 and unaltered P2X4 levels compared to the wildtype mouse. Despite the limitations of the sEGFP mouse, the pull-down assay might be carried out using samples from this mouse model, which overexpresses P2X7 and shows much higher expression of P2X4. Taking that high amounts of P2X4 protein show a tendency to aggregate (see Figure 7 of the Results section), there is a possibility that the pull-down shows a positive result for the P2X4-P2X7 interaction using this approach.

Another possibility might be that the interactions in the hypothetical P2X4/P2X7 complexes are only transient and not detected by the end of our experiments, possibly due to the use of detergents. An alternative approach for mouse tissue and HEK293 cells might be to use crosslinking as a strategy to stabilize these interactions.

Lastly, a cell-specific approach might be used in order to look for an interaction via pull-down and for interrelation between both receptors at the cellular level. A possibility would be to use microglia cells, given the role of both receptors in this cell type (Montilla et al., 2020; Raouf et al., 2007; Zabala et al., 2018) and that the protocol for microglia isolation from adult mouse brain has been established in the laboratory, as explained in this dissertation.

In conclusion, the interaction of P2X4 and P2X7 receptors could not be proved in the lung tissue from the P2X7-EGFP mouse line, nor in HEK293 cells expressing P2X4 and EGFP-tagged P2X7. In spite of the limitations of this study, it appears that this interaction might be only restricted to heterologous expression systems that show an artefactual interaction as a product of the exacerbated expression of both subunits in non-physiological conditions, given the restricted evidence from *in vivo* studies that is available in the literature. Likewise, we did not find significant interrelation effects using the P2X7-EGFP and the *P2rx4* and *P2rx7* mouse models. Similarly, a model expressing higher levels of either P2X4R or P2X7R subunits might be needed to prove an interrelation, but the usefulness of such findings may be limited due to a lack of relevance in the physiological conditions.

4.3 Comparative proteomic analysis of tissue/cells from wt and P2X7 knockout mice

Liquid chromatography coupled to mass spectrometry is a powerful, widely used tool in proteomics for the study of general protein expression profiles. The quantitative analysis

in comparative proteomics allows the study of signaling pathways that are promoted or restricted upon varying conditions, such as different levels of expression of a target gene or application of different pharmacological treatments, among others (Carrasco-Navarro et al., 2016; Harsha et al., 2013; Pandey et al., 2021).

In this project, the study of protein expression profiles under different levels of P2X7 receptor was proposed. We used the P2X7$^{-/-}$, wildtype and the P2X7-EGFP mice to study the protein expression patterns under deleted, basal and overexpressed P2X7 conditions. To this aim, protocols were developed for the preparation of mouse tissue samples prior to LC-MS. These included the homogenization of the original mouse tissue, digestion and alkylation of the samples, as well as precipitation of the proteins with acetone or trichloroacetate, in accordance with reported protocols (Bruderer et al., 2017; Wiśniewski, 2018). From these, the Filter-Aided Sample Preparation (FASP) protocol provided by a PreOmics GmbH commercial kit led to more efficient and reproducible results.

Following the sample preparation and analysis, a list was obtained containing identified and quantified proteins that were detected in the samples. A statistical comparison was carried out and several proteins were detected that seemed to show differential expression levels under the three genotypical backgrounds. However, a false discovery rate analysis from this list revealed that all of the candidates should be considered false-positive results. Nevertheless, out of the hits that resulted from the analysis, some might be worth pointing out.

VCAM-1, encoded by the gene *Vcam1* (vascular cell adhesion molecule 1), appears in higher amounts in the P2X7-EGFP mouse samples. VCAM1 is a mediator of the interaction and adhesion between endothelial cells and leukocytes, participating in the signal transduction. This protein has been linked to P2X7 in a previous study (Mishra et al., 2016), Here, the authors report that P2X7 mediates VCAM1 release from alveolar type I (ATI) cells into the alveolar space and exerts chemoattraction of neutrophils. They conclude that targeting P2X7 or VCAM1 might open the possibility of a strategy for neutrophil-related host defenses.

MCAM (melanoma cell adhesion molecule), also known as CD146 or cell surface glycoprotein MUC18, was not identified in the samples from the P2X7-EGFP mouse model, but in the P2X7 knockout and wildtype mice. MCAM is another adhesion molecule involved in signal transduction in the alveolar space. MCAM shedded during inflammation mediates leukocyte migration (Bardin et al., 2009), and it was identified in a proteomic study of enriched, ARTC2.1-mediated ADP ribosylated proteins from microglia stimulated with LPS/U0126. This might have a relation with P2X7R signaling, since the P2X7R is a target of ART2.1-mediated ribosylation (Rissiek et al., 2017).

4.3.1 Limitations and future perspectives using a cell-specific approach

Given the complexity of the samples that are analyzed using mouse brain tissue, the lack of significant hits in our analysis might be explained by the heterogeneity of the cells

involved in the experiment. Furthermore, a quantitative analysis on mouse tissue requires extremely precise tissue collection of the same amount and from the same areas, making it a very challenging procedure in the case of hippocampus.

As an alternative procedure, a cell-specific approach was proposed that consists in the proteomic analysis of samples from isolated microglia. This might be an interesting approach that possibly leads to more accurate results through LC-MS. Microglia, along with macrophages, is one of the cell types that shows highest levels of P2X7R (Bhattacharya & Biber, 2016; Bianco et al., 2006; Janks et al., 2018; Wewers & Sarkar, 2009). Furthermore, microglia cells are found widespread over the brain, and protocols have been developed and are currently available for microglia isolation and proteomic analysis (Bohlen et al., 2019; Woo et al., 2017). Therefore, it may be assumed that the prepared samples for LC-MS should be enriched in P2X7R and mediators of its signaling pathways.

Through this dissertation, I have proved and shown an efficient protocol for the isolation of microglia from adult mouse brain. However, the microglia isolation protocol uses fetal bovine serum. This is one of the limitations that we have faced in the process, as it leads to detection of proteins that do not belong to the initial samples and decreases the signal-to-noise ratio. Therefore, the protocol will need an adjustment in the sample preparation before applying the modified FASP protocol prior to the proteomic analysis.

Following the isolation of microglia and the analysis of samples through LC-MS, comparison of the three different genotypical backgrounds might lead to candidates that are overexpressed or underexpressed under three different levels of expression of P2X7, and this might help elucidating signaling pathways in which P2X7 is involved. Some of the candidates found in my analysis may be worth looking at, with careful attention. Interestingly, MCAM was found enriched in cross-linked, GFP-immunoprecipitated samples from the P2X7-EGFP mouse by my colleague Robin Kopp (Kopp, 2020). However, MCAM appeared in my analysis as highly expressed in the wildtype mouse and the *P2rx7*$^{-/-}$ but not in the P2X7-EGFP model, which is counterintuitive and should be taken as a false positive result, as previously mentioned, likely due to a high abundance of this protein in the brain.

Furthermore, The LC-MS analysis has its own limitations, and the results should be carefully taken into consideration. For example, in the previously mentioned report of MCAM being present in microglia activated with LPS/U0126 after enrichment of ARTC2.1-mediated ADP ribosylated proteins, P2X7 was not found in the resulting list even though P2X7 is a target for ADP ribosylation mediated by ARTC2.1 in other cell types, such as macrophages and T cells, and it is highly expressed in microglia (Rissiek et al., 2017). Also, the authors show that P2X7 is a target for ADP ribosylation in microglia via immunoprecipitation followed by autoradiography, revealing limitations of the proteomic approach.

In conclusion, given the drawbacks of the chosen preparation protocol from mouse tissue and the promising perspectives of the optimized protocol for microglia isolation, future

work should be carried out in order to perform proteomic analysis on the three genotypical backgrounds. This might provide confirmation of signaling pathways in which P2X7 receptor is involved, as well as hints of undiscovered ones. Once the procedure is optimized, this might be applied to other cell types in which P2X7 is expressed *e.g.* oligodendrocytes and others outside of the CNS such as lymphocytes and macrophages.

References

Abbracchio, M. P., & Burnstock, G. (1994). Purinoceptors: Are there families of P2X and P2Y purinoceptors? *Pharmacology & Therapeutics*, *64*(3), 445–475.

Adinolfi, E., Callegari, M. G., Ferrari, D., Bolognesi, C., Minelli, M., Wieckowski, M. R., Pinton, P., Rizzuto, R., & di Virgilio, F. (2005). Basal Activation of the P2X7 ATP Receptor Elevates Mitochondrial Calcium and Potential, Increases Cellular ATP Levels, and Promotes Serum-independent Growth. *Molecular Biology of the Cell*, *16*(7), 3260–3272.

Adinolfi, E., Cirillo, M., Woltersdorf, R., Falzoni, S., Chiozzi, P., Pellegatti, P., Callegari, M. G., Sandona, D., Markwardt, F., Schmalzing, G., & di Virgilio, F. (2010). Trophic activity of a naturally occurring truncated isoform of the P2X7 receptor. *The FASEB Journal*, *24*(9), 3393–3404.

Adinolfi, E., Raffaghello, L., Giuliani, A. L., Cavazzini, L., Capece, M., Chiozzi, P., Bianchi, G., Kroemer, G., Pistoia, V., & di Virgilio, F. (2012). Expression of P2X7 Receptor Increases In Vivo Tumor Growth. *Cancer Research*, *72*(12), 2957–2969.

Adinolfi, E., Giuliani, A. L., De Marchi, E., Pegoraro, A., Orioli, E., & Di Virgilio, F. (2018). The P2X7 receptor: A main player in inflammation. *Biochemical Pharmacology*, *151*, 234–244.

Albalawi, F., Lu, W., Beckel, J. M., Lim, J. C., McCaughey, S. A., & Mitchell, C. H. (2017). The P2X7 Receptor Primes IL-1β and the NLRP3 Inflammasome in Astrocytes Exposed to Mechanical Strain. *Frontiers in Cellular Neuroscience*, *11,* 227.

Amoroso, F., Falzoni, S., Adinolfi, E., Ferrari, D., & di Virgilio, F. (2012). The P2X7 receptor is a key modulator of aerobic glycolysis. *Cell Death & Disease*, *3*(8), e370.

Amoroso, F., Capece, M., Rotondo, A., Cangelosi, D., Ferracin, M., Franceschini, A., Raffaghello, L., Pistoia, V., Varesio, L., & Adinolfi, E. (2015). The P2X7 receptor is a key modulator of the PI3K/GSK3β/VEGF signaling network: Evidence in experimental neuroblastoma. *Oncogene*, *34*(41), 5240–5251.

Anderson, C. M., & Nedergaard, M. (2006). Emerging challenges of assigning P2X7 receptor function and immunoreactivity in neurons. *Trends in Neurosciences*, *29*(5), 257–262.

Andrejew, R., Oliveira-Giacomelli, Á., Ribeiro, D. E., Glaser, T., Arnaud-Sampaio, V. F., Lameu, C., & Ulrich, H. (2020). The P2X7 Receptor: Central Hub of Brain Diseases. *Frontiers in Molecular Neuroscience,* 13, 124

Antonio, L. S., Stewart, A. P., Xu, X. J., Varanda, W. A., Murrell-Lagnado, R. D., & Edwardson, J. M. (2011). P2X4 receptors interact with both P2X2 and P2X7 receptors in the form of homotrimers. *British Journal of Pharmacology*, *163*(5), 1069–1077.

Babelova, A., Moreth, K., Tsalastra-Greul, W., Zeng-Brouwers, J., Eickelberg, O., Young, M. F., Brucker, P., Pfeilschifter, J., Schaefer, R. M., Gröne, H. J., & Schaefer, L. (2009). Biglycan, a danger signal that activates the NLRP3 inflammasome via toll-like and P2X receptors. *Journal of Biological Chemistry*, *284*(36), 24035–24048.

Bardin, N., Blot-Chabaud, M., Despoix, N., Kebir, A., Harhouri, K., Arsanto, J. P., Espinosa, L., Perrin, P., Robert, S., Vely, F., Sabatier, F., Le Bivic, A., Kaplanski, G., Sampol, J., & Dignat-George, F. (2009). CD146 and its soluble form regulate monocyte transendothelial migration. *Arteriosclerosis, Thrombosis, and Vascular Biology*, *29*(5), 746–753.

Baricordi, O., Ferrari, D., Melchiorri, L., Chiozzi, P., Hanau, S., Chiari, E., Rubini, M., & Di Virgilio, F. (1996). An ATP-activated channel is involved in mitogenic stimulation of human T lymphocytes. *Blood*, *87*(2), 682–690.

Baricordi, O. R., Melchiorri, L., Adinolfi, E., Falzoni, S., Chiozzi, P., Buell, G., & di Virgilio, F. (1999). Increased proliferation rate of lymphoid cells transfected with the P2X7 ATP receptor. *Journal of Biological Chemistry*, *274*(47), 33206–33208.

Barski, J. J., Hartmann, J., Rose, C. R., Hoebeek, F., Mörl, K., Noll-Hussong, M., De Zeeuw, C. I., Konnerth, A., & Meyer, M. (2003). Calbindin in Cerebellar Purkinje Cells Is a Critical Determinant of the Precision of Motor Coordination. *The Journal of Neuroscience*, *23*(8), 3469–3477.

Bartlett, R., Stokes, L., & Sluyter, R. (2014). The P2X7 Receptor Channel: Recent Developments and the Use of P2X7 Antagonists in Models of Disease. *Pharmacological Reviews*, *66*(3), 638–675.

Bartlett, R., Sluyter, V., Watson, D., Sluyter, R., & Yerbury, J. J. (2017). P2X7 antagonism using brilliant blue G reduces body weight loss and prolongs survival in female SOD1G93A amyotrophic lateral sclerosis mice. *PeerJ*, *5,* e3064.

Beil, J., Fairbairn, L., Pelczar, P., & Buch, T. (2012). Is BAC transgenesis obsolete? State of the art in the era of designer nucleases. *Journal of Biomedicine and Biotechnology*, *2012*, 308414.

Bertin, E., Deluc, T., Pilch, K. S., Martinez, A., Pougnet, J. T., Doudnikoff, E., Allain, A. E., Bergmann, P., Russeau, M., Toulmé, E., Bezard, E., Koch-Nolte, F., Séguéla, P., Lévi, S., Bontempi, B., Georges, F., Bertrand, S. S., Nicole, O., & Boué-Grabot, E. (2020). Increased surface P2X4 receptor regulates anxiety and memory in P2X4 internalization-defective knock-in mice. *Molecular Psychiatry 26, 629-644*.

Bhattacharya, A., & Biber, K. (2016). The microglial ATP-gated ion channel P2X7 as a CNS drug target. *Glia*, *64*(10), 1772–1787.

Bianco, F., Ceruti, S., Colombo, A., Fumagalli, M., Ferrari, D., Pizzirani, C., Matteoli, M., di Virgilio, F., Abbracchio, M. P., & Verderio, C. (2006). A role for P2X7 in microglial proliferation. *Journal of Neurochemistry*, *99*(3), 745–758.

Biswas, D., Qureshi, O. S., Lee, W. Y., Croudace, J. E., Mura, M., & Lammas, D. A. (2008). ATP-induced autophagy is associated with rapid killing of intracellular mycobacteria within human monocytes/macrophages. *BMC Immunology*, *9, 35*.

Blume, A. J., Dalton, C., & Sheppard, H. (1973). *Adenosine-Mediated Elevation of Cyclic 3': 5'-Adenosine Monophosphate Concentrations in Cultured Mouse Neuroblastoma Cells (nerve cells/phosphodiesterase inhibitors). Proceedings of the National Academy of Sciences*, *70(11),* 3099-3102.

Bohlen, C. J., Bennett, F. C., & Bennett, M. L. (2019). Isolation and Culture of Microglia. *Current Protocols in Immunology*, *125*(1), 1–21.

Boumechache, M., Masin, M., Edwardson, J. M., Górecki, D. C., & Murrell-Lagnado, R. (2009). Analysis of assembly and trafficking of native P2X4 and P2X7 receptor complexes in rodent immune cells. *The Journal of Biological Chemistry*, *284*(20), 13446–13454.

Bowler, J. W., Jayne Bailey, R., Alan North, R., & Surprenant, A. (2003). P2X4, P2Y1 and P2Y2 receptors on rat alveolar macrophages. *British Journal of Pharmacology*, *140*(3), 567–575.

Bradl, M., & Lassmann, H. (2010). Oligodendrocytes: Biology and pathology. *Acta Neuropathologica 119*(1), 37–53.

Braun, K. (1990). Calcium-Binding Proteins in Avian and Mammalian Central Nervous System: Localization, Development and Possible Functions. *Progress in Histochemistry and Cytochemistry*, *21*(1), 1–64.

Bröer, S. (2003). Xenopus laevis Oocytes. *Methods in Molecular Biology Clifton, N.J.), 637,* 295–310.

Brown, A. M., Arancillo, M., Lin, T., Catt, D. R., Zhou, J., Lackey, E. P., Stay, T. L., Zuo, Z., White, J. J., & Sillitoe, R. V. (2019). Molecular layer interneurons shape the spike activity of cerebellar Purkinje cells. *Scientific Reports*, *9*(1), 1742.

Bruderer, R., Bernhardt, O. M., Gandhi, T., Xuan, Y., Sondermann, J., Schmidt, M., Gomez-Varela, D., & Reiter, L. (2017). Optimization of experimental parameters in data-independent mass spectrometry significantly increases depth and reproducibility of results. *Molecular and Cellular Proteomics*, *16*(12), 2296–2309.

Burnstock, G., Campbell, G., Satchell, D., & Smythe, A. (1970). Evidence that adenosine triphosphate or a related nucleotide is the transmitter substance released by non-adrenergic inhibitory nerves in the gut. *British Journal of Pharmacology*, *40*(4), 668–688.

Burnstock, G. (1972). Purinergic nerves. *Pharmacological Reviews*, *24*(3), 509–581.

Burnstock, G. (1976). Do some nerve cells release more than one transmitter? *Neuroscience*, *1*(4), 239–248.

Burnstock, G. (1978). A basis for distinguishing two types of purinergic receptor. In R. Straub & Bolis L (Eds.), *Cell Membrane Receptors for Drugs and Hormones: A Multidisciplinary Approach, Edited by Straub RW and Bolis L* (pp. 107–118). Raven Press.

Burnstock, G., & Kennedy, C. (1985). Is there a basis for distinguishing two types of P2-purinoceptor? *General Pharmacology: The Vascular System*, *16*(5), 433–440.

Burnstock, G., & Knight, G. E. (2004). Cellular distribution and functions of P2 receptor subtypes in different systems. *International Review of Cytology*, *240*(SPEC.ISS.), 31–304.

Burnstock, G., & Kennedy, C. (2011). P2X Receptors in Health and Disease. In *Advances in Pharmacology*, *61,* 333–372.

Burnstock, G., & Knight, G. E. (2018). The potential of P2X7 receptors as a therapeutic target, including inflammation and tumour progression. *Purinergic Signalling*, *14*(1), 1–18.

Calovi, S., Mut-Arbona, P., Tod, P., Iring, A., Nicke, A., Mato, S., Vizi, E. S., Tønnesen, J., & Sperlagh, B. (2020). P2X7 Receptor-Dependent Layer-Specific Changes in Neuron-Microglia Reactivity in the Prefrontal Cortex of a Phencyclidine Induced Mouse Model of Schizophrenia. *Frontiers in Molecular Neuroscience*, *13,* 566251.

Calzaferri, F., Ruiz-Ruiz, C., de Diego, A. M. G., de Pascual, R., Méndez-López, I., Cano-Abad, M. F., Maneu, V., de los Ríos, C., Gandía, L., & García, A. G. (2020). The purinergic P2X7 receptor as a potential drug target to combat neuroinflammation in neurodegenerative diseases. *Medicinal Research Reviews*, *40*(6), 2427–2465.

Calzaferri, F., Narros-Fernández, P., de Pascual, R., de Diego, A. M. G., Nicke, A., Egea, J., García, A. G., & de Los Ríos, C. (2021). Synthesis and Pharmacological Evaluation of Novel Non-nucleotide Purine Derivatives as P2X7 Antagonists for the Treatment of Neuroinflammation. *Journal of Medicinal Chemistry*, *64*(4), 2272–2290.

Cao, Q., Zhong, X. Z., Zou, Y., Murrell-Lagnado, R., Zhu, M. X., & Dong, X. P. (2015). Calcium release through P2X4 activates calmodulin to promote endolysosomal membrane fusion. *Journal of Cell Biology*, *209*(6), 879–894.

Carrasco-Navarro, U., Vera-Estrella, R., Barkla, B. J., Zúñiga-León, E., Reyes-Vivas, H., Fernández, F. J., & Fierro, F. (2016). Proteomic analysis of the signaling pathway mediated by the heterotrimeric Ga protein Pga1 of Penicillium chrysogenum. *Microbial Cell Factories*, *15(1)*, 173.

Casas-Pruneda, G., Reyes, J. P., Pérez-Flores, G., Pérez-Cornejo, P., & Arreola, J. (2009). Functional interactions between P2X4 and P2X7 receptors from mouse salivary epithelia. *The Journal of Physiology*, *587*(Pt 12), 2887–2901.

Chen, Y., Molet, J., Gunn, B. G., Ressler, K., & Baram, T. Z. (2015). Diversity of reporter expression patterns in transgenic mouse lines targeting corticotropin- releasing hormone-expressing neurons. *Endocrinology*, *156*(12), 4769–4780.

Chessell, I. P., Simon, J., Hibell, A. D., Michel, A. D., Barnard, E. A., & Humphrey, P. P. A. (1998). Cloning and functional characterisation of the mouse P2X7 receptor. *FEBS Letters*, *439*(1–2), 26–30.

Cisneros-Mejorado, A. J., Pérez-Samartín, A., Domercq, M., Arellano, R. O., Gottlieb, M., Koch-Nolte, F., & Matute, C. (2020). P2X7 Receptors as a Therapeutic Target in Cerebrovascular Diseases. *Frontiers in Molecular Neuroscience*, *13*, 92.

Cobbin, L. B., Einstein, R., & Maguire, M. H. (1974). Studies on the coronary dilator actions of some adenosine analogues. *British Journal of Pharmacology*, *50(1), 25-33*.

Collins, M., & Bowser, R. (2017). Molecular Mechanisms of Amyotrophic Lateral Sclerosis. In *Molecular and Cellular Therapies for Motor Neuron Diseases* (pp. 61–99). Academic Press.

Conte, G., Menéndez-Méndez, A., Bauer, S., El-Naggar, H., Alves, M., Nicke, A., Delanty, N., Rosenow, F., Henshall, D. C., Engel, T., & Yarwood, S. (2021). Circulating P2X7 Receptor Signaling Components as Diagnostic Biomarkers for Temporal Lobe Epilepsy. *Cells, 10*(9), 2444.

Cox, J., Neuhauser, N., Michalski, A., Scheltema, R. A., Olsen, J. V., & Mann, M. (2011). Andromeda: A peptide search engine integrated into the MaxQuant environment. *Journal of Proteome Research*, *10*(4), 1794–1805.

Cox, J., Hein, M. Y., Luber, C. A., Paron, I., Nagaraj, N., & Mann, M. (2014). Accurate Proteome-wide Label-free Quantification by Delayed Normalization and Maximal Peptide Ratio Extraction, Termed MaxLFQ. *Molecular & Cellular Proteomics*, *13*(9), 2513–2526.

Craigie, E., Birch, R. E., Unwin, R. J., & Wildman, S. S. (2013). The relationship between P2X4 and P2X7: A physiologically important interaction? *Frontiers in Physiology*, *4, 216*.

Csóka, B., Németh, Z. H., Szabó, I., Davies, D. L., Varga, Z. V., Pálóczi, J., Falzoni, S., Di Virgilio, F., Muramatsu, R., Yamashita, T., Pacher, P., & Haskó, G. (2018). Macrophage P2X4 receptors augment bacterial killing and protect against sepsis. *JCI Insight*, *3*(11), e99431.

Danzer, S. C., & McNamara, J. O. (2004). Localization of brain-derived neurotrophic factor to distinct terminals of mossy fiber axons implies regulation of both excitation

and feedforward inhibition of CA3 pyramidal cells. *Journal of Neuroscience*, *24*(50), 11346–11355.

Darville, T., Welter-Stahl, L., Cruz, C., Sater, A. A., Andrews, C. W., & Ojcius, D. M. (2007). Effect of the Purinergic Receptor P2X 7 on Chlamydia Infection in Cervical Epithelial Cells and Vaginally Infected Mice . *The Journal of Immunology*, *179*(6), 3707–3714

De Marchi, E., Orioli, E., Dal Ben, D., & Adinolfi, E. (2016). P2X7 Receptor as a Therapeutic Target. *Advances in Protein Chemistry and Structural Biology, 104*, 39-79.

De Nardo, D., De Nardo, C. M., & Latz, E. (2014). New insights into mechanisms controlling the NLRP3 inflammasome and its role in lung disease. *American Journal of Pathology*, *184*(1), 42–54

de Sá, K. S. G., Amaral, L. A., Rodrigues, T. S., Ishimoto, A. Y., de Andrade, W. A. C., de Almeida, L., Freitas-Castro, F., Batah, S. S., Oliveira, S. C., Pastorello, M. T., Fabro, A. T., & Zamboni, D. S. (2023). Gasdermin-D activation promotes NLRP3 activation and host resistance to Leishmania infection. *Nature Communications*, *14*(1), 1049.

de Salis, S. K. F., Li, L., Chen, Z., Lam, K. W., Skarratt, K. K., Balle, T., & Fuller, S. J. (2022). Alternatively Spliced Isoforms of the P2X7 Receptor: Structure, Function and Disease Associations. In *International Journal of Molecular Sciences*, *23*(15), 8174.

Delarasse, C., Gonnord, P., Galante, M., Auger, R., Daniel, H., Motta, I., & Kanellopoulos, J. M. (2009). Neural progenitor cell death is induced by extracellular ATP via ligation of P2X7 receptor. *Journal of Neurochemistry*, *109*(3), 846–857.

Delarasse, C., Auger, R., Gonnord, P., Fontaine, B., & Kanellopoulos, J. M. (2011). The purinergic receptor P2x7 triggers α-secretase-dependent processing of the amyloid precursor protein. *Journal of Biological Chemistry*, *286*(4), 2596–2606.

Deussing, J. M., & Arzt, E. (2018). P2X7 Receptor: A Potential Therapeutic Target for Depression? In *Trends in Molecular Medicine*, *24*(9), 736–747).

Di, A., Xiong, S., Ye, Z., Malireddi, R. K. S., Kometani, S., Zhong, M., Mittal, M., Hong, Z., Kanneganti, T. D., Rehman, J., & Malik, A. B. (2018). The TWIK2 Potassium Efflux Channel in Macrophages Mediates NLRP3 Inflammasome-Induced Inflammation. *Immunity*, *49*(1), 56-65.e4.

Di Virgilio, F. (2007). Liaisons dangereuses: P2X7 and the inflammasome. *Trends in Pharmacological Sciences*, *28*(9), 465–472.

Di Virgilio, F., Vultaggio-Poma, V., Falzoni, S., & Giuliani, A. L. (2023). Extracellular ATP: A powerful inflammatory mediator in the central nervous system. *Neuropharmacology*, *224*, 109333.

Domercq, M., & Matute, C. (2019). Targeting P2X4 and P2X7 receptors in multiple sclerosis. *Current Opinion in Pharmacology,* 47, 119–125. Elsevier Ltd.

Doná, F., Ulrich, H., Persike, D. S., Conceição, I. M., Blini, J. P., Cavalheiro, E. A., & Fernandes, M. J. S. (2009). Alteration of purinergic P2X4 and P2X7 receptor expression in rats with temporal-lobe epilepsy induced by pilocarpine. *Epilepsy Research*, *83*(2–3), 157–167

Drill, M., Powell, K. L., Kan, L. K., Jones, N. C., O'Brien, T. J., Hamilton, J. A., & Monif, M. (2020). Inhibition of purinergic P2X receptor 7 (P2X7R) decreases granulocyte-macrophage colony-stimulating factor (GM-CSF) expression in U251 glioblastoma cells. *Scientific Reports*, *10*(1), 1–11.

Drury, A. N., & Szent-Györgyi, A. (1929). The physiological activity of adenine compounds with especial reference to their action upon the mammalian heart1. *The Journal of Physiology*, *68*(3), 213–237.

Dubyak, G. R. (2012). P2X7 receptor regulation of non-classical secretion from immune effector cells. *Cellular Microbiology*, *14*(11), 1697–1706.

Emmelin, N., & Feldberg, W. (1948). Systemic effects of adenosine triphosphate. *British Journal of Pharmacology and Chemotherapy*, *3*(4), 273–284.

Engel, T., Gomez-Villafuertes, R., Tanaka, K., Mesuret, G., Sanz-Rodriguez, A., Garcia-Huerta, P., Miras-Portugal, M. T., Henshall, D. C., & Diaz-Hernandez, M. (2012). Seizure suppression and neuroprotection by targeting the purinergic P2X7 receptor during status epilepticus in mice. *The FASEB Journal*, *26*(4), 1616–1628.

Feng, Y. H., Li, X., Zeng, R., & Gorodeski, G. I. (2006). Endogenously expressed truncated P2X7 receptor lacking the C-terminus is preferentially upregulated in epithelial cancer cells and fails to mediate ligand-induced pore formation and apoptosis. *Nucleosides, Nucleotides and Nucleic Acids*, *25*(9–11), 1271–1276.

Feng, Y.-H., Li, X., Wang, L., Zhou, L., & Gorodeski, G. I. (2006). A Truncated P2X7 Receptor Variant (P2X 7-j) Endogenously Expressed in Cervical Cancer Cells Antagonizes the Full-length P2X7 Receptor through Hetero-oligomerization. *J Biol Chem*, *281*(25), 17228–17237.

Ferrari, D., Chiozzi, P., Falzoni, S., Dal Susino, M., Collo, G., Buell, G., & di Virgilio, F. (1997). ATP-mediated cytotoxicity in microglial cells. *Neuropharmacology*, *36*(9), 1295–1301.

Ferrari, D., la Sala, A., Panther, E., Norgauer, J., di Virgilio, F., & Idzko, M. (2006). Activation of human eosinophils via P2 receptors: novel findings and future perspectives. *Journal of Leukocyte Biology*, *79*(1), 7–15.

Ferrari, D., Pizzirani, C., Adinolfi, E., Lemoli, R. M., Curti, A., Idzko, M., Panther, E., & Di Virgilio, F. (2006). The P2X7 Receptor: A Key Player in IL-1 Processing and Release. *The Journal of Immunology*, *176*(7), 3877–3883.

Franceschini, a., Capece, M., Chiozzi, P., Falzoni, S., Sanz, J. M., Sarti, a. C., Bonora, M., Pinton, P., & di Virgilio, F. (2015). The P2X7 receptor directly interacts with the NLRP3 inflammasome scaffold protein. *The FASEB Journal*, 1–12.

Francistiová, L., Bianchi, C., di Lauro, C., Sebastián-Serrano, Á., de Diego-García, L., Kobolák, J., Dinnyés, A., & Díaz-Hernández, M. (2020). The Role of P2X7 Receptor in Alzheimer's Disease. In *Frontiers in Molecular Neuroscience* , 13, 94.

Fredholm, B. B., IJzerman, A. P., Jacobson, K. A., Klotz, K. N., & Linden, J. (2001). International Union of Pharmacology. XXV. Nomenclature and classification of adenosine receptors. *Pharmacological Reviews*, *53*(4), 527–552.

Fuller, S. J., Stokes, L., Skarratt, K. K., Gu, B. J., & Wiley, J. S. (2009). Genetics of the P2X7 receptor and human disease. *Purinergic Signalling,* 5, 257-262.

Gerfen, C. R., Paletzki, R., & Heintz, N. (2013). GENSAT BAC Cre-Recombinase Driver Lines to Study the Functional Organization of Cerebral Cortical and Basal Ganglia Circuits. *Neuron*, *80*(6), 1368–1383.

Ginhoux, F., Lim, S., Hoeffel, G., Low, D., & Huber, T. (2013). Origin and differentiation of microglia. *Frontiers in Cellular Neuroscience*, *7*, 45.

Giuliani, A. L., Sarti, A. C., Falzoni, S., & di Virgilio, F. (2017). The P2X7 receptor-interleukin-1 liaison. *Frontiers in Pharmacology*, *8*, 123.

Gong, S., Zheng, C., Doughty, M. L., Losos, K., Didkovsky, N., Schambra, U. B., Nowak, N. J., Joyner, A., Leblanc, G., Hatten, M. E., & Heintz, N. (2003). A gene expression atlas of the central nervous system based on bacterial artificial chromosomes. *Nature*, *425*(6961), 917–925.

Gong, S., Kus, L., & Heintz, N. (2010). Rapid bacterial artificial chromosome modification for large-scale mouse transgenesis. *Nature Protocols*, *5*(10), 1678–1696.

Gulyls, A. I., Mettinen, R., Jacobowitz, D. M., & Fretrnd, T. F. (1992). Calretinin is present in non-pyramidal cells of the rat hippocampus-I. A new type of neuron specifically associated with the mossy fibre system. *Neuroscience*, 48 (1), 1-27.

Guo, C., Masin, M., Qureshi, O. S., & Murrell-Lagnado, R. D. (2007). Evidence for functional P2X4/P2X7 heteromeric receptors. *Molecular Pharmacology*, *72*(6), 1447–1456.

Guo, H., Callaway, J. B., & Ting J. P. (2015). Inflammasomes: mechanism of action, role in disease, and therapeutics. *Nature Medicine*, 21(7), 677–687.

Hamdan, N., Kritsiligkou, P., & Grant, C. M. (2017). ER stress causes widespread protein aggregation and prion formation. *Journal of Cell Biology*, *216*(8), 2295–2304.

Harsha, H. C., Pinto, S. M., & Pandey, A. (2013). *Proteomic Strategies to Characterize Signaling Pathways*, 1007, 359–377.

Heintz, N. (2001). Bac to the future: The use of bac transgenic mice for neuroscience research. *Nature Reviews Neuroscience*, *2*(12), 861–870.

Holton, P. (1959). The liberation of adenosine triphosphate on antidromic stimulation of sensory nerves. *The Journal of Physiology*, *145*(3), 494–504.

Hooper, A., & Maguire, J. (2016). Characterization of a novel subtype of hippocampal interneurons that express corticotropin-releasing hormone. *Hippocampus*, *26*(1),

Humphreys, B. D. (2000). SAPK/JNK activation and apoptotic induction by the macrophage P2X7 nucleotide receptor. *Journal of Biological Chemistry*, *275*(35), 26792–26798.

Hung, S. C., Choi, C. H., Said-Sadier, N., Johnson, L., Atanasova, K. R., Sellami, H., Yilmaz, Ö., & Ojcius, D. M. (2013). P2X4 Assembles with P2X7 and Pannexin-1 in Gingival Epithelial Cells and Modulates ATP-induced Reactive Oxygen Species Production and Inflammasome Activation. *PLoS ONE*, *8*(7), e70210.

Idzko, M., Ferrari, D., & Eltzschig, H. K. (2014). Nucleotide signalling during inflammation. *Nature*, 509(7500), 310–317.

Illes, P., Khan, T. M., & Rubini, P. (2017). Neuronal P2X7 Receptors Revisited: Do They Really Exist? *The Journal of Neuroscience*, *37*(30), 7049–7062.

Illes, P., Müller, C. E., Jacobson, K. A., Grutter, T., Nicke, A., Fountain, S. J., Kennedy, C., Schmalzing, G., Jarvis, M. F., Stojilkovic, S. S., King, B. F., & Di Virgilio, F. (2020). Update of P2X receptor properties and their pharmacology: IUPHAR Review 30. *British Journal of Pharmacology*, *178*(3), 489–514.

Jacob, F., Novo, C. P., Bachert, C., & van Crombruggen, K. (2013). Purinergic signaling in inflammatory cells: P2 receptor expression, functional effects, and modulation of inflammatory responses. *Purinergic Signalling*, 9(3), 285–306.

Jacobson, K. A., & Müller, C. E. (2016). Medicinal chemistry of adenosine, P2Y and P2X receptors. *Neuropharmacology*, *104*, 31–49.

Janks, L., Sharma, C. V. R., & Egan, T. M. (2018). A central role for P2X7 receptors in human microglia. *Journal of Neuroinflammation*, *15*(1), 1–18.

Jiang, Y., Ye, F., Du, Y., Zong, Y., & Tang, Z. (2021). P2X7R in Mast Cells is a Potential Target for Salicylic Acid and Aspirin in Treatment of Inflammatory Pain. *Journal of Inflammation Research*, *14*, 2913–2931.

Jimenez-Mateos, E. M., Smith, J., Nicke, A., & Engel, T. (2019). Regulation of P2X7 receptor expression and function in the brain. *Brain Research Bulletin,* 151, 153–163).

Jimenez-Pacheco, A., Mesuret, G., Sanz-Rodriguez, A., Tanaka, K., Mooney, C., Conroy, R., Miras-Portugal, M. T., Diaz-Hernandez, M., Henshall, D. C., & Engel, T.

(2013). Increased neocortical expression of the P2X7 receptor after status epilepticus and anticonvulsant effect of P2X7 receptor antagonist A-438079. *Epilepsia*, *54*(9), 1551–1561.

Jimenez-Pacheco, A., Diaz-Hernandez, M., Arribas-Blázquez, M., Sanz-Rodriguez, A., Olivos-Oré, L. A., Artalejo, A. R., Alves, M., Letavic, M., Teresa Miras-Portugal, M., Conroy, R. M., Delanty, N., Farrell, M. A., O'Brien, D. F., Bhattacharya, A., Engel, T., & Henshall, D. C. (2016). Transient P2X7 receptor antagonism produces lasting reductions in spontaneous seizures and gliosis in experimental temporal lobe epilepsy. *Journal of Neuroscience*, *36*(22), 5920–5932.

Kaczmarek-Hájek, K., Lörinczi, É., Hausmann, R., & Nicke, A. (2012). Molecular and functional properties of P2X receptors-recent progress and persisting challenges. *Purinergic Signalling,* 8, 375-417.

Kaczmarek-Hájek, K., Zhang, J., Kopp, R., Grosche, A., Rissiek, B., Saul, A., Bruzzone, S., Engel, T., Jooss, T., Krautloher, A., Schuster, S., Magnus, T., Stadelmann, C., Sirko, S., Koch-Nolte, F., Eulenburg, V., & Nicke, A. (2018). Re-evaluation of neuronal P2X7 expression using novel mouse models and a P2X7-specific nanobody. *ELife*, *7,* e36217.

Kanayama, T., Tomita, H., Binh, N. H., Hatano, Y., Aoki, H., Okada, H., Hirata, A., Fujihara, Y., Kunisada, T., & Hara, A. (2019). Characterization of a BAC transgenic mouse expressing Krt19-driven iCre recombinase in its digestive organs. *PLoS ONE*, *14*(8), 1–16.

Kanellopoulos, J. M., & Delarasse, C. (2019). Pleiotropic Roles of P2X7 in the Central Nervous System. *Frontiers in Cellular Neuroscience*, *13*, 401.

Kanellopoulos, J. M., Almeida-da-Silva, C. L. C., Rüütel Boudinot, S., & Ojcius, D. M. (2021). Structural and Functional Features of the P2X4 Receptor: An Immunological Perspective. *Frontiers in Immunology*, *12*, 645834.

Karmakar, M., Katsnelson, M. A., Dubyak, G. R., & Pearlman, E. (2016). Neutrophil P2X7 receptors mediate NLRP3 inflammasome-dependent IL-1β secretion in response to ATP. *Nature Communications*, *7*, 10555

Kasatkina, L. A., & Verkhusha, V. V. (2022). Transgenic mice encoding modern imaging probes: Properties and applications. *Cell Reports,* 39(8), 110845.

Kawano, A., Tsukimoto, M., Noguchi, T., Hotta, N., Harada, H., Takenouchi, T., Kitani, H., & Kojima, S. (2012). Involvement of P2X4 receptor in P2X7 receptor-dependent cell death of mouse macrophages. *Biochemical and Biophysical Research Communications*, *419*(2), 374–380.

Khakh, B. S., & North, R. (2006). P2X receptors as cell-surface ATP sensors in health and disease. *Nature*, *442*(7102), 527–532.

Kim, H., Kim, M., Im, S.-K., & Fang, S. (2018). Mouse Cre-LoxP system: general principles to determine tissue-specific roles of target genes. *Laboratory Animal Research*, *34*(4), 147.

King, B. F., Townsend-Nicholson, A., Wildman, S. S., Thomas, T., Spyer, K. M., & Burnstock, G. (2000). Coexpression of Rat P2X2 and P2X6 Subunits in Xenopus Oocytes. *The Journal of Neuroscience*, *20*(13), 4871–4877.

Kopp, R., Krautloher, A., Ramírez-Fernández, A., & Nicke, A. (2019). P2X7 Interactions and Signaling – Making Head or Tail of It. *Frontiers in Molecular Neuroscience*, 12, 183.

Kopp, R. (2020). *Analysis of P2X7 protein complexes in a P2X7-EGFP BAC transgenic mouse model* [Doctoral Thesis, Ludwig-Maximilians-Universität München].

Koshimizu, T. A., Koshimizu, M., & Stojilkovic, S. S. (1999). Contributions of the C-terminal domain to the control of P2X receptor desensitization. *Journal of Biological Chemistry*, *274*(53), 37651–37657.

Kostopoulos, G. K., Limacher, J. J., & Phillis, J. W. (1975). Action of various adenine derivatives on cerebellar Purkinje cells. *Brain Research*, *88*(1), 162–165.

Kuroda, Y., Saito, M., & Kobayashi, K. (1976). Concomitant changes in cyclic AMP level and postaynaptic potentials of olfactory cortex slices induced by adenosine derivatives. In *Brain Research*, 109(1), 196-201.

Langen, P., & Hucho, F. (2008). Karl Lohmann and the Discovery of ATP. *Angewandte Chemie International Edition*, *47*(10), 1824–1827.

le Feuvre, R. A., Brough, D., Iwakura, Y., Takeda, K., & Rothwell, N. J. (2002). Priming of macrophages with lipopolysaccharide potentiates P2X7-mediated cell death via a caspase-1-dependent mechanism, independently of cytokine production. *Journal of Biological Chemistry*, *277*(5), 3210–3218.

Lê, K.-T., Babinski, K., & Séguéla, P. (1998). Central P2X4 and P2X6 Channel Subunits Coassemble into a Novel Heteromeric ATP Receptor. *The Journal of Neuroscience*, *18*(18), 7152–7159.

Lenertz, L. Y., Gavala, M. L., Zhu, Y., & Bertics, P. J. (2011). Transcriptional control mechanisms associated with the nucleotide receptor P2X7, a critical regulator of immunologic, osteogenic, and neurologic functions. *Immunologic Research,* 50(1), 22–38.

Li, H., & Sun, S. (2021). Protein aggregation in the ER: Calm behind the storm. *Cells,* 10(12), 3337.

Liu, X., Zhang, Z., Ruan, J., Pan, Y., Magupalli, V. G., Wu, H., & Lieberman, J. (2016). Inflammasome-activated gasdermin D causes pyroptosis by forming membrane pores. *Nature*, *535*(7610), 153–158.

Lohmann, K. (1929). Über die Pyrophosphatfraktion im Muskel. *Die Naturwissenschaften*, *17*(31), 624–625.

Lopez-Castejon, G., & Brough, D. (2011). Understanding the mechanism of IL-1β secretion. *Cytokine and Growth Factor Reviews*, *22*(4), 189–195.

Lu, W., Albalawi, F., Beckel, J. M., Lim, J. C., Laties, A. M., & Mitchell, C. H. (2017). The P2X7 receptor links mechanical strain to cytokine IL-6 up-regulation and release in neurons and astrocytes. *Journal of Neurochemistry*, *141*(3), 436–448.

Ma, W., Korngreen, A., Weil, S., Cohen, E. B. T., Priel, A., Kuzin, L., & Silberberg, S. D. (2006). Pore properties and pharmacological features of the P2X receptor channel in airway ciliated cells. *Journal of Physiology*, *571*(3), 503–517.

Mackenzie, A. B., Young, M. T., Adinolfi, E., & Surprenant, A. (2005). Pseudoapoptosis Induced by Brief Activation of ATP-gated P2X7 Receptors. *Journal of Biological Chemistry*, *280*(40), 33968–33976.

Martel-Gallegos, G., Rosales-Saavedra, M. T., Reyes, J. P., Casas-Pruneda, G., Toro-Castillo, C., Pérez-Cornejo, P., & Arreola, J. (2010). Human neutrophils do not express purinergic P2X7 receptors. *Purinergic Signalling*, *6*(3), 297–306.

Martínez-Frailes, C., Di Lauro, C., Bianchi, C., De Diego-García, L., Sebastián-Serrano, Á., Boscá, L., & Díaz-Hernández, M. (2019). Amyloid peptide induced neuroinflammation increases the P2X7 receptor expression in microglial cells, impacting on its functionality. *Frontiers in Cellular Neuroscience*, *13*, 143.

Martínez-Gil, N., Kutsyr, O., Noailles, A., Fernández-Sánchez, L., Vidal, L., Sánchez-Sáez, X., Sánchez-Castillo, C., Lax, P., Cuenca, N., García, A. G., & Maneu, V. (2022). Purinergic Receptors P2X7 and P2X4 as Markers of Disease Progression in the rd10 Mouse Model of Inherited Retinal Dystrophy. *International Journal of Molecular Sciences*, *23*(23), 14758.

Martinian, L., Catarino, C. B., Thompson, P., Sisodiya, S. M., & Thom, M. (2012). Calbindin D28K expression in relation to granule cell dispersion, mossy fibre sprouting and memory impairment in hippocampal sclerosis: A surgical and post mortem series. *Epilepsy Research*, *98*(1), 14–24.

Masin, M., Young, C., Lim, K., Barnes, S. J., Xu, X. J., Marschall, V., Brutkowski, W., Mooney, E. R., Gorecki, D. C., & Murrell-Lagnado, R. (2012). Expression, assembly and function of novel C-terminal truncated variants of the mouse P2X7 receptor: re-evaluation of P2X7 knockouts. *British Journal of Pharmacology*, *165*(4), 978–993.

Matute, C. (2008). P2X7 receptors in oligodendrocytes: A novel target for neuroprotection. *Molecular Neurobiology,* 38(2), 123–128.

McCarthy, A. E., Yoshioka, C., & Mansoor, S. E. (2019). Full-Length P2X7 Structures Reveal How Palmitoylation Prevents Channel Desensitization. *Cell*, *179*(3), 659-670.e13.

Messemer, N., Kunert, C., Grohmann, M., Sobottka, H., Nieber, K., Zimmermann, H., Franke, H., Nörenberg, W., Straub, I., Schaefer, M., Riedel, T., Illes, P., & Rubini, P. (2013). P2X7 receptors at adult neural progenitor cells of the mouse subventricular zone. *Neuropharmacology*, *73*, 122–137.

Metzger, M. W., Walser, S. M., Aprile-Garcia, F., Dedic, N., Chen, A., Holsboer, F., Arzt, E., Wurst, W., & Deussing, J. M. (2017). Genetically dissecting P2rx7 expression within the central nervous system using conditional humanized mice. *Purinergic Signalling*, *13*(2), 153–170.

Miller, C. M., Boulter, N. R., Fuller, S. J., Zakrzewski, A. M., Lees, M. P., Saunders, B. M., Wiley, J. S., & Smith, N. C. (2011). The role of the P2X7 receptor in infectious diseases. *PLoS Pathogens*, *7*(11).

Minkiewicz, J., de Rivero Vaccari, J. P., & Keane, R. W. (2013). Human astrocytes express a novel NLRP2 inflammasome. *Glia*, *61*(7), 1113–1121.

Miras-Portugal, M. T., Sebastián-Serrano, Á., De Diego García, L., & Díaz-Hernández, M. (2017). Neuronal P2X7 Receptor: Involvement in Neuronal Physiology and Pathology. *Journal of Neuroscience*, *37*(30), 7063–7072.

Mishra, A., Guo, Y., Zhang, L., More, S., Weng, T., Chintagari, N. R., Huang, C., Liang, Y., Pushparaj, S., Gou, D., Breshears, M., & Liu, L. (2016). A Critical Role for P2X7 Receptor–Induced VCAM-1 Shedding and Neutrophil Infiltration during Acute Lung Injury. *The Journal of Immunology*, *197*(7), 2828–2837.

Mohanty, J. G., Raible, D. G., McDermott, L. J., Pelleg, A., & Schulman, E. S. (2001). Effects of purine and pyrimidine nucleotides on intracellular Ca2+ in human eosinophils: Activation of purinergic P2Y receptors. *Journal of Allergy and Clinical Immunology*, *107*(5 SUPPL.), 849–855.

Monif, M., Reid, C. A., Powell, K. L., Smart, M. L., & Williams, D. A. (2009). The P2X7 receptor drives microglial activation and proliferation: A trophic role for P2X7R pore. *Journal of Neuroscience*, *29*(12), 3781–3791.

Montilla, A., Mata, G. P., Matute, C., & Domercq, M. (2020). Contribution of p2x4 receptors to cns function and pathophysiology. *International Journal of Molecular Sciences*, *21*(15), 1–16.

Morandini, A., Savio, L., & Coutinho-Silva, R. (2014). The role of p2x7 receptor in infectious inflammatory diseases and the influence of ectonucleotidases. *Biomedical Journal, 37*(4), 169–177.

Müller, T., Vieira, R. P., Grimm, M., Dürk, T., Cicko, S., Zeiser, R., Jakob, T., Martin, S. F., Blumenthal, B., Sorichter, S., Ferrari, D., di Virgillio, F., & Idzko, M. (2011). A potential role for P2X7R in allergic airway inflammation in mice and humans. *American Journal of Respiratory Cell and Molecular Biology*, *44*(4), 456–464.

Murrell-Lagnado, R. D. (2018). A role for P2X4 receptors in lysosome function. *Journal of General Physiology*, *150*(2), 185–187.

Murrell-Lagnado, R. D., & Frick, M. (2019). P2X4 and lysosome fusion. *Current Opinion in Pharmacology*, *47*, 126–132.

Mutini, C., Falzoni, S., Ferrari, D., Chiozzi, P., Morelli, A., Roberto Baricordi, O., Collo, G., Ricciardi-Castagnoli, P., & di Virgilio, F. (1999). Mouse Dendritic Cells Express the P2X 7 Purinergic Receptor: Characterization and Possible Participation in Antigen Presentation 1. In *The Journal of Immunology*, 163(4), 1958-65

Nicke, A. (2008). Homotrimeric complexes are the dominant assembly state of native P2X7 subunits. *Biochemical and Biophysical Research Communications*, *377*(3), 803–808.

Nicke, A., Kuan, Y.-H., Masin, M., Rettinger, J., Marquez-Klaka, B., Bender, O., Górecki, D. C., Murrell-Lagnado, R. D., & Soto, F. (2009). A Functional P2X7 Splice Variant with an Alternative Transmembrane Domain 1 Escapes Gene Inactivation in P2X7 Knock-out Mice. *Journal of Biological Chemistry*, *284*(38), 25813–25822.

North, R. A. (2002). Molecular physiology of P2X receptors. *Physiological Reviews*, *82*(4), 1013–1067.

North, R. A., & Jarvis, M. F. (2013). P2X receptors as drug targets. *Molecular Pharmacology*, *83*(4), 759–769.

Novak, I. (2008). Purinergic receptors in the endocrine and exocrine pancreas. *Purinergic Signalling, 4*(3), 237–253.

Novak, I. (2011). Purinergic signalling in epithelial ion transport: regulation of secretion and absorption. *Acta physiologica,* 202(3), 501–522

Orioli, E., de Marchi, E., Giuliani, A. L., & Adinolfi, E. (2017). P2X7 Receptor Orchestrates Multiple Signalling Pathways Triggering Inflammation, Autophagy and Metabolic/Trophic Responses. *Current Medicinal Chemistry*, *24*(21).

Ortega, F., Gomez-Villafuertes, R., Benito-León, M., Martínez de la Torre, M., Olivos-Oré, L. A., Arribas-Blazquez, M., Gomez-Gaviro, M. V., Azcorra, A., Desco, M., Artalejo, A. R., Puelles, L., & Miras-Portugal, M. T. (2021). Salient brain entities labelled in P2rx7-EGFP reporter mouse embryos include the septum, roof plate glial specializations and circumventricular ependymal organs. *Brain Structure and Function*, *226*(3), 715–741.

Pandey, P., Zaman, K., Prokai, L., & Shulaev, V. (2021). Comparative proteomics analysis reveals unique early signaling response of saccharomyces cerevisiae to oxidants with different mechanism of action. *International Journal of Molecular Sciences*, *22*(1), 1–17.

Pelegrin, P., & Surprenant, A. (2006). Pannexin-1 mediates large pore formation and interleukin-1beta release by the ATP-gated P2X7 receptor. *The EMBO Journal*, *25*(21), 5071–5082.

Pérez-flores, G., Lévesque, S. A., Pacheco, J., Vaca, L., Pérez-cornejo, P., & Arreola, J. (2015). The P2X7/P2X4 Interaction Shapes The Purinergic Response In Murine Macrophages. *Biochemical and Biophysical Research Communications, 467*(3), 484–490.

Qu, Y., & Dubyak, G. R. (2009). P2X7 receptors regulate multiple types of membrane trafficking responses and non-classical secretion pathways. *Purinergic Signalling*, 5, 163–173.

Qureshi, O. S., Paramasivam, A., Yu, J. C. H., & Murrell-Lagnado, R. D. (2007). Regulation of P2X4 receptors by lysosomal targeting, glycan protection and exocytosis. *Journal of Cell Science*, *120*(21), 3838–3849.

Ramírez-Fernández, A., Urbina-Treviño, L., Conte, G., Alves, M., Rissiek, B., Durner, A., Scalbert, N., Zhang, J., Magnus, T., Koch-Nolte, F., Plesnila, N., Deussing, J. M., Engel, T., Kopp, R., & Nicke, A. (2020). Deviant reporter expression and P2X4 passenger gene overexpression in the soluble EGFP BAC transgenic P2X7 reporter mouse model. *Scientific Reports*, *10*(1), 1–17.

Raouf, R., Chabot-Doré, A. J., Ase, A. R., Blais, D., & Séguéla, P. (2007). Differential regulation of microglial P2X4 and P2X7 ATP receptors following LPS-induced activation. *Neuropharmacology*, *53*(4), 496–504.

Ren, W., Rubini, P., Tang, Y., Engel, T., & Illes, P. (2022). Inherent p2x7 receptors regulate macrophage functions during inflammatory diseases. In *International Journal of Molecular Sciences*, 23(1), 232.

Requardt, R. P., Kaczmarczyk, L., Dublin, P., Wallraff-Beck, A., Mikeska, T., Degen, J., Waha, A., Steinhäuser, C., Willecke, K., & Theis, M. (2009). Quality control of astrocyte-directed Cre transgenic mice: The benefits of a direct link between loss of gene expression and reporter activation. *GLIA*, *57*(6), 680–692.

Resende, R. R., Majumder, P., Gomes, K. N., Britto, L. R. G., & Ulrich, H. (2007). P19 embryonal carcinoma cells as in vitro model for studying purinergic receptor expression and modulation of N-methyl-d-aspartate-glutamate and acetylcholine receptors during neuronal differentiation. *Neuroscience*, *146*(3), 1169–1181.

Ribeiro, D. E., Roncalho, A. L., Glaser, T., Ulrich, H., Wegener, G., & Joca, S. (2019). P2X7 receptor signaling in stress and depression. *International Journal of Molecular Sciences*, 20(11), 2778.

Rissiek, B., Menzel, S., Leutert, M., Cordes, M., Behr, S., Jank, L., Ludewig, P., Gelderblom, M., Rissiek, A., Adriouch, S., Haag, F., Hottiger, M. O., Koch-Nolte, F., &

Magnus, T. (2017). Ecto-ADP-ribosyltransferase ARTC2.1 functionally modulates FcγR1 and FcγR2B on murine microglia. *Scientific Reports*, *7*(1), 16477.

Rittiner, J. E., Korboukh, I., Hull-Ryde, E. A., Jin, J., Janzen, W. P., Frye, S. V., & Zylka, M. J. (2012). AMP is an adenosine A 1 receptor agonist. *Journal of Biological Chemistry*, *287*(8), 5301–5309.

Rogers, J. H. (1989). Immunoreactivity for calretinin and other calcium-binding proteins in cerebellum. *Neuroscience*, 31(3), 711-721.

Roguev, A., & Krogan, N. J. (2008). BAC to the future : functional genomics in mammals Metastasis : two assays explore the two roads traveled. *Nature Methods*, *5*(5), 383–384.

Rubio, M. E., & Soto, F. (2001). Distinct Localization of P2X Receptors at Excitatory Postsynaptic Specializations. *The Journal of Neuroscience*, *21*(2), 641–653.

Ruiz-Ruiz, C., Calzaferri, F., & García, A. G. (2020). P2X7 Receptor Antagonism as a Potential Therapy in Amyotrophic Lateral Sclerosis. *Frontiers in Molecular Neuroscience*, *13*, 93.

Ruiz-Ruiz, C., García-Magro, N., Negredo, P., Avendaño, C., Bhattacharya, A., Ceusters, M., & García, A. G. (2020). Chronic administration of P2X7 receptor antagonist JNJ-47965567 delays disease onset and progression, and improves motor performance in ALS SOD1 G93A female mice. *Disease Models & Mechanisms*, *13*(10), dmm045732.

Saul, A., Hausmann, R., Kless, A., & Nicke, A. (2013). Heteromeric assembly of P2X subunits. *Frontiers in Cellular Neuroscience*, *7*, 250.

Savio, L. E. B., Mello, P. de A., da Silva, C. G., & Coutinho-Silva, R. (2018). The P2X7 receptor in inflammatory diseases: Angel or demon? *Frontiers in Pharmacology*, *9*, 52.

Schilling, W. P., Sinkins, W. G., & Estacion, M. (1999). Maitotoxin activates a nonselective cation channel and a P2Z/P2X7-like cytolytic pore in human skin fibroblasts. *American Journal of Physiology*, *277*(4), C755–C765.

Schmidt, H., Stiefel, K. M., Racay, P., Schwaller, B., & Eilers, J. (2003). Mutational analysis of dendritic Ca2+ kinetics in rodent Purkinje cells: Role of parvalbumin and calbindin D28k. *Journal of Physiology*, 551(1), 13–32.

Schmöle, A. C., Lundt, R., Gennequin, B., Schrage, H., Beins, E., Krämer, A., Zimmer, T., Limmer, A., Zimmer, A., & Otte, D. M. (2015). Expression analysis of CB2-GFP BAC transgenic mice. *PLoS ONE*, *10*(9), 1–16.

Schneider, M., Prudic, K., Pippel, A., Klapperstück, M., Braam, U., Müller, C. E., Schmalzing, G., & Markwardt, F. (2017). Interaction of Purinergic P2X4 and P2X7 Receptor Subunits. *Frontiers in Pharmacology*, *8, 860*.

Schwindt, T. T., Trujillo, C. A., Negraes, P. D., Lameu, C., & Ulrich, H. (2011). Directed differentiation of neural progenitors into neurons is accompanied by altered expression of P2X purinergic receptors. *Journal of Molecular Neuroscience*, *44*(3), 141–146.

Sebastián-Serrano, A., Engel, T., De Diego-García, L., Olivos-Oré, L. A., Arribas-Blázquez, M., Martínez-Frailes, C., Pérez-Díaz, C., Luis Millán, J., Artalejo, A. R., Miras-Portugal, M. T., Henshall, D. C., & Díaz-Hernández, M. (2016). Neurodevelopmental alterations and seizures developed by mouse model of infantile hypophosphatasia are associated with purinergic signalling deregulation. *Human Molecular Genetics*, *25*(19), 4143–4156.

Sebastián-Serrano, Á., de Diego-García, L., di Lauro, C., Bianchi, C., & Díaz-Hernández, M. (2019). Nucleotides regulate the common molecular mechanisms that underlie neurodegenerative diseases; Therapeutic implications. *Brain Research Bulletin*, *151*, 84–91.

Serganova, I., & Blasberg, R. G. (2019). Molecular Imaging with Reporter Genes: Has Its Promise Been Delivered? *Journal of Nuclear Medicine*, *60*(12), 1665–1681.

Shuen, J. A., Chen, M., Gloss, B., & Calakos, N. (2008). Drd1a-tdTomato BAC transgenic mice for simultaneous visualization of medium spiny neurons in the direct and indirect pathways of the basal ganglia. *Journal of Neuroscience*, *28*(11), 2681–2685.

Sikora, A., Liu, J., Brosnan, C., Buell, G., Chessel, I., & Bloom, B. R. (1999). Cutting Edge: Purinergic Signaling Regulates Radical-Mediated Bacterial Killing Mechanisms in Macrophages Through a P2X7-Independent Mechanism. *The Journal of Immunology*, *163*(2), 558–561.

Silinsky, E. M., Hunt, J. M., Solsona, C. S., & Hirsh, J. K. (1990). Prejunctional Adenosine and ATP Receptors. *Annals of the New York Academy of Sciences*, *603*, 324–334.

Silva-Ramos, M., Silva, I., Faria, M., Ferreirinha, F., & Correia-De-Sá, P. (2020). Activation of prejunctional P2x2/3 heterotrimers by ATP enhances the cholinergic tone in obstructed human urinary bladders. *Journal of Pharmacology and Experimental Therapeutics*, *372*(1), 63–72.

Silverman, W. R., de Rivero Vaccari, J. P., Locovei, S., Qiu, F., Carlsson, S. K., Scemes, E., Keane, R. W., & Dahl, G. (2009). The pannexin 1 channel activates the inflammasome in neurons and astrocytes. *Journal of Biological Chemistry*, *284*(27), 18143–18151.

Sim, J. A., Chaumont, S., Jo, J., Ulmann, L., Young, M. T., Cho, K., Buell, G., North, R. A., & Rassendren, F. (2006). Altered hippocampal synaptic potentiation in P2X4 knock-out mice. *Journal of Neuroscience*, *26*(35), 9006–9009.

Sluyter, R., Adriouch, S., Fuller, S. J., Nicke, A., Sophocleous, R. A., & Watson, D. (2023). Animal Models for the Investigation of P2X7 Receptors. *International Journal of Molecular Sciences,* 24(9), 8225.

Solle, M., Labasi, J., Perregaux, D. G., Stam, E., Petrushova, N., Koller, B. H., Griffiths, R. J., & Gabel, C. A. (2001). Altered cytokine production in mice lacking P2X7receptors. *Journal of Biological Chemistry*, *276*(1), 125–132.

Sparwasser, T., & Eberl, G. (2007). BAC to immunology - Bacterial artificial chromosome-mediated transgenesis for targeting of immune cells. *Immunology*, *121*(3), 308–313.

Sperlágh, B., & Illes, P. (2014). P2X7 receptor: an emerging target in central nervous system diseases. *Trends in Pharmacological Sciences*, *35*(10), 537–547.

Srinivasan, K., Friedman, B. A., Larson, J. L., Lauffer, B. E., Goldstein, L. D., Appling, L. L., Borneo, J., Poon, C., Ho, T., Cai, F., Steiner, P., van der Brug, M. P., Modrusan, Z., Kaminker, J. S., & Hansen, D. v. (2016). Untangling the brain's neuroinflammatory and neurodegenerative transcriptional responses. *Nature Communications*, *7*(1), 11295.

Stelmashenko, O., Lalo, U., Yang, Y., Bragg, L., North, R. A., & Compan, V. (2012). Activation of Trimeric P2X2 Receptors by Fewer than Three ATP Molecules. *Molecular Pharmacology*, *82*(4), 760–766.

Sudji, I. R., Subburaj, Y., Frenkel, N., García-Sáez, A. J., & Wink, M. (2015). Membrane disintegration caused by the steroid saponin digitonin is related to the presence of cholesterol. *Molecules*, *20*(11), 20146–20160.

Suh, B.-C., Kim, J.-S., Namgung, U., Ha, H., & Kim, K.-T. (2001). P2X7 Nucleotide Receptor Mediation of Membrane Pore Formation and Superoxide Generation in Human Promyelocytes and Neutrophils. *The Journal of Immunology*, *166*(11), 6754–6763.

Sun, B.-X., Peng, A.-S., Liu, P.J., Wang, M.-J., Ding, H.L., Hu, Y.-S., & Kang, L. (2023). Neuroprotection of exercise: P2X4R and P2X7R regulate BDNF actions. *Purinergic Signalling,* 19(1), 297–303.

Suurväli, J., Boudinot, P., Kanellopoulos, J., & Rüütel Boudinot, S. (2017). P2X4: A fast and sensitive purinergic receptor. *Biomedical Journal*, *40*(5), 245–256.

Svensson, E., Apergis-Schoute, J., Burnstock, G., Nusbaum, M. P., Parker, D., & Schiöth, H. B. (2019). General principles of neuronal co-transmission: Insights from multiple model systems. *Frontiers in Neural Circuits, 12*, 117.

Swanson, K. v., Deng, M., & Ting, J. P. Y. (2019). The NLRP3 inflammasome: molecular activation and regulation to therapeutics. *Nature Reviews Immunology*, 19 (8), 477–489.

Tammaro, P., Shimomura, K., & Proks, P. (2008). Xenopus Oocytes as a Heterologous Expression System for Studying Ion Channels with the Patch-Clamp Technique. *Methods in Molecular Biology (Clifton, N.J.), 491*, 127–139.

Tanaka, K., Choi, J., Cao, Y., & Stacey, G. (2014). Extracellular ATP acts as a damage-associated molecular pattern (DAMP) signal in plants. In *Frontiers in Plant Science, 5*, 446.

Tenneti, L., Gibbons, S. J., & Talamo, B. R. (1998). Expression and Trans-synaptic Regulation of P2x4 and P2z Receptors for Extracellular ATP in Parotid Acinar Cells. *Journal of Biological Chemistry*, *273*(41), 26799–26808.

Territo, P. R., & Zarrinmayeh, H. (2021). P2X7 Receptors in Neurodegeneration: Potential Therapeutic Applications From Basic to Clinical Approaches. *Frontiers in Cellular Neuroscience, 15*, 617036.

Torres, G. E., Egan, T. M., & Voigt, M. M. (1999). Hetero-oligomeric Assembly of P2X Receptor Subunits. *Journal of Biological Chemistry*, *274*(10), 6653–6659.

Tozaki-Saitoh, H., Takeda, H., & Inoue, K. (2022). The Role of Microglial Purinergic Receptors in Pain Signaling. *Molecules*, *27*(6), 1–17.

Trang, M., Schmalzing, G., Müller, C. E., & Markwardt, F. (2020). Dissection of P2X4 and P2X7 receptor current components in BV-2 microglia. *International Journal of Molecular Sciences*, *21*(22), 1–20.

Tsoa, R. W., Coskun, V., Ho, C. K., de Vellis, J., & Sun, Y. E. (2014). Spatiotemporally different origins of NG2 progenitors produce cortical interneurons versus glia in the mammalian forebrain. *Proceedings of the National Academy of Sciences*, *111*(20), 7444–7449.

Tsuda, M., Tone, Y., Ogawa, C., Nagaoka, Y., Katsumata, M., Necula, A., Howie, D., Masuda, E., Waldmann, H., & Tone, M. (2017). A bacterial artificial chromosome reporter system for expression of the human FOXP3 gene in mouse regulatory T-cells. *Frontiers in Immunology*, *8*, 279.

Tusher, V. G., Tibshirani, R., & Chu, G. (2001). Significance analysis of microarrays applied to the ionizing radiation response. *Proceedings of the National Academy of Sciences*, *98*(9), 5116–5121.

Tyanova, S., Temu, T., & Cox, J. (2016). The MaxQuant computational platform for mass spectrometry-based shotgun proteomics. *Nature Protocols*, *11*(12), 2301–2319.

Urbina-Treviño, L., von Mücke-Heim, I. A., & Deussing, J. M. (2022). P2X7 Receptor-Related Genetic Mouse Models – Tools for Translational Research in Psychiatry. *Frontiers in Neural Circuits, 16*, 876304.

Valera, S., Hussy, N., Evans, R. J., Adami, N., North, R. A., Surprenant, A., & Buell, G. (1994). A new class of ligand-gated ion channel defined by P2X receptor for extracellular ATP. *Nature*, *371*(6497), 516–519.

Vénéreau, E., Ceriotti, C., & Bianchi, M. E. (2015). DAMPs from Cell Death to New Life. *Frontiers in Immunology*, *6, 422.*

Verhoef, P. A., Estacion, M., Schilling, W., & Dubyak, G. R. (2003). P2X7 Receptor-Dependent Blebbing and the Activation of Rho-Effector Kinases, Caspases, and IL-1β Release. *The Journal of Immunology*, *170*(11), 5728–5738.

Virginio, C., Church, D., North, R. A., & Surprenant, A. (1997). Effects of Divalent Cations, Protons and Calmidazolium at the Rat P2X7 Receptor, *Neuropharmacology,* 36(9), 1285-1294.

Wang, C., Yang, T., Xiao, J., Xu, C., Alippe, Y., Sun, K., Kanneganti, T. D., Monahan, J. B., Abu-Amer, Y., Lieberman, J., & Mbalaviele, G. (2021). NLRP3 inflammasome activation triggers gasdermin D–independent inflammation. *Science Immunology*, *6*(64).

Webb, T. E., Simon, J., Krishek, B. J., Bateson, A. N., Smart, T. G., King, B. F., Burnstock, G., & Barnard, E. A. (1993). Cloning and functional expression of a brain G-protein-coupled ATP receptor. *FEBS Letters*, *324*(2), 219–225.

Wei, W., Ryu, J. K., Choi, H. B., & McLarnon, J. G. (2008). Expression and function of the P2X7 receptor in rat C6 glioma cells. *Cancer Letters*, *260*(1–2), 79–87.

Weinhold, K., Krause-Buchholz, U., Rödel, G., Kasper, M., & Barth, K. (2010). Interaction and interrelation of P2X7 and P2X4 receptor complexes in mouse lung epithelial cells. *Cellular and Molecular Life Sciences*, *67*(15), 2631–2642.

Wewers, M. D., & Sarkar, A. (2009). P2X7 receptor and macrophage function. *Purinergic Signalling*, *5*(2), 189–195.

Wiley, J. S., & Gu, B. J. (2012). A new role for the P2X7 receptor: A scavenger receptor for bacteria and apoptotic cells in the absence of serum and extracellular ATP. *Purinergic Signalling*, *8*(3), 579–586.

Wilhelm, K., Ganesan, J., Müller, T., Dürr, C., Grimm, M., Beilhack, A., Krempl, C. D., Sorichter, S., Gerlach, U. v., Jüttner, E., Zerweck, A., Gätner, F., Pellegatti, P., di Virgilio, F., Ferrari, D., Kambham, N., Fisch, P., Finke, J., Idzko, M., & Zeiser, R. (2010). Graft-versus-host disease is enhanced by extracellular ATP activating P2X7R. *Nature Medicine*, *16*(12), 1434–1439.

Wilson, H. L., Varcoe, R. W., Stokes, L., Holland, K. L., Francis, S. E., Dower, S. K., Surprenant, A., & Crossman, D. C. (2007). P2X receptor characterization and IL-1/IL-1Ra release from human endothelial cells. *British Journal of Pharmacology*, *151*(1), 96–108.

Winkelmann, V. E., Thompson, K. E., Neuland, K., Jaramillo, A. M., Fois, G., Schmidt, H., Wittekindt, O. H., Han, W., Tuvim, M. J., Dickey, B. F., Dietl, P., & Frick, M. (2019). Inflammation-induced upregulation of p2x 4 expression augments mucin secretion in airway epithelia. *American Journal of Physiology - Lung Cellular and Molecular Physiology*, *316*(1), L58–L70.

Wirsching, E., Fauler, M., Fois, G., & Frick, M. (2020). P2 purinergic signaling in the distal lung in health and disease. *International Journal of Molecular Sciences*, *21*(14), 1–25.

Wiśniewski, J. R., Zougman, A., Nagaraj, N., & Mann, M. (2009). Universal sample preparation method for proteome analysis. *Nature Methods*, *6*(5), 359–362.

Wiśniewski, J. R. (2018). Filter-Aided Sample Preparation for Proteome Analysis, *Methods in Molecular Biology*, 1841, 3–10.

Woo, J., Han, D., Wang, J. I., Park, J., Kim, H., & Kim, Y. (2017). Quantitative Proteomics Reveals Temporal Proteomic Changes in Signaling Pathways during BV2 Mouse Microglial Cell Activation. *Journal of Proteome Research*, *16*(9), 3419–3432.

Xiang, Z., & Burnstock, G. (2005). Expression of P2X receptors on rat microglial cells during early development. *Glia*, *52*(2), 119–126

Xiao, L., Magupalli, V. G., & Wu, H. (2023). Cryo-EM structures of the active NLRP3 inflammasome disc. *Nature*, *613*(7944), 595–600.

Xu, J., Bernstein, A. M., Wong, A., Lu, X. H., Khoja, S., Yang, X. W., Davies, D. L., Micevych, P., Sofroniew, M. V., & Khakh, B. S. (2016). P2X4 receptor reporter mice: Sparse brain expression and feeding-related presynaptic facilitation in the arcuate nucleus. *Journal of Neuroscience*, *36*(34), 8902–8920.

Yang, X. W., Model, P., & Heintz, N. (1997). Homologous recombination based modification in Esherichia coli and germline transmission in transgenic mice of a bacterial artificial chromsome. *Nature Biotechnology*, *15*(9), 859–865.

Yang, X. W., & Gong, S. (2005). An Overview on the Generation of BAC Transgenic Mice for Neuroscience Research. *Current Protocols in Neuroscience*, *31*(1), 5-20.

Yang, X. W. (2009). BAC Use in the Study of the CNS. In *Encyclopedia of Neuroscience* (pp. 13–20). Academic Press.

Yip, L., Woehrle, T., Corriden, R., Hirsh, M., Chen, Y., Inoue, Y., Ferrari, V., Insel, P. A., & Junger, W. G. (2009). Autocrine regulation of T-cell activation by ATP release and P2X7 receptors. *The FASEB Journal*, *23*(6), 1685–1693.

Young, C. N. J., Sinadinos, A., Lefebvre, A., Chan, P., Arkle, S., Vaudry, D., & Gorecki, D. C. (2015). A novel mechanism of autophagic cell death in dystrophic muscle regulated by P2RX7 receptor large-pore formation and HSP90. *Autophagy*, *11*(1), 113–130.

Zabala, A., Vazquez-Villoldo, N., Rissiek, B., Gejo, J., Martin, A., Palomino, A., Perez-Samartín, A., Pulagam, K. R., Lukowiak, M., Capetillo-Zarate, E., Llop, J., Magnus, T., Koch-Nolte, F., Rassendren, F., Matute, C., & Domercq, M. (2018). P2X4 receptor controls microglia activation and favors remyelination in autoimmune encephalitis. *EMBO Molecular Medicine*, *10*(8), 1-20.

Zech, A., Wiesler, B., Ayata, C. K., Schlaich, T., Dürk, T., Hoßfeld, M., Ehrat, N., Cicko, S., & Idzko, M. (2016). P2rx4 deficiency in mice alleviates allergen-induced airway inflammation. *Oncotarget*, *7*(49), 80288–80297.

Zhao, X. F., Alam, M. M., Liao, Y., Huang, T., Mathur, R., Zhu, X., & Huang, Y. (2019). Targeting microglia using Cx3cr1-Cre lines: Revisiting the specificity. *ENeuro*, *6*(4), 1–11.

Zhao, Y. F., Tang, Y., & Illes, P. (2021). Astrocytic and Oligodendrocytic P2X7 Receptors Determine Neuronal Functions in the CNS. *Frontiers in Molecular Neuroscience*, *14*, 641570.

Zoghbi, H. Y. (2003). BAC-to-BAC images of the brain. *Nature*, *425*(6961), 907–908.

Acknowledgements

I would like to start by thanking Prof. Dr. Annette Nicke, for the opportunity that I was given to work in her laboratory. I am grateful for your guidance and the help that you gave me, especially during Covid-19 time when the situation was difficult. I have learned many things from working in your laboratory, thanks to which I am a better scientist now.

I am grateful for the help provided by Dr. Thomas Fröhlich, who gave us quality advice about proteomics and performed the LC-MS analyses. I extend my gratitude to all the collaborators that helped in our research and help with the preparation of the Scientific Reports article.

This work would not have been possible without the help and support from my colleagues at the Nicke laboratory. Thank you for all the lessons that I learned and all the good times that we had. I want to thank Robin Kopp for being not only a mentor but a friend since the first day. I want to thank you for the help that you gave me, your effort in trying to learn Spanish, your (always useful) knowledge of German grammar and your patience and honesty when I needed them. I also want to mention Anna Durner (Krauti) for all the nice (and not so nice) music sessions at the institute and for always being there for a nice conversation or a caffeine boost. I will never forget all the help that you gave me by going through administration procedures when I had just arrived and we didn't know each other. I am sorry, but I still think koalas are better than sloths! Special thanks to Heinz Janser, for always having a smile for me when the days were rough, for never saying "no" when technical help was needed (even if I had to pay with chocolate) and for all the jokes in the laboratory. You have been a real hero for me during these years! I also want to thank Yves Haufe for all of his advice (either work-related or Germany-related), for your enthusiasm and for reminding me that there is always time for sports and anime.

I want to extend my gratitude to my other colleagues and the group leaders at the Walther Straub Institute for their advice. Special thanks to Carla Abrahamian, Isabel Müller, Fabienne Geiger, Anna Scotto Rosato, Julia Böck, Suhasini Rajan and Philipp Alt for all of the tea times/lunch times and for making Covid19 time a period that I will remember for all the fun I had. Thank you for the help, the good times, the never-ending conversations about languages and the support when the situations were difficult and I just needed to complain about everything.

I am really grateful for having the best colleagues and friends I could have ever expected at the PurinesDX consortium. Together, we learned many things and had great times during our trips and meetings that I will not forget. These were full of enriching experiences, scientific talks, and discussions for which I want to thank all the project leaders involved, but specially Prof. Emeritus Antonio García-García and Prof. Dr. Béata Sperlágh, for having me in their research laboratories during my secondments, and to Dr. Isabela Aparicio and Dr. Tobias Engel for the organization and for making sure that we were all doing well.

Moving back to Spain, I want to thank my uncles, aunts, cousins and also my friends for all their support and for keeping in touch, making sure I was alright while I was away.

I want to thank my parents Antonio and Carmen, for never saying “no” and for supporting me in all of my life choices, for taking care of me in the distance and for always being there to talk, advice and comfort.

I want to thank my brother Fernando, for joining me in this adventure from the first day, for helping me during my worst times and for always being willing to support and give advice. I also want to dedicate this to my grandmother Amparo for being my biggest fan and for the unconditional love. I also thank my grandfather Fernando for the support in every aspect of my life, whether you had to take us to school or carry my saxophone around, and for all the fun and good times. Lastly, I dedicate this to my late grandfather Paco, for all the lessons, the love and for being the first one to encourage me to go to Granada to study and live there with him.

Finally, I want to thank Cris, for accepting and supporting my choices, for being there in all kinds of situations, for always finding a way to make things right when everything seems to be wrong, and for making every day worthwhile.

Thank you everyone! This would not have been possible without you!

Funding: This project has received funding from the European Union’s Horizon 2020 research and innovation programme under the Marie Skłodowska-Curie grant agreement No. 766124

Affidavit

LMU LUDWIG-MAXIMILIANS-UNIVERSITÄT MÜNCHEN

Promotionsbüro
Medizinische Fakultät

MMRS

Affidavit

Ramírez Fernández, Antonio

Surname, first name

I hereby declare, that the submitted thesis entitled:

"Characterization of a P2X7 BAC reporter mouse model and investigation of the P2X4/P2X7 interaction in mouse lung tissue"

is my own work. I have only used the sources indicated and have not made unauthorised use of services of a third party. Where the work of others has been quoted or reproduced, the source is always given.

I further declare that the dissertation presented here has not been submitted in the same or similar form to any other institution for the purpose of obtaining an academic degree.

Málaga, 11.12.2023 — Antonio Ramírez-Fernández

place, date — Signature doctoral candidate

Confirmation of congruency

LMU LUDWIG-MAXIMILIANS-UNIVERSITÄT MÜNCHEN

Promotionsbüro
Medizinische Fakultät

MMRS

Confirmation of congruency between printed and electronic version of the doctoral thesis

Ramírez Fernández, Antonio

Surname, first name

I hereby declare, that the submitted thesis entitled:

"Characterization of a P2X7 BAC reporter mouse model and investigation of the P2X4/P2X7 interaction in mouse lung tissue"

……

is congruent with the printed version both in content and format.

Málaga, 11.12.2023
place, date

Antonio Ramírez-Fernández
Signature doctoral candidate

Use of previously published illustrations

In the course of my doctoral project, I have published part of my work as a research article with the following reference:

“Ramírez-Fernández, A., Urbina-Treviño, L., Conte, G., Alves, M., Rissiek, B., Durner, A., Scalbert, N., Zhang, J., Magnus, T., Koch-Nolte, F., Plesnila, N., Deussing, J. M., Engel, T., Kopp, R., & Nicke, A. (2020). Deviant reporter expression and P2X4 passenger gene overexpression in the soluble EGFP BAC transgenic P2X7 reporter mouse model. *Scientific Reports, 10*(1), 1–17.”

I have included full or slightly changed figures from this article in this dissertation and I have included the reference in each figure legend.

As part of the Open Access policy from Scientific Reports, all articles are published under the Creative Commons Attribution 4.0 International License. This license “allows for maximum dissemination and re-use of open access materials (...). Under this license, users are free to share (copy, distribute and transmit) and remix (adapt) the contribution including for commercial purposes, providing they attribute the contribution in the manner specified by the author or licensor”.

Further information about the Creative Commons Attribution 4.0 International License (CC BY 4.0) may be found in the following link https://creativecommons.org/licenses/by/4.0/legalcode.

Furthermore, according to Springer Nature, “authors have the right to reuse their article’s Version of Record, in whole or in part, in their own thesis. Additionally, they may reproduce and make available their thesis, including Springer Nature content, as required by their awarding academic institution. (...) Authors must properly cite the published article in their thesis according to current citation standards.”

This information is available in the following link https://www.nature.com/nature-portfolio/reprints-and-permissions/permissions-requests#Author%20reuse.

These figures are the results from the experiments that I have carried in the course of my doctoral project. As the first author from the cited research article, I take responsibility for their use in this dissertation.

Antonio Ramírez Fernández

Málaga, 11.12.2023